ABSTRACT

Title of Document:	LONG-RANGE SIGNALING AT THE INTESTINAL-NEURAL AXIS PROMOTES ORGANISMAL HEME HOMEOSTASIS IN *C. ELEGANS*
	Jason Sinclair, Doctor of Philosophy, 2014
Directed By:	Professor Dr. Iqbal Hamza, Department of Animal and Avian Sciences

Metazoans synthesize and regulate intracellular heme in a cell autonomous manner although genetic evidence in vertebrates suggests that cell non-autonomous mechanisms may exist at the organismal level. In *C. elegans*, a heme auxotroph, extraintestinal tissues are intrinsically dependent on the intestine, which acquires dietary heme for sustenance, supporting the concept that intestinal heme status must be coordinated at the systemic level to regulate whole-organism heme homeostasis. Here we show, by conducting a functional genome-wide RNAi screen in an intestinal-restricted heme sensor worm, that an interorgan heme signaling pathway exists and that >30% of the genes identified from the RNAi screen altered heme homeostasis in the intestine even though these genes are not expressed in the intestine. The biological basis for this signaling is underscored by HRG-7, a cathepsin protease-like protein secreted by the intestine and internalized by distally-located neurons. HRG-7 is specifically secreted from the intestine during heme limitation and *hrg-7* depletion causes embryonic lethality concomitant with a heme deficiency response. Reciprocally, neuron-to-intestine heme signaling is mediated by the bone

morphogenic protein homolog DBL-1, which recapitulates *hrg-7* deficiency when depleted. Remarkably, depletion of both genes simultaneously results in markedly enhanced growth and heme deficiency phenotypes, suggesting that bidirectional signaling between the intestine and neurons mediates systemic heme homeostasis. Our results have uncovered an unexpected role for a protease family member in long-range communication between organs at the intestinal-neural axis to regulate systemic heme homeostasis in metazoa. As humans have over thirty cathepsin and cathepsin-like proteases, several of which are secreted, we anticipate that these proteins may play analogous roles in mammalian biology.

LONG-RANGE SIGNALING AT THE INTESTINAL-NEURAL AXIS
PROMOTES ORGANISMAL HEME HOMEOSTASIS IN *C. ELEGANS*

By

Jason Sinclair

Dissertation submitted to the Faculty of the Graduate School of the
University of Maryland, College Park, in partial fulfillment
of the requirements for the degree of
Doctor of Philosophy
2014

Advisory Committee:
Professor Iqbal Hamza, Chair
Dr. Lisa Taneyhill
Dr. Jiuzhou Song
Dr. Michael Krause
Dr. Najib El-Sayed

Dedication

To my friends, family, and mentors who made this possible

Acknowledgements

This dissertation would not have been possible without the help and support from family, friends, advisors, committee members, coworkers and colleagues. Thanks to all for your friendship, patience, financial support when needed, and a positive word during the tougher times.

I have to thank my family first. That starts with my parents. They have never complained when I couldn't come home for a holiday because I had to do an experiment, and always offered their full support, no matter what. Thank you to my two sisters, Margaret and Jackie, who, whether it was giving me an Xbox or just coming down to Maryland to hang out, have been awesome throughout my time in graduate school. Thank you to my Grandmothers Joan and Bea, who always had money for me (and wouldn't take no for an answer) and who have always supported me. And of course, thank you to my aunts, uncles, and cousins. I would like to give a special thanks to the Peters, my closest local relatives.

Thank you to my former housemates Adam and Erin who didn't complain when I turned the kitchen table into a study zone before my preliminary exams, and turned a blind eye when I skipped my house chores because I was at the lab. We may not live together anymore but we'll be lifetime friends, I have no doubt. Thanks to my friends Will and Brian, my best friends from high school and college. I will soon join your ranks as someone who is no longer in school.

Thank you to Joe and Steve, the guys with whom I have been making "beautiful" music with for over ten years now, before either of you were fathers.

You've been there as an outlet during my entire graduate school tenure, and we've had some fun times. Rock on!

And of course, thank you to my lovely girlfriend Jen. You have not only been a rock and had to put up with me more than anyone else, but as a fellow scientist I could always give you my practice presentations or have you read over anything I wrote. And you cook! Thanks so much for everything.

Thank you to my committee: Dr. Lisa Taneyhill, Dr. Michael Krause, Dr. Jiuzhou Song, and Dr. Najib El-Sayed. You have been a fantastic committee and without your input and guidance, this dissertation would not have been possible. Through your questions, suggestions, and just putting in the time you have pushed me to become a better scientist. I hope you enjoy reading this work.

Thank you to all the Hamza lab members, past and present. Thank you Abbhi, as you probably wanted to kill me when I joined the lab as a Master's student and had endless questions. Thank you to Scott, who read and edited everything I wrote for my first few years in the lab. You were a bastion of knowledge and really helped me get through the initial difficulties a beginning graduate student faces. Thank you to Tamika, who has contributed to the work presented in this dissertation. We spent a lot of long days at the NIH together and usually closed up the Hanover lab. Thank you to Kate, who for the last two years has facilitated the generation of data for this work tremendously. I'm not sure where this project would be without your help! And thanks to Kevin, the former undergraduate student who helped initiate this work. You'll be writing your acknowledgements before you know it!

Thank you to the members of the Baltimore-Washington Worm Club. Not only was this an amusing name to my non-scientist friends, but presenting my work at Worm Club made me really believe that I could be a successful scientist. A special thanks to Dr. John Hanover who let Tamika, Scott and I use his worm sorter at will. This project would not have been possible without it.

Thank you to my former advisor Sige Zou. During our time at the NIA you made me believe that I had the ability to get a PhD. If you hadn't supported me during the earliest days of my scientific career I would have never have gotten to this point.

And, thank you to my advisor, Dr. Iqbal Hamza. You convinced me to come to UMD and join your lab, and I haven't looked back since. You have pushed me to be the best scientist I can be, and I can't believe how far I've come since beginning my Master's degree in 2006. When I first joined your lab, I would have never thought that I would one day be a three time ANSC oral presentation winner and PhD student of the year. Thanks to your guidance, I am armed with the skills and confidence to continue my career. Hopefully one day we will be corresponding as colleagues.

<div align="center">Thanks again to all!</div>

Table of Contents

List of Tables and Figures

Chapter 1

Chapter 3

Chapter 4

Chapter 5

Chapter 6

List of Abbreviations

ACC	Anterior cingulate cortex
ACE	Angiotensin-converting-enzyme
AGRP	Agouti-related peptide
ALA	5-aminolevulinic acid
ALAS	Aminolevulinic acid synthase
ANS	Autonomic nervous system
BMP	Bone morphogenic protein
CP motif	Cysteine proline motif
CRH	Corticotropin releasing hormone
DDM	n-Dodecyl β-D-maltoside
DiI	1,1'-dioctadecyl-3,3,3',3'-tetramethylindocarbocyanine perchlorate
DMSO	Dimethyl formamide
DNMV	Dorsal motor nucleus of vagus
dsRNA	Double-stranded RNA
DVC	Dorsal vagal complex
EDTA	Ethylenediaminetetraacetic acid
EECs	Enteroendocrine cells
EGF	Epidermal growth factor
EICs	Enteric immune cells
ENS	Enteric nervous system
EP	Erythrophagocytosis
FITC	5-fluorescein isothiocyanate
GaPP	gallium protoporphyrin
HERE	Heme-responsive element
HGF	Hepatocyte growth factor
HO	Heme oxygenase
HRG	Heme repsonsive gene
HSCR	Hirschsprung's disease
ICS	Intercistronic SL2 sequence
INS	Insula
IPANs	Intrinsic primary afferent neurons
IPTG	Isopropyl-β-D-thioglactopyranoside
IRE	Iron response element
IRP	Iron regulatory protein
LB	Luria-Bertani broth

LCR	Locus control region
MARE	Maf recognition element
MCH	Melanin concentrating hormone
MCS	Multiple cloning sequence
MMP	Matrix metalloproteases
MuDPIT	Multi-dimensional protein identification technology
NGM	Nematode growth medium
NPY	Neuropeptide Y
NTS	Nucleus tractus solitarii
PAG	Periaqueductal grey
PARs	Protease activated receptors
PBS	Phosphate-buffered saline
PFC	Prefrontal cortex
RAS	Renin-angiotensin system
RBC	Red blood cell
ROI	Region of interest
RVLM	Rostro–ventro–lateral medulla
SDS	Sodium dodecyl sulfate polyacrylamide gel electrophoresis
Shh	Sonic hedgehog
succinyl-CoA	Succinyl-coenzyme A
UTR	Untranslated region
ZnMP	Zinc mesopophyrin

Chapter 1: Introduction

Heme homeostasis

Heme is an iron-containing tetrapyrrole that is required as a cofactor for proteins involved in numerous cellular functions including hemoglobin for oxygen binding, cytochromes for electron transfer, and guanylate cyclase for cell signaling [1, 2]. In humans, over sixty percent of iron in the body is heme-iron coordinated in hemoglobin. Additionally, iron is more efficiently absorbed from the diet as heme-iron [3-6]. However, despite its necessity free heme is also cytotoxic due to its inherent peroxidase reactivity and ability to produce reactive oxygen species [7-9]. Moreover, heme is hydrophobic due to the porphyrin side chains and, *a priori*, cannot freely diffuse through the aqueous cytosol. Therefore, cells must be able to carefully regulate heme levels, compartmentalization, and transport to target hemoproteins whilst preventing toxicity. Although the regulatory processes of heme synthesis and degradation have been well characterized, other homeostatic mechanisms have remained elusive. This is primarily due to the difficulty in uncoupling heme synthesis from downstream processes such as heme trafficking. However, the discovery that the soil-dwelling nematode, *C. elegans*, contains hemoproteins but is unable to synthesize heme has led to the identification of several intracellular and intercellular heme transporters [10-13]. In *C. elegans*, all organismal heme must pass through the intestine before distribution to other tissues, and therefore it is not surprising that worms possess an intercellular transport system to mobilize heme from the intestine to tissues such as neurons, muscles, and developing embryos [1]. However, it had

been presumed that in heme producing organisms such as mammals, heme synthesis and degradation function in a cell-autonomous manner and that is sufficient to maintain cellular heme levels without a need for an intercellular transport pathway. However, recent evidence suggests that such pathways do exist in vertebrates [14-17]. The mechanisms of cellular heme homeostasis and evidence for intercellular heme transport in vertebrates will be discussed.

Heme homeostasis in *C. elegans*

The nematode *C. elegans* is a unique model in which to study systemic heme homeostasis. Worms offer several general advantages as a model organism as they are genetically tractable, optically transparent, amenable for genetic screens and cell biological studies, and have a high percentage of genes that are conserved in humans [18]. More specifically and crucially for studying heme homeostasis, *C. elegans* is a heme auxotroph. All heme that is utilized by the worm must pass through the intestinal brush border where it will be used directly by the intestine, stored for later use, or transported to extraintestinal tissues. Heme destined for extraintestinal tissues must be transported through the intestinal epithelial cells and exported from the basolateral membrane to the pseudocoelom, the worm's circulatory system. Once in the pseudocoelom, extraintestinal tissues will have access to intestinal-derived heme. Using *C. elegans* as a model organism, these pathways can be studied without interference from confounding factors such as cellular iron transport and heme synthesis. Based on transcriptomic analyses in *C. elegans*, several of the heme transporters have been identified and will be discussed.

As the source of all heme in the worm, the intestine plays an essential role in organismal heme homeostasis, and thus expresses several genes necessary for adaptation to varying environmental heme availability. As mentioned, all heme must pass through the intestinal brush border of the worm. HRG-4 is a high-affinity heme permease involved in this process. HRG-4 is specifically expressed in the *C. elegans* intestine at low heme and localizes to the apical intestinal membrane where it imports dietary heme [13, 19, 20]. RNAi knockdown of *hrg-4* results in an intestinal heme deficiency signal, diminished intestinal accumulation of the fluorescent heme analog zinc mesoporphyrin (ZnMP), and protection from the toxic heme analog gallium protoporphyrin IX (GaPP) [20]. These data indicate that HRG-4 imports heme from the lumen into the intestine. However, a genetic deletion of *hrg-4* does not result in a growth phenotype, suggesting redundant pathways for heme uptake. This redundancy is likely due to two HRG-4 paralogs, HRG-5 and HRG-6. Unlike HRG-4, HRG-5 and HRG-6 are not transcriptionally regulated by heme and therefore may mediate heme transport into the intestine in heme replete conditions when HRG-4 would normally be repressed.   Once in the intestine, at least a portion of heme will be compartmentalized into vesicles. HRG-1, another paralog of HRG-4, is also upregulated by low heme specifically in the intestine but localizes to ZnMP-containing intracellular vesicles. RNAi depletion of *hrg-1* results in vesicular ZnMP accumulation, suggesting that under heme limiting conditions, upregulation of HRG-1 allows compartmentalized heme to be mobilized for utilization. Interestingly, worms harboring mutations in both *hrg-1* and *hrg-4* exhibit a synthetic growth phenotype in low heme [19]. This suggests that after transport into the intestine,

heme may be partitioned into separate labile and compartmentalized pools. It is also possible that HRG-1 traffics via the apical plasma membrane and compensates for the lack of HRG-4 **(Figure 1.1).**

Transport studies in *Saccharomyces cerevisiae* have identified the residues within these permeases that are important for heme transport [19]. HRG-4 transports heme by utilizing a histidine in the exoplasmic (E2) loop and a conserved FARKY motif near the C terminus. Under low heme conditions when maximum transport activity is required, an additional tyrosine in TMD2 is necessary. HRG-1, meanwhile, requires both a histidine in the predicted second transmembrane domain (TMD2) and the FARKY motif. For optimal activity under heme-limiting conditions, HRG-1 requires a histidine in the E2 loop. The presence of tyrosines rather than histidines in HRG-4 may help stabilize oxidized heme imported from the lumen [21, 22].

Interestingly, despite both genes being upregulated in the intestine by low heme, *hrg-1* and *hrg-4* appear to be transcriptionally regulated by different pathways. The heme-dependent regulation of *hrg-1* is driven by a heme-responsive element (HERE) in conjunction with GATA sites, elements that bind the GATA transcription factor ELT-2 and are responsible for intestinal transcription in the worm [23, 24]. Although the *hrg-4* 5' flanking region also has GATA sites, it does not have a HERE, indicating different pathways are responsible for the heme-responsiveness of *hrg-1* and *hrg-4*.

Figure 1.1: Model of heme homeostasis in *C. elegans*

In order to adapt to varying environmental heme conditions, *C. elegans* has adopted

several mechanisms to ensure that tissue heme requirements are fulfilled but heme

toxicity is prevented. In high environmental heme conditions, expression of high

affinity heme transporters is repressed, and excess heme is compartmentalized in

vesicles. When the worm encounters low environmental heme, high affinity heme

importers HRG-4 and HRG-1 are expressed to increase intestinal heme uptake and

release heme stored in vesicles, respectively. The heme exporter MRP-5 is slightly

upregulated to facilitate heme availability to extraintestinal tissues. HRG-3 is

expressed to provide oocytes and developing embryos with sufficient heme, and

genes such as HRG-2 in the hypodermis are upregulated in peripheral tissues to

increase heme utilization. It is likely that homeostatic adaptation is controlled at the

systemic level by bidirectional signaling between the intestine and extraintestinal
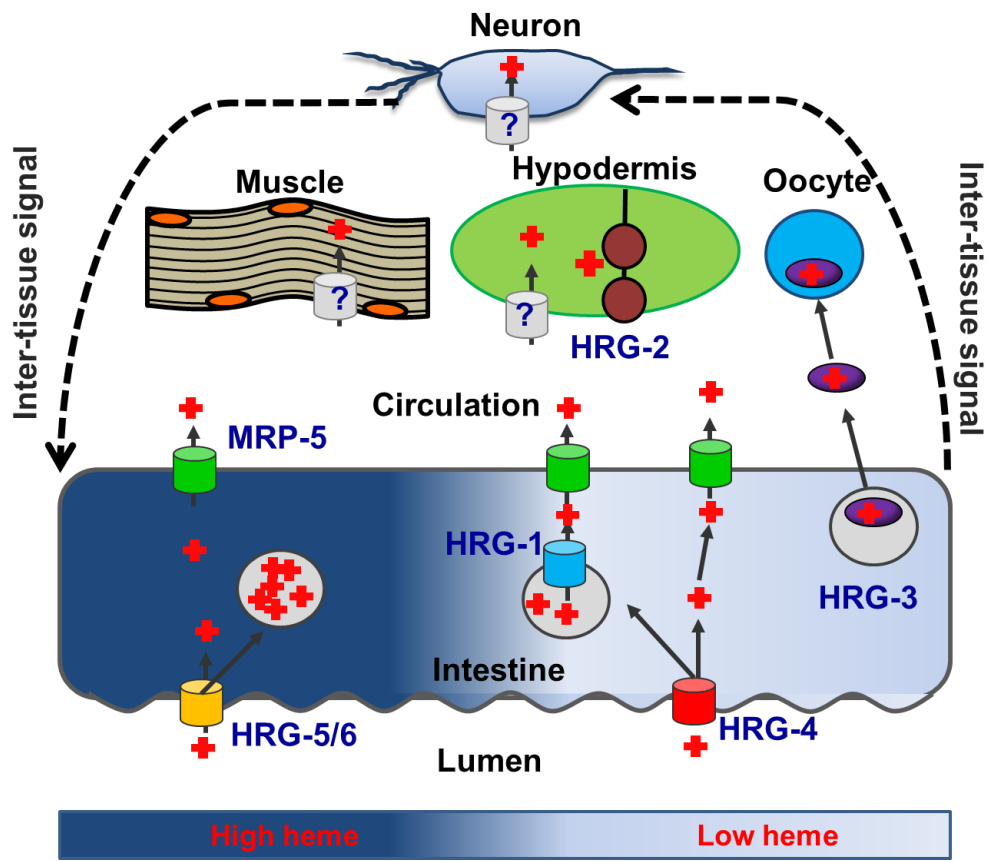
tissues.

Before heme can be utilized by extraintestinal tissues after uptake, it must be transported across the intestinal basolateral membrane. Unlike the redundancy observed for heme importers, there appears to be one main intestinal heme exporter in the *C. elegans* intestine, MRP-5 (**Figure 1.1**). MRP-5 is an ABC-transporter that localizes to the basolateral membrane and basolateral sorting vesicles of the *C. elegans* intestine. Both a genetic deletion and RNAi depletion of MRP-5 result in embryonic lethality due to heme being trapped in the mother's intestine, showing a lack of functional redundancy in intestinal heme export. This lethality can be overcome by supplementing the worm growth medium with >200 μM heme. In addition to embryonic lethality, depletion of MRP-5 leads to accumulation of ZnMP in the intestine and protection from GaPP, presumably by preventing it from being transported to extraintestinal tissues. MRP-5 is also expressed in extraintestinal tissues such as the hypodermis, pharynx and some neurons, although it is unclear whether MRP-5 exports heme from these tissues or provides heme to hemoproteins in the secretory pathway, a function attributed to mammalian MRP5.

Microarray and qRT-PCR data have shown that *mrp-5* is upregulated by low heme, and bioinformatic analyses suggest that *mrp-5*, like *hrg-1*, has a conserved HERE and GATA cis-elements in the 5' flanking region. However, unlike *hrg-1*, *mrp-5* continues to be expressed in high heme conditions, which is not surprising due to a lack of functional redundancy. Unexpectedly, knockdown of *mrp-5* results in a heme deficiency signal in the intestine despite also resulting in intestinal heme accumulation [12, 20]. This result suggests that when heme is trapped in the intestine, heme-depleted extraintestinal tissues signal to the intestine to acquire more

heme. Thus it appears that though the intestine is the source of all heme in *C. elegans*, extraintestinal tissue have regulatory input over intestinal heme transport by regulating HRG-1 and possibly other transporters, indicating that heme homeostasis is maintained on an organismal level through intertissue communication **(Figure 1.1)**.

While MRP-5 is required for embryonic survival over a broad range of heme concentrations, *C. elegans* has adapted an "emergency" mechanism at critically low heme conditions to ensure that oocytes developing within the germline receive the heme required for embryogenesis and larval development [11]. This is accomplished by upregulation of HRG-3, a 8.1 kDa heme chaperone that binds heme in a 2:1 (protein: heme) stoichiometry, possibly through two conserved histidine residues [11]. Although *hrg-3* is not detectable at heme concentrations greater than 6 μM, it is upregulated in the intestine more than 900 fold at 1.5 μM. A genetic deletion of *hrg-3* results in embryonic lethality and L1 arrest, while chimeric HRG-3::mCherry is secreted from the intestine and localizes to developing oocytes. Taken together, these data indicate that HRG-3 delivers maternal heme to developing oocytes. It is unclear whether HRG-3 acquires heme in the secretory pathway or in the pseudocoelom post secretion, or if heme loading is dependent on MRP-5. Further analyses will be required to establish the relationship between different mechanisms of intestinal heme export. Interestingly, HRG-3 is expressed in zygotes, all larval stages and in males, suggesting function beyond delivery of heme to the germline.

In addition to HRGs in the intestine, we have characterized another heme-responsive gene in the hypodermis termed *hrg-2* [25]. HRG-2 is a single pass type I transmembrane protein that localizes to the ER and apical plasma membrane of the

hypodermis. In addition to the transmembrane domain, HRG-2 has a thioredoxin-like fold and a glutathione S-transferase-like domain on the carboxyl terminus. Under heme limited conditions, *hrg-2* is upregulated over 200 fold in the hypodermis. A genetic deletion of *hrg-2* results in an aberrant cytochrome heme profile, and ectopic expression of HRG-2 in a heme deficient strain of yeast facilitates growth in submicromolar concentrations of exogenous heme. Together these data suggest that HRG-2 is involved in heme utilization in the hypodermis. Although HRG-2 can bind heme, as a single pass membrane protein it is unlikely that HRG-2 itself is a heme transporter. However, it may function as on oxidoreductase, which may facilitate heme uptake, similar to how DcytB and Steap3 facilitate iron uptake [26, 27]. Circulating iron is in the Fe(III) oxidation state but is reduced during cellular uptake. A similar oxidation reduction pattern may exist for heme as it is transported between the cytoplasm, intracellular compartments, and extracellular space.

The characterization of heme-responsive genes demonstrates that *C. elegans* has adapted several mechanisms to cope with varying environmental heme availability. However, heme homeostasis is intrinsically linked to metabolism due to the requirement of heme for respiration amongst other metabolic processes. Therefore, cellular heme requirements will vary according to metabolic fluctuations independent of environmental heme availability. One such regulator of metabolism is circadian rhythm [28]. In. *C elegans*, temperature fluctuations are one of the environmental cues that drive circadian rhythm. Many heme-responsive genes, including all the genes discussed above, are transcriptionally regulated during entrained shifts in temperature, indicating that heme homeostasis is in part regulated

by circadian rhythm [29]. In mammals there is a reciprocal relationship between circadian rhythm and heme homeostasis. Two transcription factors involved in mammalian circadian rhythm, Rev-erb alpha and Per2, are regulated by bound heme [30, 31]. In return, the circadian clock controls heme levels through NPAS-2/BMAL1, a core clock component complex, which regulates expression of the first enzyme in the heme biosynthetic pathway, ALAS1. [32]. How such metabolic fluctuations are influenced and integrated with heme availability *in C. elegans* has yet to be elucidated.

It is interesting that the worm has adopted several transcriptional pathways for the upregulation of intestinal genes in low heme. We speculate that each pathway is specific to a particular response. For example, while *mrp-5* depletion results in upregulation of *hrg-1* through the HERE, *hrg-3* is downregulated, suggesting that the HERE is predominately regulated by extraintestinal signals while the regulation of the *hrg-3* promoter is dominated by intestinal heme status. In this model, as *hrg-1* and *mrp-5* both have a HERE, heme mobilization from storage vesicles in the intestine would be released to the extraintestinal tissues for general usage as an initial heme deficiency response, but the directed delivery of heme to embryos would not occur until intestinal heme stores were sufficiently low. These different mechanisms would enable tight control over systemic heme homeostasis and possibly establish a hierarchy of tissue heme distribution under heme limiting conditions. In support of this postulation, RNAi knockdown of *mrp-5* or *hrg-4* results in upregulation of *hrg-1*, but only knockdown of *mrp-5* results in upregulation of *hrg-2*. This suggests that the intestinal heme stores are mobilized prior to the upregulation of heme-responsive

genes in extraintestinal tissues, which are only turned on once systemic heme availability is low. The "sensors", transcription factors or otherwise, that sense and initiate a response to varying heme conditions in each tissue have yet to be elucidated. Uncovering how each tissue senses and communicates heme levels will be crucial to understanding organismal heme homeostasis.

Heme homeostasis in mammals

In mammals, different tissue types have vastly different heme requirements. Erythrocytes have the highest heme requirement and highest synthesis rate due to hemoglobin production [2]. Adult humans have about 25 trillion red blood cells (RBCs), and each second we recycle about 5 million RBCs by erythrophagocytosis (EP) in macrophages of the reticuloendothelial system [6]. Therefore, heme synthesis and degradation must be highly regulated processes that are coordinated between, but also differ in, various cell types. To date, synthesis is the most thoroughly characterized mechanism of regulating cellular heme levels, with most regulatory differences found between red blood cells and other tissues.

Intracellular heme homeostasis

In most eukaryotes and prokaryotes, heme is synthesized via a conserved eight-step pathway. In eukaryotes, the first and last three reactions take place in the mitochondria, while the remainder of the reactions occurs in the cytosol. Disruptions to the heme synthesis pathway can result in the porphyrias, or the toxic accumulation heme precursors [8]. The first step in heme biosynthesis is catalyzed by

11

aminolevulinic acid synthase (ALAS), which synthesizes 5-aminolevulinic acid (ALA) from glycine and succinyl-coenzyme A (succinyl-CoA). The human genome encodes two ALAS genes; ALAS1 is ubiquitously expressed whereas ALAS2 is red blood cell specific. At the transcriptional level, *ALAS2* is upregulated during erythropoiesis through the binding of erythroid-specific transcription factors, such as GATA-1 and NF-E1, to their target sequences in the *ALAS2* promoter [33]. Interestingly, while *ALAS1* is negatively regulated by heme, *ALAS2* is not, which may be expected due to the high demand of heme for hemoglobin production in red blood cells. Rather, *ALAS2* is regulated post-transcriptionally by iron to prevent the accumulation of toxic heme intermediates when there is insufficient iron for heme synthesis [34]. The *ALAS2* transcript contains an iron response element (IRE) in the 5' untranslated region (UTR) which is regulated by the iron regulatory protein (IRP) when under iron deplete conditions, thereby blocking *ALAS2* translation. Sufficient iron results in IRP dissociation from the *ALAS2* 5' UTR to allow translation. Post-transcriptional regulation of *ALAS2* enables erythroid cells to couple heme synthesis with iron availability with more immediate effect than regulation at the transcriptional level.

The second, third, and fourth genes in the heme biosynthetic pathway, *ALAD*, *PBGD*, and *UROS*, all achieve higher expression in erythroid cells compared to other tissues due to erythroid specific promoters [35, 36]. The erythroid specific promoters of *ALAD* and *UROS* bind the erythroid specific transcription factor GATA-1, while the erythroid specific promoter of PBGD binds NF-E1 and NF-E2. The final four

genes, *UROD*, *CPOX*, *PPOX*, and *FECH* all have higher expression in erythroid cells compared to other tissues independent of tissue specific promoters [37-39].

In addition to synthesis, cellular heme levels are mediated by heme oxygenase 1 (HO-1) and heme oxygenase 2 (HO-2) which degrade heme into iron, CO, and biliverdin. Heme itself is a regulator of HO-1 through the heme-binding transcriptional repressor Bach1 [40]. Bach1 heterodimerizes with small Maf proteins to bind MAf Recognition Element (MARE) sequences and repress transcription. MARE sequences are present in the *Hmox1* promoter. In high heme conditions, heme binds Bach1 through four cysteine proline (CP) heme regulatory motifs, resulting in Bach1 transport out of the nucleus, followed by degradation [40-42]. This will result in the Maf proteins forming new heterodimers with p45, the large subunit of the erythroid-specific transcription factor NF-E2. This heterodimer acts as an activator when bound to the MARE. Therefore, Bach1 mediated repression only occurs in low heme conditions. When heme levels are high, negative feedback allows derepression of the MARE and upregulation of HO-1 to degrade excess heme. In addition to HO-1, the locus control region (LCR) of hemoglobin has MARE elements, thereby coupling heme levels to globin chain production [43].

Heme can be regulated not only by cellular levels but by sequestration and transport into and out of vesicles. After EP of senescent erythrocytes by macrophages, heme transport out of the phagolysosome for degradation by HO-1 is mediated by HRG1 [44]. HRG1 localizes to the phagolysosome and depletion of *hrg-1* by siRNA results in lower mRNA expression of *Hmox1, Fpn1,* and reduction in ferritin accumulation following EP, all markers of cellular iron availability.

Interestingly, macrophages also express two heme exporters, FLVCR1 and MRP5. This suggests the possibility that a pool of heme transported by HRG1 out of the phagolysome is exported *in toto* out of the macrophage. HRG1 itself is upregulated by cellular heme, which may in part be Bach1 dependent [45]. In addition to macrophages, HRG1 is expressed in brain, heart, kidney, muscle, placenta and intestine, suggesting a role for HRG1 beyond heme transport out of phagolysosomes [13]. Accordingly, in zebrafish morpholino knockdown of *hrg1* results in anemia, hydrocephalus, and a curved body with shortened yolk tube. Remarkably these phenotypes can be rescued with *C. elegans* HRG1 despite the two proteins sharing only 20% identity. This demonstrates that conserved mechanisms of heme homeostasis exist between the heme auxotroph *C. elegans* and vertebrates that synthesize heme.

Correspondingly, zebrafish MRP5 is essential for normal morphology and hemoglobinization of red blood cells [12]. In mammalian cells MRP5 localizes to both the plasma membrane and to endosomal compartments where it appears to facilitate incorporation of heme into hemoproteins in the secretory pathway. Therefore, in addition to its role in cellular heme export, MRP5 may transport heme from the cytosol to the secretory pathway.

In conjunction with synthesis, degradation, and compartmentalization, cells may be able to regulate heme levels by efflux. Another heme exporter, FLVCR1, has been described which belongs to the major facilitator superfamily. FLVCR1, unlike MRP5, only localizes to the plasma membrane and mediates efflux of ZnMP from rat renal epithelial and hematopoietic K562 cells [46]. Interestingly, FLVCR1 was

shown to be required for erythropoiesis. However, this is likely due to a second, mitochondrial isoform of FLVCR1 (FLVCR1B) which controls mitochondrial heme efflux. Due to an alternative start site, FLVCR1B has a shortened amino terminus with a mitochondrial localization signal [47]. Specific silencing of *Flvcr1b* resulted in termination of erythroid differentiation, while silencing the plasma membrane isoform, *Flvcr1a*, did not affect erythropoiesis but still lead to hemorrhage, edema, and skeletal abnormalities.

Intercellular heme homeostasis

Free heme and heme complexed to hemoglobin is released from mammalian cells into the blood stream in response to disease, inflammation, or intravascular red blood cell hemolysis. Two serum proteins, both related to proteases, have been identified that scavenge heme and hemoglobin to preserve iron and inhibit oxidative stress caused by extracellular heme. Haptoglobin, which is related to S1 proteases and is secreted mainly by hepatocytes, binds free hemoglobin in the plasma with a Kd $\approx 10^{-12}$ M [48, 49]. The haptoglobin-hemoglobin complex is bound by the receptor CD163 and endocytosed by tissue macrophages [50]. The macrophages subsequently degrade the heme to release iron, which will be reutilized by erythroid cells for hemoglobin production [51, 52].

Hemopexin, which is related to matrix metalloproteases and also produced predominately by the liver, binds free heme in the plasma with a Kd $\approx 10^{-13}$ [53]. The hemopexin-heme complex is bound by the LRP1 (CD91) receptor, which is expressed in several cell types, including macrophages, hepatocytes, placental

syncytiotrophoblast, and neurons [54]. When the hemopexin / CD91 complex is endocytosed by the liver, heme is removed and the rest of the complex is recycled [53, 55]. Interestingly, hemopexin has been shown to directly bind FLVCR1 and the presence of hemopexin in cell culture media increased heme export by macrophages more than 100 fold. [16]. Furthermore, cell cultures studies have shown that a portion of heme obtained by macrophages after erythrophagocytosis is transported out of the cell intact [56]. Based on this data, it is possible that hemopexin facilitates the delivery of heme *in toto* from macrophages to the liver. The liver itself has mechanisms for heme import, as patients with acute porphyria who are administered intravenous heme complexed to albumin show increased heme-dependent enzyme activity in the liver [57].

Recently, Haldar *et. al* showed that during hemolysis, heme from senescent red blood cells serves as a signal for monocytes to differentiate into macrophages through regulation of SPI-C [17]. The transcription factor SPI-C is expressed in splenic red pulp macrophages and is required for their development. The heme-induced expression of *Spic* is through derepression of Bach1, indicating that heme from erythrocytes must be transported into the nucleus of monocytes. These results predict that a portion of heme that crosses the phagolysosomal membrane after EP is not immediately degraded by heme oxygenase but must remain intact for function, implicating that the intertissue transport of heme is essential for cellular differentiation.

In addition to macrophage EP of red blood cells, another major source of heme is the intestine. Although most dietary heme is postulated to be degraded by

enterocytes and utilized for iron, evidence exists that some heme may be directly exported from the intestinal basolateral membrane [58-60]. Interestingly, studies in Caco2 cells have demonstrated that a portion of heme remains intact and is transported from the basolateral membrane out of the cell [61]. Therefore, a percentage of dietary heme may be distributed to peripheral tissues intact.

Similar to HRG-3 in *C. elegans*, there may be specific pathways for maternal fetal heme transfer in vertebrates. Zebrafish defective in heme synthesis survive 10-25 days post-fertilization [62]. Due to the high energy demands of a developing embryo, this suggests a possible maternal heme contribution. Along these lines, FLVCR1 expression in human placenta is correlated with LRP1 expression and neonatal iron status. Moreover, HRG-1 is expressed in the placenta [13]. Therefore, the placenta expresses the necessary transporters for heme import from maternal blood and heme export to the fetus, which may become a significant source of iron during development [15, 16].

There is also evidence for heme uptake in neurons. Neurons require heme for respiration, growth, and differentiation, and both heme depletion and accumulation have been linked to neurodegeneration [63]. Therefore neuronal heme levels must be tightly controlled, and evidence suggests that this may in be part accomplished through intertissue heme transfer. In chicken dorsal root ganglion cultures treated with ALA, only the Schwann cells and macrophages showed fluorescence from heme biosynthesis intermediates despite all three cell types taking up ALA, suggesting the heme synthesis pathway in neurons was less active [64]. Due to their high consumption of oxygen and therefore reliance on mitochondrial cytochrome activity,

it is unlikely that neurons simply require less heme. Additionally, premature

senescence of heme depleted neurons can be rescued by exogenous heme, and they

can endocytose hemopexin-heme complexes, indicating that neurons can import heme

[65-67]. Interestingly, the brain itself expresses hemopexin and FLVCR1, and

depletion of *hrg1* in zebrafish embryos results in a defect in hindbrain-midbrain

formation [13, 46, 68]   These results hint at the intriguing possibility that neurons

may in part regulate heme levels by intertissue trafficking.

Taken together, these studies indicate that intertissue heme transport may not

just be limited to obligate heme auxotrophs. However, more research is required to

understand to what extent heme transfer between cells is required compared to iron

transfer for cell-autonomous heme synthesis. Direct heme transfer between cells may

become more relevant under specific conditions, such as low iron availability or

pathogenesis.

The brain – gut axis

The bilateral communication between the central nervous system and the

gastrointestinal system, referred to as the brain-gut axis, plays a key role in metazoan

homeostasis. In mammals, both sugar and lipid sensing in the gut, through

enteroendocrine cells (EECs) and I cells, can stimulate the central nervous system

through neuropeptides and peptide hormones [69-71]. Direct neuronal connections

are also maintained between central nervous system and the enteric nervous system

through the vagus nerve. The close relationship between nervous system and gut is

conserved across phyla. Carbohydrate homeostasis in *Drosophila* involves brain

suppression of sugar intake, while in *C. elegans* metabolism and energy balance,

development, and stress are all regulated on a systemic level through communication between the nervous system and intestine [72-76]. Furthermore, the *C. elegans* intestine has endocrine function and has been shown to directly communicate with the nervous system via a secreted neuropeptide to regulate the defecation cycle [77]. The enteric nervous system and communication between the intestine and brain will be discussed in further detail below.

The enteric nervous system

In the early twentieth century, Byron Robinson, MD, described a second brain in the abdomen which he believed was just as important as the cranial brain [78]. Robinson hypothesized that the abdominal brain presided over nutrition and was in fact the center of life itself. Today we refer to this "second brain" as the enteric nervous system (ENS). The ENS is found throughout the animal kingdom, including invertebrates such as insects and mollusks [79]. In fact, it has been hypothesized that the ganglia which compose the primitive brain of helminths evolved from gut circuits [69]. The ENS is derived from neural crest cells and is composed of about 100 million neurons, or about as many as the spinal cord, that are divided into eighteen functional classes [80]. It is arranged into two concentric plexuses, the outer myenteric, or Auberbachs plexus, and the inner submucosal, or Meissner's plexus. The ENS receives mechanical and chemical information from the gut lumen via intrinsic primary afferent neurons (IPANS) that innervate the intestine, and functions such as intestinal motility, absorption, secretion, and blood flow are carried out by efferent motor neurons. Although communication between the central nervous system,

especially the hypothalamus and the nucleus tractus solitarii (NTS), are maintained

through the vagus nerve, the ENS continues to function when this nerve is severed,

indicating that the ENS can function autonomously [81, 82].

Neuropathology of the ENS usually results in impaired gut function [80]. The

most recognized neuropathy is Hirschsprung's disease (HSCR), which is a congenital

disorder resulting from the absence of ganglia [83]. Several genes have been

implicated in HSCR, including *RET* and *EDNRB*, which are both involved in neural

crest cell migration [84]. Another gene involved in the development of the ENS,

neuregulin 3 of the epidermal growth factor (EGF) family, has also been implicated

in HSCR [85]. It has also been suggested that the pathology associated with

enterocolitis and Crohn's disease, an immune disease, may develop in part due to loss

of glial cells associated with the ENS. Of note, dominant neurovisceral porphyrias

can be inherited with HSCR and other ENS pathologies [86, 87]. Similarly, carbon

monoxide signaling impairment due to a lack of HO-2 has also been linked HSCR

[88, 89]. These studies indicate there is an interconnection between heme metabolism

and ENS function which warrants further investigation.

Gut to Brain signaling

As the largest interface between the environment and our bodies, the

gastrointestinal tract has an integral role in homeostasis and must be able to

communicate with the master regulator, the central nervous system. Additionally, the

gut has by far the largest population of commensal organisms of all the body surfaces,

with 100 trillion microorganisms from 40 thousand species inhabiting the

gastrointestinal tract [90]. It is becoming clear how important these microorganisms are in the function of the brain-gut axis [91]. Accordingly, two thirds of the body's immune cells are found within the gut. Moreover, the gut has thousands of endocrine cells that produce at least 20 different hormones. The gut can communicate with the brain through three main mechanisms: through the nervous system, through immune cells, and through EECs.

Signaling from the gut to the brain through the nervous system begins with intrinsic primary afferent neurons. These neurons do not receive luminal signals directly but from endocrine or immune cells [92]. Extrinsic afferent neurons from the vagus nerve and spinal cord also have connections in the gut. Specific populations of these extrinsic primary afferents synapse with dorsal horn neurons in the spinal dorsal horn or with cell bodies in the vagal NTS. These connections provide the brain with a wide range of gut-related information. While most intestinal function is regulated by IPAN and efferent motor neuron reflex loops within the ENS, gastric function is mediated through vagal reflexes.

Endocrine cells in the gut constitute the largest endocrine organ in the body. As previously mentioned, endocrine signaling can function through the ENS. However, signals initiated from EECs can also directly communicate to vagal afferents and to the hypothalamus. Activation of EECs can take place through several mechanisms, including mechanosensitive cation channels and various macronutrient receptors. In fact, several nutrient receptors that are expressed on the tongue are also expressed in the intestinal EECs, including the sugar receptors T1R2 /TR13. When these receptors are activated by sugars, the EECs secrete GLP-1 and GIP that target

the brain (hypothalamus) and pancreas, resulting in altered feeding behavior and increased insulin secretion [76]. Here, environmental probing by the gut results in systemic sugar homeostasis through the coordination of endocrine and nervous system signaling.

The enteric immune system is presented with a unique challenge: Tolerance of commensal bacteria but response to pathogens [93]. It is thought that commensal bacteria are recognized by EICs and don't elicit an immune response. When pathogens are encountered, microfold cells deliver antigens, through transcytosis, to antigen processing cells within Peyer's patches to elicit an immune response. Vagal afferents located near EICs respond to several signaling factors, including proteases, histamine, serotonin and corticotropin releasing factor [94]. Remarkably, gut microbiota may play an integral role in neurodevelopment, especially during childhood and adolescence [95]. Perturbations of microbiota during these time periods have the potential to disrupt the brain-gut axis and increase the risk of neurological disorders. In addition to the immune response and signaling to the nervous system, immune cells can also influence EEC function.

Brain to gut signaling

The brain can communicate with the viscera through parallel pathways, including the autonomic nervous system (ANS) and the hypothalamus **(Figure 1.2)** [69]. Although the ANS input is triggered by reflexes originating from the ENS, it can be overridden by the central nervous system [96, 97]. Prolonged alterations to the ANS may results in perturbed gut to brain signaling and anxiety disorders. Both

Figure 1.2: Reflex circuits of the brain-gut axis

Both top-down (brain to gut) and bottom up (gut to brain) environmentally stimulated responses optimize homeostatic regulation of intestinal function. Blue boxes are neuron types, yellow boxes are location. Anterior cingulate cortex (ACC), nucleus tractus solitarius (NTS), dorsal motor nucleus of vagus (DMNV). The NTS and DMNV make up the dorsal vagal complex (DVC). A1, A2 and A5 are medullary catecholaminergic nuclei to autonomic effector regions in the rostro–ventro–lateral medulla (RVLM) and ventromedial medulla (VMM). Periaqueductal grey (PAG), prefrontal cortex (PFC), the insula (INS), autonomic nervous system (ANS). Image adapted from [69]
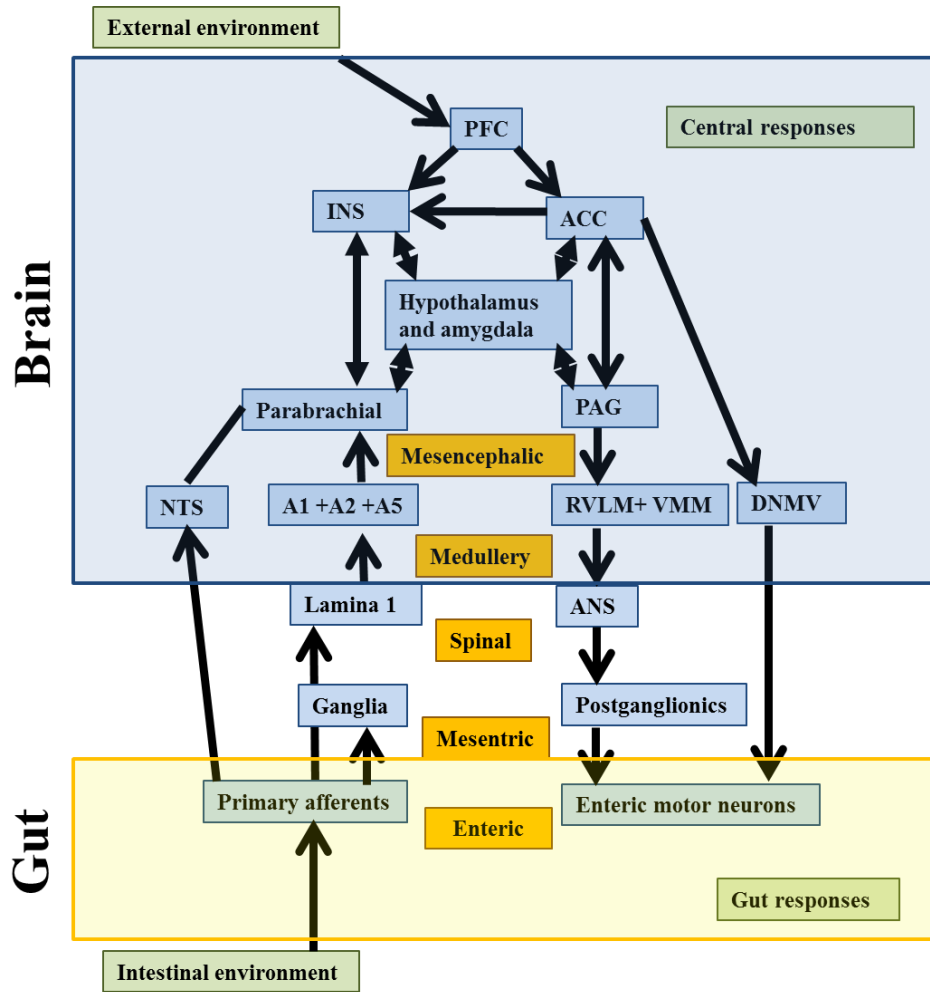
the sympathetic and parasympathetic divisions of the ANS provide feedback to the gut. The overall effect of sympathetic signaling to the gut is inhibitory, slowing transit and secretion. In addition to modulating endocrine and motor function, another subset of sympathetic postganglionic neurons are involved in mucosal immune modulation, including modulation of Peyer's patches. Parasympathetic innervation of the gastrointestinal tract includes vagal and sacral division, and, as mentioned previously the vagal input is crucial for gastric function through both motor neurons and endocrine cells. Top-down engagement from both sympathetic and parasympathetic postganglionic neurons influence emotion-related changes in motor, secretory and immune activity in the gastrointestinal tract [97].

Much of the focus on CNS control of nutrient homeostasis has been on satiety in response to signals such as leptin, ghrelin, insulin, peptide YY, cholecystokinin, and GLP-1 from the viscera [98, 99]. The hypothalamus, which receives both neural and endocrine signals, is particularly important to the satiety response. Feedback from the viscera initiates a neurotransmitter cascade within the hypothalamus. The cascade begins with neurons that produce neuropeptide Y (NPY) or agouti-related peptide (AgRP) and ends with neurons producing appetite stimulating neuropeptides melanin concentrating hormone (MCH) and orexin or the appetite suppressing neuropeptide corticotropin releasing hormone (CRH) to alter feeding behavior [100].

Proteases

A protease is an enzyme that can disrupt the peptide bond between amino acids through hydrolysis. The human genome contains over 1200 proteases or

protease homologs, which can be grouped into four broad classes based on the catalytic residues of the active site: serine/threonine proteases, metalloproteases, aspartic acid proteases, and cysteine proteases **(Figure 1.3)** [101]. Some organisms also express asparagine and glutamic acid proteases.

Proteases are involved in a wide array of functions, ranging from general turnover to signaling through activation of a specific substrate. They are often synthesized as zymogens which require propeptide removal before becoming active. Many also have a signal peptide for entry into the secretory pathway upon translation. The four major classes of proteases will be discussed, as will protease signaling and proteases in parasitic organisms.

Classes of proteases

Mammalian aspartic proteases can be divided into two clans: AA (families A1, A2, A28, A33) and AD (family A22). The A1 family has been the most extensively studied and includes pepsin, renin, cathepsin D and cathepsin E. Most studies of the A22 family have focused on prenesilin, due to its purported role in familial Alzheimer's disease [103]. Aspartic acid proteases utilize a catalytic dyad of two aspartic acids for proteolysis, and are typically active at low pH. In general, low pH induces activation through autocatalysis of the propeptide. Examples of autoactivation include pepsin in the stomach and cathepsin D in the lysosome. A notable exception is renin, which requires trans-activation by another protease. Many aspartic acid proteases are secreted, however cathepsin D is mainly lysosomal; cathepsin E is in non-lysosomal compartments or associates with the inner leaflet of

Figure 1.3: The active sites of the four major classes of proteases

A) Serine proteases use a catalytic triad of histidine, serine and aspartic acid. The histidine, with the aid of the proton-withdrawing aspartate, deprotonates the serine hydroxyl, enabling nucleophilic attack on the substrate carbonyl carbon. **B)** Cysteine proteases employ a similar mechanism as serine proteases, but the nucleophile is the sulphur atom of a cysteine residue. **C)** Aspartic proteases utilize two aspartic acid residues that act in a general acid–base mechanism. A water molecule coordinated between the aspartic acids is activated by the abstraction of a proton, enabling the polarized water to attack the carbonyl carbon of the substrate's scissile bond. **D)** Metalloproteases utilize a coordinated metal, typically zinc, in their catalytic mechanism. In many soluble metalloproteases, such as thermolysin and the matrix metalloproteases, coordination is accomplished by three histidines, or two histidines and an acidic side chain. A water molecule serving as an additional zinc ligand is hydrogen-bonded to a glutamate, which abstracts a proton from the attacking water molecule. Red arrows indicate movement of electron pairs. Blue dotted lines represent hydrogen bonds or other electrostatic interactions. Grey lines represent the continuation of the substrate polypeptide to either side of the peptide bond that is represented explicitly. Adapted from [102].
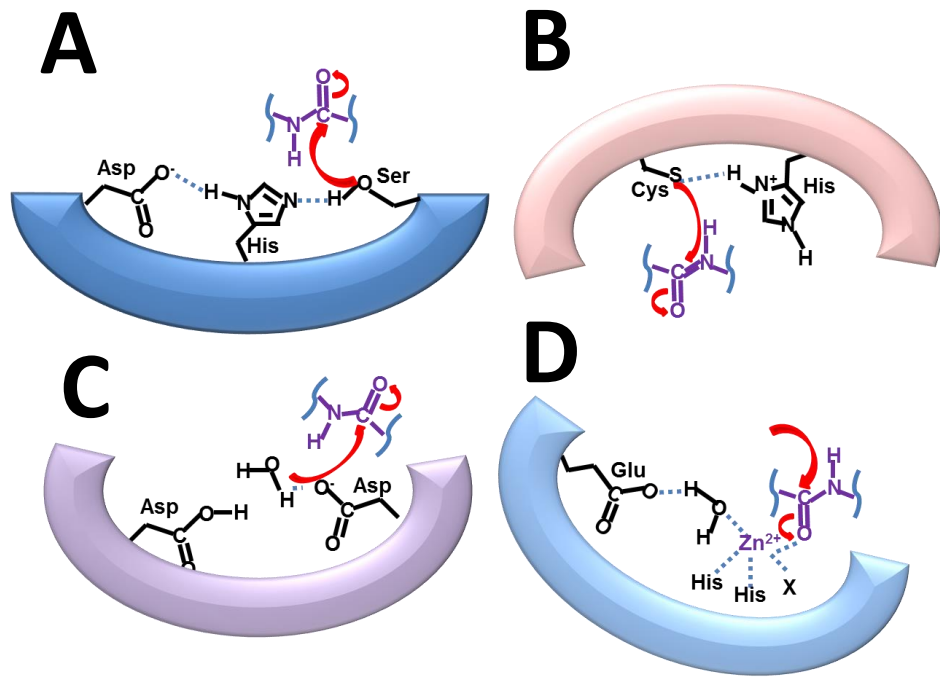
the plasma membrane depending on cell type; and presenilin is membrane-bound [104-106]. The active site specificity of these proteases can vary depending on function. Pepsin and cathepsin D, which are involved in digestion and protein turnover, respectively, require broad specificity due to the variety of substrates encountered [107]. Renin, in contrast, is involved specifically in regulation of systemic blood pressure, and is only known to cleave angiotensinogen at a single leucine- valine bond [108].

Mammals have several families of cysteine proteases, with the most extensively studied being the cathepsins (family C1) and calpains (family C2) of clan CA and the caspases (family C14) of clan CD. Cysteine proteases use a catalytic dyad of a cysteine and histidine residue for proteolysis.

Caspases have been studied in detail due to their key role in apoptosis. As mediators of cell death, they lack a signal peptide and are not translocated to the secretory pathway, but rather members are present in the cytosol, mitochondria, and nucleus [109]. They can be divided into two classes: initiator caspases and effector caspases. Initiator caspases are activated by increased mitochondrial permeability, TNF alpha signaling from macrophages, and Fas signaling from T lymphocytes [110, 111]. Once activated, initiator caspases activate effector caspases by catalytic removal of effector propeptides. Subsequently, effector caspases then cleave effector proteins such as lamins, which will result in apoptotic cell death.

The majority of cathepsins are C1 proteases, with include cathepsin B, cathepsin L, and cathepsin K. There are two known types of endogenous inhibitors of this family of peptidases: cystatins and cytotoxic T-lymphocyte associated protein 2

(CTLA-2), which allow the regulation of activated proteases. Cathepsin K, a secreted cathepsin, plays a critical role in bone resorption under calcium limiting-conditions [112]. Cathepsin L was traditionally thought be to be involved in general protein turnover within the lysosome, although it may also have more specific roles such as neuropeptide processing [113]. Cathepsin B is unique in that it can serve as both an endopeptidase and peptidyldipeptidase peptidase (removal of a carboxyl terminal dipeptide), which is attributed to the presence of a 20 amino acid insert called the occluding loop [114]. It has been suggested that the occluding loop blocks the active site of cathepsin B at low pH, resulting in the enzyme now functioning as a dipeptidase. However, at basic or neutral pH, the loop is displaced, resulting in cathepsin B functioning as an endopeptidase [115]. Cathepsin B usually resides in the acidic lysosome, suggesting that it functions primarily as a dipeptidase. In support of this, cathepsin B knockout mice do not have protein turnover defects, although this is likely, at least in part, due to functional redundancies with other proteases [116].

The calpains are a family of calcium-dependent proteases that are mainly resident in the cytosol, and therefore, like caspases, do not have signal peptides. They are not involved in degradation but selectively respond to calcium signaling. An example is the cleavage of cytoskeletal proteins to facilitate cell migration [117, 118].

Serine proteases play pivotal roles in many mammalian processes, including blood coagulation and digestion. Serine proteases typically have a catalytic triad consisting of a serine, histidine, and aspartic acid. The majority of serine proteases in mammals, and in fact the largest protease family overall, are the trypsin-like S1

30

proteases [107]. Members include trypsin, cathepsin G, and the membrane-bound matriptases. Many S1 proteases are secreted and thus have a signal peptide on the amino terminus, followed by a propeptide, or amino terminal extension. In blood coagulation proteases such as plasmin and thrombin, the amino terminal extension contains other domains, including Kringle domains, which are important for mediating the protein-protein interactions between blood coagulation factors [119]. Activation of these proteases requires cleavage of the amino terminal extension, which nonetheless remains bound via disulfide bridges serving as the heavy chain subunit of the protease [120]. The exposure of the new amino terminus after cleavage initiates a structural rearrangement, in which the newly exposed amino terminus binds to the aspartic acid within the active site. Endogenous serpins inhibit S1 proteases. Other notable serine proteases include signal peptidase (family S26), furin (family S8), the rhomboid proteases (family S54), and serine carboxypeptidase A, also called cathepsin A (family S10).

Metalloproteases are the most diverse class of proteases. Most of these proteases utilize a zinc ion coordinated by two or three histidines and a glutamic acid in the active site. Cobalt is occasionally used instead of zinc. Metalloproteases are placed in groups according to the primary structure of their catalytic sites and include the gluzincins, metzincins, inuzincins, carboxypeptidases, and DD carboxypeptidases [121]. The metzincin subgroup (mainly clan MA) is further divided into serralysins (family M10), astacins and adamalysins (family M12), and matrixins (family M10) [122]. The latter two families have been the described in detail as they comprise the ADAMs and matrix metalloproteases (MMPs), respectively. The ADAMs mainly

function as sheddases, cleaving cell membrane proteins for signaling and turnover [123]. MMPs are involved in matrix remodeling through cleavage of extracellular matrix proteins, but function in other processes as well [124]. Both of these families utilize three histidines for zinc coordination and a catalytic glutamic acid. In addition to the metalloprotease domain, ADAM family members have EGF domains, cysteine rich domains, and disintegrin domains which likely assist in substrate specificity and activity [125]. MMPs have fibronectin II-like and hemopexin-like domains, which may help these proteins bind to the extracellular matrix.

Protease signaling

Although once assumed to be mainly involved in general protein turnover, it is becoming clear that proteases are essential for a number of biological processes, including a crucial role in cell signaling. Each of the main classes of proteases have active members or related pseudoproteases that are involved in cell signaling. Their role in signaling varies from receptor processing to acting directly as a ligand. Protease signaling often involves cascades involving multiple cleavages of a single substrate, or proteases that act as substrates for each other, providing added levels of regulation [126]. Protease signaling mediates several essential physiological processes, including blood pressure, iron homeostasis, and the inflammatory response, which will be discussed below.

Serine proteases have an abundant and diverse role in protease and pseudoprotease signaling in mammals. Furin is a convertase responsible for activating a variety of substrates through propeptide removal. Substrates include

signaling ligands such as TGFβ and parathyroid hormone, but also other proteases which can in turn effect signaling [127]. One target of furin is TACE, or ADAM metalloprotease-17. Furin processing of TACE occurs in the Golgi apparatus, and then TACE traffics to the plasma membrane where it facilitates TNFα shedding to initiate an inflammatory response [128]. Remarkably, TACE trafficking from the ER to Golgi requires chaperone activity from a proteolytically inactive rhomboid protease homolog, or pseudoprotease, iRhomb2 [129]. In the absence of iRhomb2, TACE remains as a zymogen trapped in the ER, ultimately resulting in failure to promote inflammation. This singular signaling event requires the coordinated actions of a metalloprotease, a serine protease, and a serine pseudoprotease. TACE is also involved in Notch signaling, although the requirement for iRhomb2 has not been established [130].

Systemic iron homeostasis is regulated by the hormone hepcidin, which is secreted from the liver when high iron is sensed. Hepcidin binds to ferroportin on the basolateral membrane of the intestine, liver and macrophages, leading to ferroportin degradation and less circulating iron. Hepcidin is positively regulated by BMP6 signaling through an iron specific BMP co-receptor called hemojuvelin. In low iron, a serine protease called TMPRSS6 (matriptase-2) is upregulated and degrades hemojuvelin, resulting in less BMP signaling and ultimately less hepcidin production, thereby allowing more iron release into circulation [131].

One of the most extensively studied examples of protease signaling is regulation of the renin-angiotensin system (RAS) by the aspartic acid protease renin. The RAS system is stimulated by a decrease in blood pressure, which results in active

renin secretion from the kidney [132]. Renin activation requires a trans-acting protease, and although the cysteine protease cathepsin B has been implicated in this process, this remains controversial [133, 134]. Circulating, active renin cleaves angiotensinogen, an α-2 globulin that functions as a hormone, secreted by the liver to produce angiotensin I. A second cleavage event by the protease angiotensin-converting-enzyme (ACE), results in active angiotensin II. Through the angiotensin II receptors, which are G-coupled protein receptors, angiotensin II induces changes in adipose, cardiac, central nervous system, adrenal gland, and kidney function to regulate systemic blood pressure [135-137]. In addition to blood pressure regulation through angiotensin, a (pro)renin receptor, the first receptor identified for an aspartic protease, has been described. The (pro)renin receptor binds pro-renin at the cell surface, resulting in active renin through a conformational change. Pro-renin or renin binding also induces activation of MAP kinases ERK1 and ERK2 [138]. However, this receptor has also been implicated in WNT signaling and vacuolar ATPase activity, and there is still much debate about its actual physiological role [139].

In addition to modulating signaling indirectly through regulation of ligands and receptors, proteases and pseudoproteases can act directly as receptor ligands. An example is S1 serine protease signaling through the protease activated receptors (PARs). PARs are G-coupled receptors that when activated, result in several downstream functions such as platelet aggregation, cell growth and division, and neuron survival [140]. PARs are unique in that rather than activation through ligand binding, activation occurs through processing of an exoplasmic amino terminus by serine proteases such as trypsin and thrombin, which results in activation. There are

four PARs (PAR1-PAR4). PAR1, -3, and -4 are activated by thrombin, while PAR-2 is primarily activated by trypsin [141]. PAR4 can also be activated by trypsin and cathepsin G. The cleavage of PARs at various peptide bonds by different proteases allows biased signaling in a context specific manner.

Pseudoproteases

It is becoming apparent that pseudoproteases play an important biological role. Two well described signaling ligands, hepatocyte growth factor (HGF) and sonic hedgehog (Shh), are pseudoproteases. HGF signaling is initiated when HGF binds the tyrosine kinase receptor Met, which results in processes such as cell proliferation and motility [142]. HGF is an S1 family pseudoprotease. Like plasmin, HGF has Kringle domains in the propeptide which is cleaved but remains attached to the light chain by disulfide bridges [142]. This processing is necessary for signaling. Although not a protease, the active site pocket is required for function. Perhaps telling, the aspartic acid, which is necessary for active serine proteases to undergo a conformational change, is conserved. Shh signaling is another example of a pseudoprotease functioning as a receptor ligand. Shh signaling is critical for normal development. Shh is a hybrid of two proteases, with a catalytically active carboxyl terminus and inactive amino terminus. Activation of Shh requires autocatalytic activity of the carboxyl terminal portion of the protein, which is similar to family C46 cysteine proteases. The amino terminal portion of the protein is then esterified and palmitoylated. Both lipid modifications are necessary for normal signaling [143]. The amino terminal portion of the protein is similar to M15 metalloproteases, and in

fact coordinates a zinc ion and has conserved catalytic residues. However, the active site is not required for signaling, as mutation of both the active site histidine and glutamic acid do not result in loss-of-signaling function. Rather, conserved surface residues outside and partly on the edge of the pseudo-active site groove lead to reduced binding to Shh receptor Ptc1 and diminished hedgehog signaling [144]. Unlike serine proteases that act as ligands through proteolytic activity, Shh acts as a ligand strictly through receptor binding.

Parasitic proteases

Proteases have been studied in parasites, from single cell pathogens to multicellular helminthic worms, for a variety of reasons. They are essential for parasite host invasion through tissue digestion and penetration, nutrient acquisition, and evasion of host immune responses. They make attractive drug targets as most families have described inhibitors. In worms, many are glycosylated and expressed in the intestine, making them possible targets for antibody therapy.

Blood-feeding parasites rely on hemoglobin as a source of nutrition, not only for amino acids, but likely heme as well. Like *C. elegans*, helminthic worms are heme auxotrophs, and therefore rely on host heme for survival. In the hookworm *Ancylostoma caninum*, an ordered proteolytic cascade involving a cathepsin D-like aspartic protease (ARP-1), a cathepsin B-like cysteine protease (CP-2), and a metalloprotease (MEP-1) is involved in hemoglobin digestion and utilization. Although the ARP-1 and CP-2 can cleave native hemoglobin, MEP-1 requires initial proteolysis by ARP-1 and CP-2 [145]. Additionally, ARP-1 from the human

hookworm *Necator americanus* can cleave native hemoglobin, whereas CP-2 requires initial cleavage by ARP-1 [146]. Interestingly, ARP-1 contributes to host specificity in hookworms, as ARP-1 from *A. caninum* cannot cleave human hemoglobin while *N. americanus* ARP-1 cannot cleave canine hemoglobin. Furthermore, inactivation of a single class of enzymes in these parasites prevents growth using hemoglobin as a nutrient source, suggesting an ordered, rather than parallel cleavage with an aspartic protease being the initiator of the cascade. Similar cascades are used by the nematode *Haemonchus contortus* [147]. *Plasmomidum* have also been shown to utilize a cascade that is initialized by an aspartic protease preceding a cysteine protease, followed by a metalloprotease, and ending with an exopeptidase for digestion into amino acids [148]. Therefore, it is likely that an aspartic-cysteine-metalloprotease cascade is conserved across blood-feeding phyla.

Proteases play an important role in helminthic skin penetration and tissue invasion. L3 infective larvae of *A. caninum* have been shown to secrete a metalloprotease which degrades gelatin, collagen, laminin, and fibronectin. Similarly, *N. americanus* larvae in the infectious stage secrete metalloproteases that degrade collagen and elastin. However, since pepstatin also inhibited invasion, an aspartic protease must also be involved [149]. In the trematode *Schistosoma mansoni*, the infective cercarial larvae utilize a serine protease similar to elastase for skin penetration and tissue invasion [150]. Furthermore, this protease may also play a role in host immune evasion as it can cleave human complement proteins and IgE [151]. The trematode *Fasciola hepatica* is a food borne pathogen that penetrates the intestinal wall, the liver capsule, and eventually enters the bile ducts where larvae

mature into adults. At 21 days of age when the worms are penetrating host tissue,

they specifically upregulate cathepsin L-like cysteine proteases. Accordingly, it was

shown that cysteine protease activity was important for gut penetration [152, 153].

Like helminths, the kinetoplastid parasites *Leishmania* and *Trypanosoma*

utilize proteases for host invasion. During the promastigote stage in the gut of the

sandfly, a metalloprotease called GP63 (family M8) on the *Leishmania* cell surface

accounts for 1% of total promastigote protein. GP63 has been implicated in host

immune evasion, phagocytosis into macrophages, and survival of the intracellular

amastigotes within macrophages [154]. *Leishmania* also express several cysteine

proteases, primarily in amastigotes. A cathepsin L-like cysteine protease, CPB, was

shown to be important for infection and virulence in mice [155]. Serine proteases

have also been implicated in *Leishmania* survival and virulence [156, 157].

Similarly, metalloprotease, serine protease, and cysteine protease activity have been

shown to be important for *Trypanosoma cruzi* virulence, with the latter also

important for *T. brucei* virulence [154, 158, 159].

Clearly proteases play an essential role in parasite metabolism and host

invasion. However, the mechanisms and the full extent to which they are required

have yet to be elucidated. In addition to degradation of host tissue for invasion and

nutrients, parasite proteases can alter host signaling for their own benefit. An

interesting interaction occurs between the parasitoid wasp *Cotesia congregata* and its

hornworm host *Manduca sexta*. The wasp coinjects the symbiotic virus, *C.

congregata Bracovirus*, long with fertilized eggs into the host. The virus is essential

for the parasitic success of the wasp because it expresses high levels of cystatins in

host tissue, which inhibits host cysteine proteases [160]. However, it is not known how these host proteases defend against parasitism. Understanding these basic biological interactions between host and parasite will be important for the development of effective drugs that target parasite proteases.

Problem Statement

Heme is required as a prosthetic group in proteins by most living organisms. Although heme levels can be regulated within each cell by heme synthesis and degradation, evidence exists that heme can also be transported *in toto* between cells. However, the pathways for the directed movement of heme between cells remain poorly defined due to interference from heme synthesis. To uncover these pathways, we have taken advantage of the nematode *C. elegans*, which is a heme auxotroph and thus relies on dietary heme to fulfill its heme requirements. To maintain a balance between heme uptake, availability, and storage we hypothesize that bidirectional signaling must exist between the intestine and extraintestinal tissues to control systemic heme homeostasis. We show that the protease homologs, HRG-7 and HRG-8, are secreted from the intestine and localize to neurons. Depletion of either gene results in an intestinal heme deficiency signal, suggesting a neuron to intestine feedback. The neurons regulate systemic heme levels by signaling to the intestine through the bone morphogenic protein homolog, DBL-1. Remarkably, depletion of HRG-7 and DBL-1 simultaneously results in an enhanced heme deficiency signal and growth phenotype, indicating that the neuron-gut axis is critical for maintaining systemic heme homeostasis.

Chapter 2: Materials and Methods

C. elegans **culture**

Worms were maintained in axenic liquid mCeHR2 medium supplemented with 20 μM heme with continuous shaking or on nematode growth medium (NGM) plates seeded with OP50 bacteria at 15°C. NGM plates contained 3 g/L NaCl, 2.5 g/L peptone, 20 g/L agar, 5 mg/L cholesterol, 0.1 M CaCl2, 0.1 M MgSO4, and 25 mM KH2PO4. [161-163]

Synchronization of *C. elegans*

Worms were collected from plates with M9 buffer (86 mM NaCl, 42 mM Na2HPO4, 22 mM KH2PO4, and 1 mM MgSO4), washed three times to remove bacteria, then resuspended in 0.1 M NaCl. Worms from liquid mCeHR-2 medium were harvested by centrifugation at 800 x g for 5 minutes, and then resuspended in 0.1 M NaCl. Gravid worms were allowed to settle on ice for 5 minutes. The supernatant was aspirated and remaining worms were bleached using a 1.1% sodium hypochlorite and 0.55 M NaOH solution. After 5 minutes, embryos were released from adult worms and the mixture was centrifuged (800 x g, 1 minute) and washed twice with sterile water. Embryos were suspended in M9 buffer and allowed to hatch overnight.

Worm strains

Worms strains used in this study are listed in Appendix I. N2, BW1496, RW10745, and VH624 were obtained from the *Caenorhabditis* Genetics Center (CGC, USA).

VC1478 was a kind gift from Dr. Yun Zhang at Harvard University. Strains IQ6011,

IQ8031, and IQ8333 were previously generated in the lab. All other strains were

generated in this study.

Restriction enzyme cloning

The *P$_{hrg-7}$::GFP* and *P$_{hrg-8}$::GFP* transcriptional fusion constructs were generated by

restriction enzyme cloning into Fire vector pPD95.67. For *hrg-7*, 0.7 kb of the 5'

flanking region was digested with HindIII and BamHI, and then ligated into the

multiple cloning sequence (MCS) of pPD95.67. For *hrg-8*, 2 kb of the 5' flanking

region was digested with HindIII and XbaI and then ligated into the pPD95.67 MCS.

Gateway cloning

All constructs apart from the *hrg-7* and *hrg-8* transcriptional reporters were generated

using Multisite Gateway recombination (Invitrogen). Promoters, coding regions, and

3' untranslated regions were amplified with sequence-specific Gateway attB primers.

PCR products were first recombined into donor plasmids, and then three donor

plasmids were recombined into expression plasmids, according to the manufacturer's

instructions (Invitrogen).

Generation of transgenic worms

Reporter constructs mixed in a 2:1 ratio with the *unc-119* rescue construct (18 µg

total DNA), were introduced into *unc-119(ed-3)* worms by microparticle

bombardment using the PDS-1000 particle delivery system (Bio-Rad). Transgenic

lines were isolated after two weeks.

Single worm PCR

For single worm PCR, worms were lysed in lysis buffer (50 mM KCl, 10 mM Tris-

HCl, 2.5 mM MgCl2, 0.45% NP-40, 0.45% Tween-20, 0.01% gelatin, 1 mg/ml

proteinase K) by incubation for 2 hours at -80°C, 1 hour at 65°C, and 30 min at 95°C.

Worm lysates were added to PCR reactions with primers to detect wild-type and

mutant alleles. Genotyping primers for *dbl-1(nk3)* and *lin-15b(nk3)* are listed in

Appendix II. For *lin-15b* genotyping, PCR product was purified with the Nucleospin

PCR cleanup kit (Macherey-Nagel) and digested overnight with restriction enzyme

BccI. PCR product amplified from *lin-15b(n744)* mutation yielded fragments of 200

and 300 bp after digestion. PCR product from wild type *lin-15b* remained as a single

band of 500 bp.

RNA Interference by feeding

RNAi experiments were performed by feeding worms the RNase III-deficient bacteria

HT115(*DE3*) expressing double-stranded RNA (dsRNA) complimentary to the gene

of interest. dsRNA expression was induced by seeding bacteria on NGM plates

containing 2 mM isopropyl-β-D-thioglactopyranoside (IPTG), 50 μg/mL

carbenicillin, and 12 μg/mL tetracycline. For the genome-wide RNAi screen,

bacterial cultures of clones from the Ahringer and Vidal RNAi libraries were grown

for 5.5 hours in LB containing 50 μg/mL carbenicillin, 12 μg/mL tetracycline, and 5

μM or 25 μM heme before seeding onto 12 well RNAi plates [164, 165]. Plates were

left at room temperature overnight for dsRNA induction. Forty L1 larvae from strain

IQ6011 which had been grown in liquid media supplemented with 10 μM heme for

five days were added to each well of the 12-well plates. Each 12-well plate had 10

wells seeded with experimental clones and one well seeded with each of the control

clones, vector and *hrg-4*. The plates were incubated at 15°C overnight then moved to

20°C for three additional days. The GFP levels in gravid adults were observed

visually using a Leica Microsystems MZ16FA stereoscope. The intensity and pattern

of GFP in gravid worms feeding on bacteria producing dsRNA against each library

clone was compared to the intensity and pattern of GFP in same-stage worms feeding

on bacteria transformed with the empty vector. For evaluating the function of HRG-

7^{PR} and HRG-8^{PR} transgenes, RNAi clones were grown with 10 μM heme. All clones

were taken from the RNAi libraries except for *hrg-7^{300bp}*, which was generated by

ligating the first 300bp of *hrg-7* into the L4440 plasmid (Fire Vector Kit, Addgene)

and transforming into HT115(*DE3*) bacteria.

RNA Interference by injection

dsRNA was prepared using the Megascript T7 transcription kit (Ambion) according

the manufactures instructions. dsRNA was amplified from *hrg-7* ORF and from the

MCS sequence of pL4440 as a control. dsRNA was injected at a concentration of 200

ng /μl into strain IQ6916 P0 adults. After injections, P0 adults were placed on RP523

seeded NGM agar plates with 1μM or 50 μM heme and allowed to lay F1 progeny for

11 hours. F1 worms were imaged after a further 72 hours.

Quantification of size and fluorescence using COPAS BioSort

Fluorescence of transgenic *C. elegans* and analyses of growth rate was quantified using COPAS BioSort (Union Biometrica). Worms were grown from L1 larvae to early adult or gravid stage on RNAi plates. For evaluation of fluorescence, three parameters were measured: time of flight (length), extinction (optical density) and GFP intensity. The settings for measuring GFP intensity in IQ6011 (P_{hrg-1}::*GFP*) were gain = 2.5 and PMT voltage = 400 and in IQ8031 (P_{hrg-3}::*GFP*) were gain = 2.5 and PMT voltage = 600. GFP was normalized to time of flight.

Quantification of GFP expression in neurons

After RNA interference (described above) in strain VC1478, adult worms were immobilized in 10 mm levamisole on a 2% agarose pad, and fluorescence microscopy images were quantified by Simple PCI software (Hamamatsu) using the region of interest (ROI) method. GFP was quantified in 20 worms for each treatment.

Embryonic lethality assay

Strain VH624 was synchronized and placed on RNAi plates with bacterial cultures grown in 1/4 Luria-Bertani broth (LB) (2.5% tryptone, 1.25% yeast extract, and 10% NaCl weight by volume, 50 μg/mL carbenicillin, 12 μg/mL tetracycline) with no added heme or 50 μM added heme. After 72 hours, adult worms were picked to fresh plates and allowed to lay embryos for 8 hours. Hatched and unhatched worms were counted 24 hours later.

Growth on RP523 bacteria

The heme-deficient *E. coli* strain RP523 was grown overnight in LB supplemented with 4 μM heme [166]. The following day, cultures were placed in fresh LB with 1 μM or 50 μM heme and grown for 5.5 hours to an OD600 of 0.2. Cultures were seeded on NGM agar plates overnight. The following day, synchronized IQ6011 and IQ6311 L1 larvae were placed on the RP523 seeded plates and incubated at 20°C. Worms grown on 50 μM heme were quantified using COPAS BioSort after 72 hours. Worms grown on 1 μM were quantified after 96 hours.

Immunoblotting

For detection of HRG-7, HRG-7-3xFLAG, and HRG-8-3xFLAG, between 2,500 and 5,000 gravid or young adult worms were lysed in phosphate-buffered saline (PBS) with protease inhibitors (1 mM phenylmethylsulfonyl fluoride, 4 mM benzamidine, 2 μg/ml leupeptin, and 1 μg/ml pepstatin), Lysing Matrix C beads (MP Biomedicals) in a FastPrep-24 Beadbeater (MP Biomedicals). Worm lysates were centrifuged 3 times at 10,000 x g for 10 minutes, then total protein concentration in the supernatants was measured using the Pierce BCA assay kit (Thermo Scientific). Unboiled samples were mixed with Laemmli sample buffer and 50 μg protein / lane were separated on a 10% SDS-PAGE gel and transferred to a nitrocellulose membrane. The membrane was incubated overnight in 4° C with anti-HRG-7 polyclonal antibody or anti-FLAG

monoclonal antibody (Sigma) at a concentration of 1:1000. Goat anti-rabbit HRP-conjugated secondary was used for anti- HRG-7, or rabbit anti-mouse HRP-conjugated secondary for anti-FLAG, at a 1:10,000 dilution, and blots were developed in SuperWest Pico Chemiluminescent Substrate (Thermo Scientific). Bio-Rad Image Lab software was used to quantify blots.

DiI, FITC pulse

To stain amphid and phasmid neurons, worms were removed from plates with M9, washed twice with M9, and resuspended in 100 µl M9. A stock solution of 2 mg/ml 5-fluorescein isothiocyanate (FITC) or 1,1'-dioctadecyl-3,3,3',3'-tetramethylindocarbocyanine perchlorate (DiI) in dimethyl formamide (DMSO) was diluted 1: 200 into the mixture. The tubes were wrapped in aluminum foil to avoid light exposure and incubated for 3 hours at room temperature. The worms were washed three times with M9 to remove excess dye, then immobilized in 10 mM levamisole on a 2% agarose pad and imaged by fluorescence microscopy.

Heme response assay

For heme response assays, eggs were obtained from worm strains maintained in mCeHR-2 medium with 20 µM heme. The following day, synchronized L1 larvae were placed mCeHR-2 medium with varying heme concentrations. After 72 hours, GFP or mCherry fluorescence was quantified with the COPAS BioSort and analyzed by fluorescent microscopy.

HRG-7 and HRG-8 recoding

To generate *hrg-7* and *hrg-8* RNAi resistant transgenes, the endogenous sequences were recoded by base pair substitution at degenerate sites and artificial introns were added using the *C. elegans* codon adapter [167]. Simultaneously, the endogenous sequences were recoded with the Genscript rare codon usage tool (http://www.genscript.com/cgi-bin/tools/rare_codon_analysis). The two recoded sequences were combined to ensure the least amount of overlap with the endogenous sequences. Finally, any contiguous stretches of six identical nucleotides between the recoded and endogenous sequences were changed manually, where applicable, to ensure RNAi resistance. The sequences were then sent to Genscript (Piscataway, NJ) for synthesis. The final recoded sequences are in appendix V. Only the first 300 bp is recoded in RNAi resistant *hrg-7* (*hrg-7^{PR}*). All of *hrg-8* is recoded (*hrg-8^{REC}*).

Microscopy

The genome-wide RNAi screen was performed with a Leica MZ16 FA stereomicroscope. Fluorescent and DIC images were captured using a Leica DMIRE2 epifluorescence microscope connected to a Retiga 1300 cooled mono 12-bit camera or a Zeiss LSM710 laser scanning confocal microscope.

Worm lysate acid titration

To evaluate HRG-7 processing, IQ7370 (*P_{vha-6}::HRG-7::3xFLAG*) were lysed in PBS + 1% n-Dodecyl β-D-maltoside (DDM). The pH of each sample was lowered with acetate solution (1 part 0.2 M sodium acetate and 9 parts 0.2 M glacial acetic acid).

The pH was brought to 8 with 0.1 M NaOH before running samples on a sodium dodecyl sulfate polyacrylamide gel electrophoresis (SDS-PAGE) gel.

RNAi of trafficking genes

Synchronized N2 or IQ7670 L1 larvae were placed in mCeHR2 media supplemented with 10 μM heme for 30 hours. Worms were then washed with M9 and transferred to RNAi plates. Worms were harvested for immunoblotting or fluorescent imaging 48 hours after transfer to RNAi plates.

MuDPIT

250,000 L1 larvae were placed in a 30 mL flask of liquid mCeHR2 medium supplemented with 4 μM and allowed to grow for 96 hours. Worms were then harvested, washed with PBS three times, and resuspended with 500 μl FLAG buffer (100 mM Tris-HCl 8.0,150 mM NaCl, 5 mM Ethylenediaminetetraacetic acid (EDTA), 5% glycerol, 0.1% NP-40). Worms were lysed using Lysing Matrix C beads in a FastPrep-24 Beadbeater. Worm lysates were centrifuged 3 times at 10,000 x g in 4°C for 10 minutes, then total protein concentration in the supernatants was measured using the Pierce BCA assay kit. 3-5 μg total protein in 500 FLAG buffer was mixed with 60 μl anti-FLAG affinity gel (M2 antibody, Sigma). The mixture was rotated at 4 °C for 2 hours. The anti-FLAG beads were then pelleted at 1000 g and washed three times with FLAG buffer and three times with FLAG buffer without NP40. Protein was eluted off beads by eluting two times with 500 μl FLAG buffer (no NP40) and 150 μg / ml 3xFLAG peptide for 25 minutes. 5% and 10% eluate

were removed for western blot and silver stain, respectively. Mass spectrophotometer

analyses was performed at the University of California, Los Angeles.

Bioinformatics

Protein and DNA alignments were performed using ClustalW2

(http://www.ebi.ac.uk/Tools/msa/clustalw2) [168]. Signal peptides were predicted

with the SignalP 4.1 server (http://www.cbs.dtu.dk/services/SignalP) [169].

Interaction networks were analyzed with geneMANIA (www.genemania.org).

Homology models were generated with I-TASSER

(http://zhanglab.ccmb.med.umich.edu/I-TASSER) [170].

Statistics

Statistical significance was determined using a Student's t-test or one-way ANOVA

in GraphPad Prism, version 5.00 (GraphPad Software, Inc.). All data are presented as

the mean ± the standard error of the mean

Chapter 3: A genome-wide RNAi screen reveals HRG-7 and HRG-8 as modulators of systemic heme homeostasis

Summary

Heme is an iron-containing tetrapyrrole that is required as a cofactor for proteins involved in diverse cellular functions [1, 2]. While heme synthesis and heme degradation have been extensively studied, other mechanisms of cellular and systemic homeostasis, such as transport, remain poorly understood. We have previously shown that *C. elegans* does not synthesize heme, but must acquire it from the environment via the intestine by the paralogous permeases HRG-1 and HRG-4 [10, 13]. Extraintestinal tissues in the worm including developing embryos, muscle, hypodermis, and neurons depend on heme exported by MRP-5 to fulfill their heme requirements. Remarkably, depletion of *mrp-5* results in upregulation of *hrg-1* in the intestine, suggesting heme deficiency, despite the accumulation of heme in this tissue. Therefore, the heme deficiency signal emanating from the intestine is a consequence of heme deficiency in extraintestinal tissues, leading us to speculate that an intertissue communication network exists to regulate systemic heme homeostasis. In order to uncover these interorgan signaling pathways we performed a genome-wide RNAi screen using the heme sensor strains IQ6011 ($P_{hrg-1}::GFP$) and IQ8031 ($P_{hrg-3}::GFP$), which express GFP from heme-responsive promoters in the intestine. Roughly 30% of the identified genes for which expression data was available were not even expressed in the intestine, confirming that intestinal heme responsiveness was regulated by extraintestinal tissues. Analyses of candidate genes with putative signal peptides revealed that two protease homologs, which we termed HRG-7 and HRG-8,

are regulators of heme homeostasis. HRG-7 and HRG-8 are upregulated by low heme in the intestine, secreted from the basolateral surface of the intestine, and internalized by neurons. Depletion of either gene results in upregulation of *hrg-1::GFP* even though sufficient heme is present to repress GFP. Together, our data suggest that communication between the intestine, the portal for heme entry, and the recipient tissue, the neuron, is essential for maintaining systemic heme homeostasis.

Results

A genome-wide RNAi screen identifies genes involved in heme homeostasis

The lab has previously demonstrated that the heme sensor strain, IQ6011 (*Phrg-1::GFP*), is a powerful tool for studying heme homeostasis [20]. In *C. elegans*, heme export from the intestine to extraintestinal tissues is mediated by the ABC transporter MRP-5 [12]. Depletion of *mrp-5* results in upregulation of intestinal GFP in IQ6011 similar to that seen for the heme importer HRG-4, indicating heme deficiency (**Figure 3.1A**). While this result is expected for *hrg-4* knockdown, which prevents heme from entering the animal, it is surprising that *mrp-5* knockdown results in a heme deficiency signal and intestinal heme accumulation [12]. However, because depletion of *mrp-5* results in a failure to export heme from the intestine, extraintestinal tissues become heme deficient under these conditions. We therefore reasoned that extraintestinal tissues must signal their heme deficiency status to the intestine, resulting in upregulation of HRG-1 to provide more heme to these tissues. In order to identify factors involved in this intertissue communication, we knocked

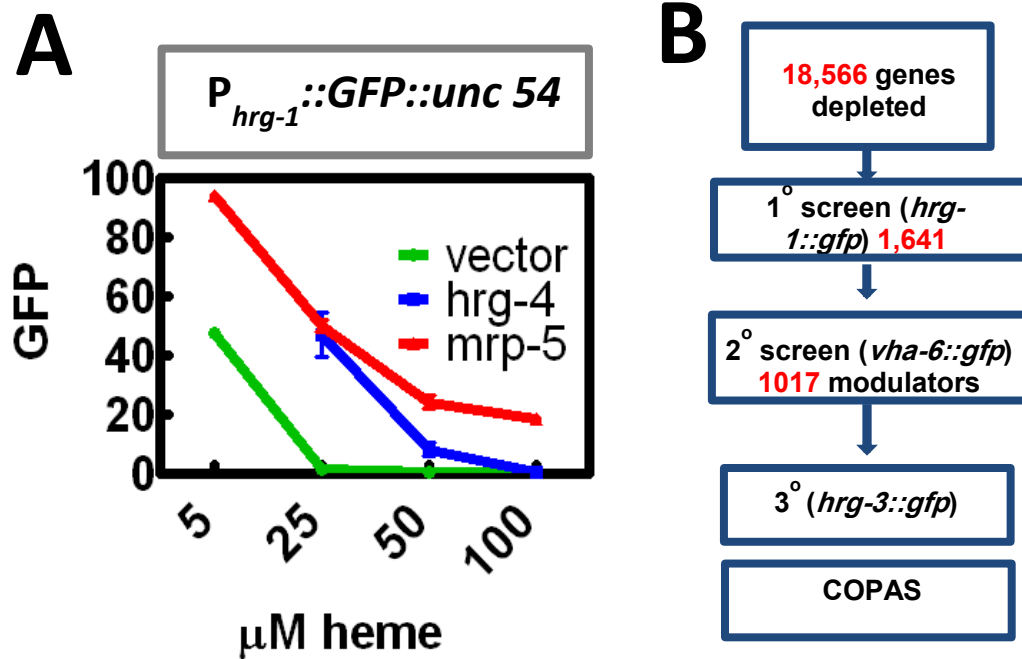**Figure 3.1: A genome-wide RNAi screen identifies genes involved in systemic heme homeostasis.** **A**) GFP fluorescence (120 worms per treatment) quantified from strain IQ6011 ($P_{hrg-1}::GFP$) fed dsRNA against control vector, *hrg-4*, or *mrp-5* at 5, 25, 50, and 100 μM heme. GFP was quantified using COPAS BioSort. **B**) Schematics of genome-wide RNAi screen for modulators of heme homeostasis.

down ≈ 18,577 genes in IQ6011 by RNAi **(Figure 3.1B)**. Knockdown of 1,641 genes

resulted in altered GFP expression compared to worms fed vector only, indicating

alterations in heme homeostasis. To rule out genes that regulate GFP expression non-

specifically, we rescreened the 1,641 modulators in worms expressing $P_{vha-6}::GFP$.

These worms also express GFP specifically in the intestine but independent of heme

concentrations. Using this strain, we validated 1,017 genes as modulators of heme

homeostasis. GFP expression after RNAi knockdown of validated genes in IQ6011

and another heme-sensor strain, IQ8031 ($P_{hrg-3}::GFP)$, was quantified using COPAS

BioSort. Like *hrg-1*, *hrg-3* is transcriptionally upregulated in the intestine by low

heme but through a different transcriptional pathway [11, 24]. Comparing the effect

of RNAi knockdown in the two strains allowed us to differentiate between genes that

had an overall effect on heme homeostasis and genes that were involved in a specific

pathway. Genes were considered candidates if knockdown resulted in upregulation of

GFP in both strains by ≥ 1.5 fold or downregulation of GFP ≥ 2 fold **(Figure 3.2A).**

In total, we found 187 genes that regulated GFP in both strains **(Figure 3.2B)**.

Systemic heme homeostasis is maintained by intertissue communication

Tissue specific expression patterns from reporter constructs or mRNA

enrichment experiments were available for 94 out of the 187 genes that regulate GFP

in IQ6011 and IQ8031 [171, 172]. Of these 94, approximately thirty percent were

reported to be exclusively expressed in extraintestinal tissues, despite regulating

intestinal GFP in both heme sensor strains **(Figure 3.3A)**. This supported our

hypothesis that intertissue communication was a key component of systemic heme
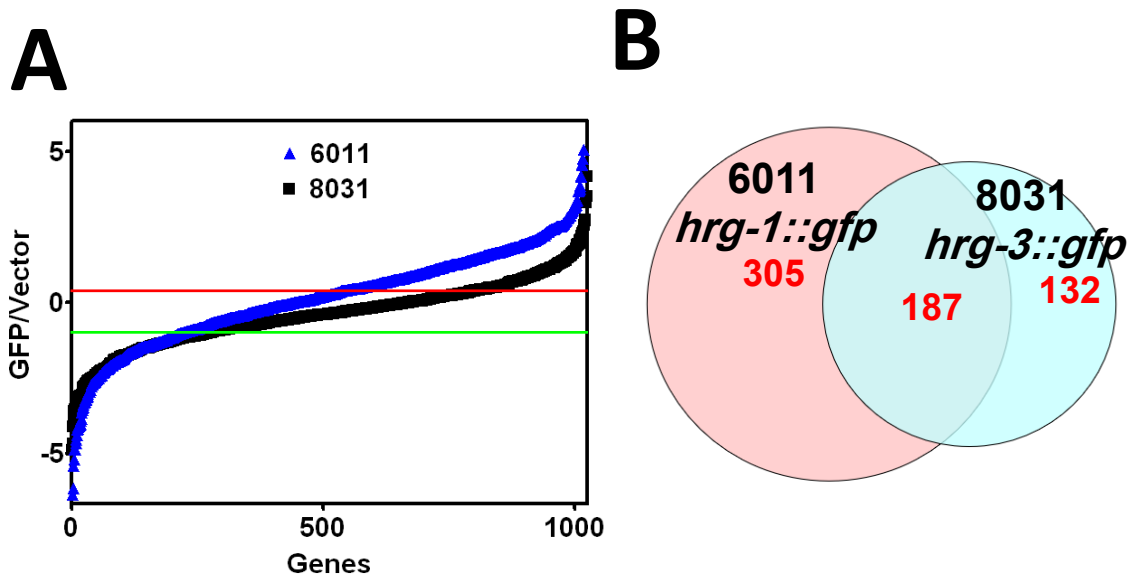
Figure 3.2: GFP quantification of candidate genes in two heme sensor strains

A) GFP fluorescence (80 worms per treatment) quantified from IQ6011 and IQ8031 fed dsRNA against genes identified from a genome-wide screen for modulators of heme homeostasis. Individual genes are plotted on the X axis by increasing GFP expression for both IQ6011 and IQ8031. GFP is normalized to GFP expression in IQ6011 and IQ8031 fed dsRNA against vector only. The red line indicates 1.5 fold increased GFP / vector GFP, the green line indicates 2 fold decreased GFP / vector GFP. **B)** Venn diagram indicating the number of genes that upregulated GFP ≥ 1.5x or downregulated GFP ≥ 2x in IQ6011, IQ8031, or both strains.
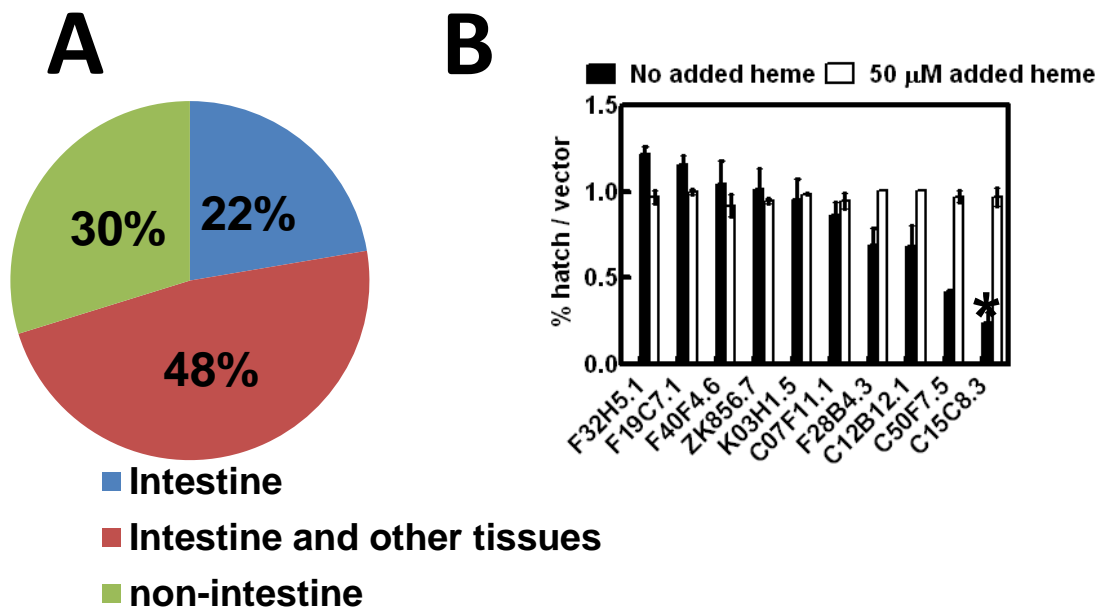
Figure 3.3: Systemic heme homeostasis is maintained by intertissue signaling.

A) Pie chart indicating percentages of tissue-specific expression patterns of genes identified from our genome-wide screen. Expression data was available for 94 out of 187 genes. **B)** Embryonic lethality in the RNAi hypersensitive strain VH624 (*nre-1*; *lin-15b* (*hd126*)) fed dsRNA against genes with putative signal peptides identified from the genome-wide RNAi screen. P0 VH624 L1 larvae were fed dsRNA against indicated genes until gravid. 5 P0 worms were then picked to fresh RNAi plates and allowed to lay F1 progeny for 8 hrs. Hatched and unhatched embryos were counted 24 hours later. *$P < 0.05$ compared to vector only in no added heme, n=3 (one-way ANOVA).

homeostasis. In order to uncover the mechanisms of heme-dependent signaling

between tissues, we analyzed the 187 modulators for putative signal peptides using

SignalP 4.1 (http://www.cbs.dtu.dk/services/SignalP) [169]. The presence of a signal

peptide is an indication that a protein is translocated to the secretory pathway during

translation and potentially secreted, thus capable of mobility and communication

between tissues. From the 187 ORFs, 10 had putative signal peptides and were

expressed in a variety of tissues **(Table 3.1)**. In order to uncover which of these

genes were crucial for heme homeostasis, we RNAi depleted each candidate gene in

the RNAi hypersensitive strain VH624 (*nre—1*; *lin15b* (*hd126*)) and found that

depletion of one candidate, C15C8.3, resulted in 90% embryonic lethality when

worms were grown in low heme **(Figure 3.3B)**. Embryonic lethality was fully

rescued by the addition of heme to RNAi bacteria cultures, indicating that this

phenotype was reversible and dependent upon heme availability. Together, our

results indicate that C15C8.3 is required for heme homeostasis under heme limiting

conditions.

HRG-7 and HRG-8 are protease homologs

   Microarray results, previously performed by our group, had indicated that

C15C8.3 was upregulated by low heme, so we termed this gene <u>h</u>eme <u>r</u>esponsive

<u>g</u>ene 7 (*hrg-7*) [20].   Blast searches against the predicted protein sequence of *hrg-7*

revealed that it is a member of the A1 aspartic protease family, which includes the

human proteases cathepsin D, cathepsin E, pepsin, and renin. Like other A1

56

Table 3.1: Candidate genes with putative signal peptides

Sequence name	Gene name	Tissue specific Expression	Description
C07F11.2	tol-1	Neuron Head mesoderm	Toll-like receptor
C12D12.1		Unknown	Glycoprotein
C15C8.3	asp-10	Intestine	Aspartic protease
C50F7.5		Neuron Hypodermis Muscle	Basic proline-rich protein
F19C7.1		Intestine	
F28B4.3		Unknown	C-type lectin
F32H5.1		Intestine	Cysteine protease homolog
F40F4.6		Unknown	C-type lectin
K03H1.5		Unknown	Sushi domain containing protein
ZK856.7		Intestine	

proteases, HRG-7 is predicted to have a signal peptide, a propeptide which keeps these enzymes as zymogens until they encounter low pH, two conserved disulfide bonds, and two aspartic acid residues which are required for proteolytic activity **(Figure 3.4A, B)**. Antibody against endogenous HRG-7 confirmed it is synthesized as a pro-protein before maturation, as indicated by the appearance of a higher molecular weight band in addition to the expected molecular weight when worm lysates were immunoblotted for HRG-7 **(Figure 3.4C)**. RNAi knockdown of *hrg-7* reduces the intensity both bands, confirming the authenticity of the pro and mature forms of HRG-7. Analyses of these candidates genes uncovered a second protease-like gene, F32H5.1, which like *hrg-7,* upregulated GFP levels in IQ6011 when depleted, indicating heme deficiency. Microarray results had showed that F32H5.1 is upregulated by low heme, so we termed this gene *hrg-8*. The predicted HRG-8 protein is homologous to the C1 cysteine proteases which include human proteases cathepsin B and cathepsin L **(Figure 3.5A, B)**. HRG-8 also has a signal peptide, a propeptide, and conserved disulfide bonds, but unlike HRG-7, lacks the catalytic diad of cysteine and histidine, which have been instead replaced by a methionine and alanine, respectively. This suggests that HRG-8 may function as something other than a protease no longer requiring a functional active site. Although attempts to obtain an antibody against endogenous HRG-8 were unsuccessful, we could detect transgenic HRG-8::3xFLAG with anti-FLAG antibody, suggesting that *hrg-8* mRNA is translated and is not a pseudogene **(Figure 3.5C)**.

Figure 3.4: HRG-7 is an A1 protease homolog

A) Conserved regions of aspartic proteases. **B)** Homology model of HRG-7 using I-TASSER. The putative active site is indicated by a red circle. The conserved disulfide bonds are indicated by green arrows. **C)** Immunoblot analysis of HRG-7 expression in *C. elegans*. Membranes were probed with polyclonal anti-HRG-7 antibody and then incubated with HRP-conjugated anti-rabbit secondary antibody. The HRG-7 antibody recognizes pro and mature HRG-7. * indicates pro-HRG-7. + indicates mature HRG-7. Arrowhead indicates tubulin.

A

Consensus
HRG-7

D T G
D S G

D T/S G
D T   A

S S

S S

Signal peptide
Propeptide
Mature form

Catalytic motif
Catalytic residue
[S-S] cysteines for
disulfide bonds

B Homology model

C α-HRG-7

RNAi: vector hrg-7

HRG-7 ▶ *
       +

─37kD

Tubulin ▶
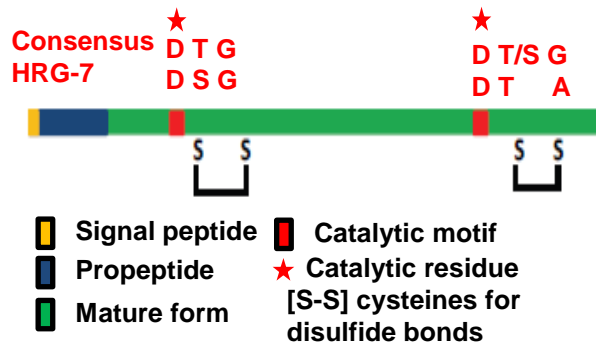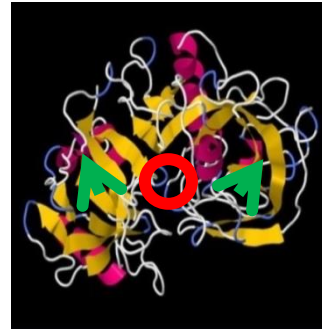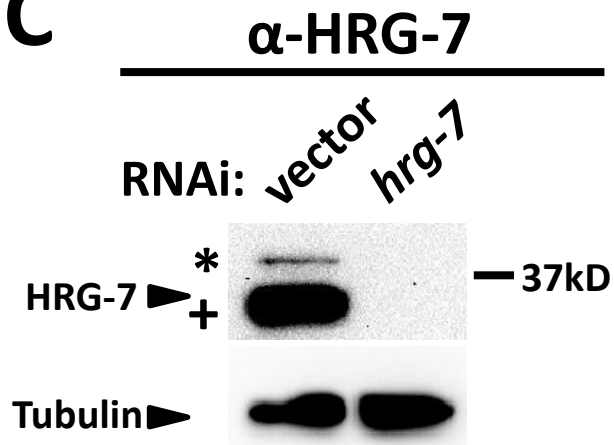
Figure 3.5: HRG-8 is a C1 protease homolog

A) Conserved regions of cysteine proteases. **B)** Homology model of HRG-8 using I-TASSER. The canonical active site of C1 proteases, which is absent in HRG-8, site is indicated by a red circle. **C)** Immunoblot analysis of HRG-8-3xFLAG expression in IQ7380 (*P*_{*vha-6*}*::HRG-8-3xFLAG::ICS::GFP*). Membranes were probed with monoclonal anti-FLAG antibody and then incubated with HRP-conjugated anti-mouse secondary antibody. The anti-FLAG antibody specifically recognizes HRG-8-3xFLAG.

A

Consensus
HRG-8

Signal · Propeptide · Mature form · Light chain

Catalytic · Catalytic · [S-S] cysteines for disulfide bonds

B
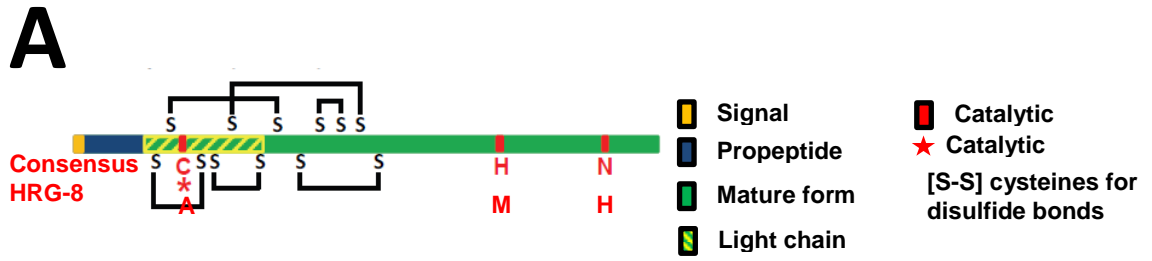
Homology model of HRG-8

C

HRG-8::3xFLAG

50kD

37kD

IQ7380   N2
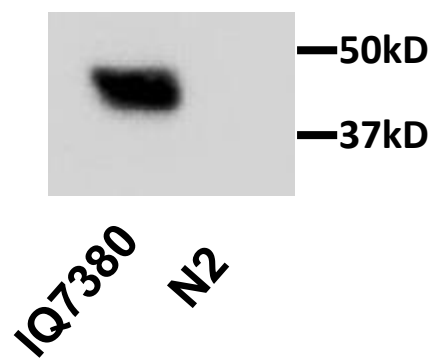
The heme-dependent regulation of *hrg-7* and *hrg-8* is specific to the intestine

Previous studies have suggested that *hrg-7* and *hrg-8* expression is enriched in the intestine [172, 173], and expression is regulated by heme [20]. Therefore, we sought to address two questions: 1) are *hrg-7* and *hrg-8* expressed at all in extraintestinal tissues, and 2) is heme-dependent expression restricted to the intestine? To answer these questions, we constructed *hrg-7* and *hrg-8* transcriptional reporters by fusing the 5' flanking region of each gene upstream of GFP. Interestingly, within the *hrg-7* 5' flanking sequence there was a highly conserved region about 200 bp upstream of the start codon which showed high similarity to the HEme Responsive Element (HERE) previously characterized in the *hrg-1* promoter **(Figure 3.6A B)** [24]. As in the *hrg-1* promoter, the putative *hrg-7* HERE was flanked by GATA sites, enhancer elements that bind the transcription factor ELT-2 and are responsible for intestinal expression in *C. elegans* [173]. Together, this analysis predicts that like *hrg-1*, *hrg-7* is upregulated by low heme specifically in the intestine. This predicted pattern of regulation was confirmed by the P_{hrg-7}*::GFP* transcriptional reporter strain IQ7701, which expressed strong GFP in the intestine when worms were grown in low heme **(Figure 3.7A)**. Worms expressing an *hrg-7* transcriptional reporter in which the seven nucleotides on the 3' end of the HERE were mutated (G→T, C→A, T → G, A→C) did not show GFP expression under low heme, indicating that the *hrg-7* HERE is functional and mediates the heme-dependent expression of *hrg-7* **(Figure 3.7B)**. Finally, western blot analyses of HRG-7 expression showed that protein levels closely mimic the heme-dependent regulation observed in IQ7701, indicating that the

Figure 3.6: The *hrg-7* 5' flanking region has a conserved HERE and GATA sites

A) ClustalW alignment of the *hrg-7* 5' flanking region with homologous sequences in *C. briggsae* and *C. remanei*. White text with black background indicates a conserved nucleotide in all three species. Red box indicates HERE. **B)** Alignment of the *hrg-1* transcriptional regulatory region with the putative *hrg-7* transcriptional regulatory region. Red box indicates HERE. White text with black background indicates conserved nucleotides in the HERE. Blue boxes indicate GATA sites.

Figure 3.7: *hrg-7* is specifically upregulated in the intestine under low heme conditions

A) GFP expression in strain IQ7701 (P_{hrg-7}*::GFP*) grown in varying heme concentrations. GFP was quantified with the COPAS BioSort. Graph represents 3 replicates with 100 worms per replicate. **B)** GFP expression in IQ7701 and IQ7702 (P_{hrg-7}^{mut}*::GFP*) in 4 μM heme. GFP was only detectable in IQ7701. **C)** Immunoblot analysis of HRG-7 expression in N2 grown in increasing heme concentrations. Membranes were probed with polyclonal anti-HRG-7 antibody and then incubated with HRP-conjugated anti-rabbit secondary antibody. * indicates pro-HRG-7. + indicates mature HRG-7. Arrowhead indicates tubulin.

A

$P_{hrg-7}::GFP::unc-54\ 3'\ UTR$

B

4 μM heme
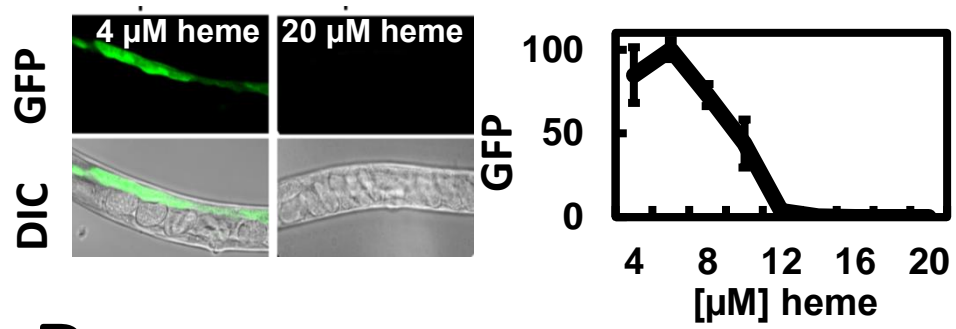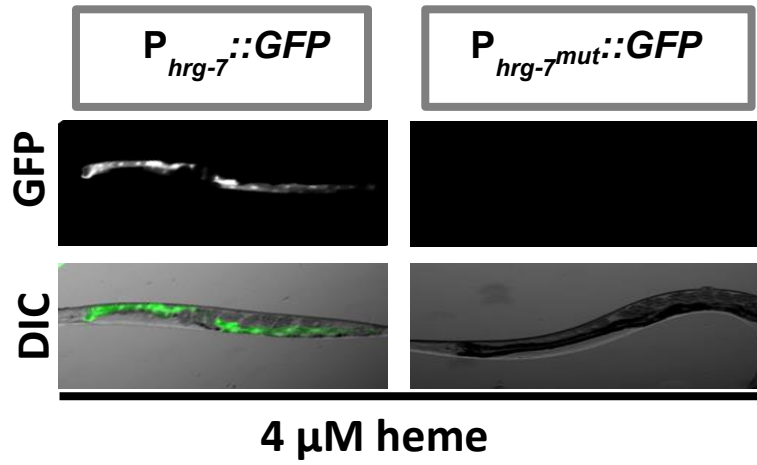
C
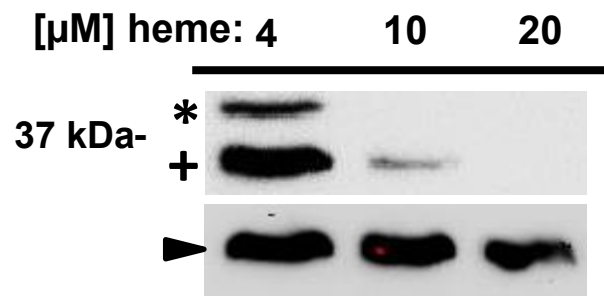
heme-dependent transcriptional regulation plays a major role in HRG-7 protein levels (**Figure 3.7C**).

Although the 5' flanking region of *hrg-8* did not contain a HERE, there were two conserved GATA sites, supporting previous reports indicating that *hrg-8* expression was enriched in the intestine (**Figure 3.8A**). As predicted, worms expressing $P_{hrg-8}::GFP$ (IQ7801) showed strong intestinal GFP expression (**Figure 3.8B**). In addition to the intestine, IQ7801 worms also expressed GFP in a single neuron pair in the head. Although these neurons did not take up DiI, which labels the plasma membranes of amphid and phasmid sensory neurons, they were situated between neurons that did, suggesting that this neuron pair could be the AFD neurons (**Figure 3.8C**). AFD neurons are also amphid sensory neurons but their dendrites are not exposed to the environment, preventing dye labeling. To examine whether *hrg-8* was indeed expressed in AFD neurons, we crossed IQ7801 to worms expressing $P_{gcy-8}::mCherry$, which is specifically expressed in the AFD neuron pair. GFP and mCherry colocalized in crossed progeny, indicating that in addition to the intestine, *hrg-8* is expressed in the AFD neuron pair (**Figure 3.8D**). Next, to confirm microarray results indicating *hrg-8* is heme-responsive, we grew IQ7801 in mCeHR-2 media supplemented with 4, 20, 100, or 500 μM heme. GFP expression was strongest at 4 μM heme but was still evident at 500 μM heme, indicating that although *hrg-8* is heme-responsive, it is expressed over a broad range of heme concentrations (**Figure 3.9A**). There were no heme-dependent changes in expression in the AFD neuron pair, indicating that the heme-dependent transcriptional regulation of *hrg-8* is restricted to the intestine (**Figure 3.9B**).

Figure 3.8: *hrg-8* **is expressed in the intestine and AFD neuron pair**

A) ClustalW alignment of the *hrg-8* 5' flanking region with homologous sequences in

C. briggsae and *C. remanei*. White text with black background indicates a conserved

nucleotides in all three species. Blue boxes indicate GATA elements. **B)** Intestinal

GFP expression in strain IQ7801(P_{hrg-8}*::GFP*). **C)** Neuronal GFP expression in strain

IQ7801(P_{hrg-8}*::GFP*) pulsed with 10 µg /ml DiI for 3 hrs. **D)** GFP and mCherry

expression in double transgenic worms expressing P_{hrg-8}*::GFP* and P_{gcy-8}*::mCherry*,

which is specifically expressed in the AFD neuron pair.

A

```
C. elegans    AACAATCTTC TATCT TTTC- TATC ---TTTCTGCTCTTTTCCCTCTC
C. remained   AACAGTCTTC TATCT TTTC- TATC CTCTTTCTGCTCTTTTCTTTCTC
C. briggsae   AACAACTTTC TATCT TTTCC TATC CCTTTATTGCTCTTTTCTCCTCTC
```

B

P_{hrg-8}::GFP::unc-54 3' UTR

P_{hrg-8}::GFP::unc-54 3' UTR

C

P_{hrg-8}:GFP DiI DIC

D

P_{hrg-8}::GFP P_{gcy-8}::mCherry Merge DIC
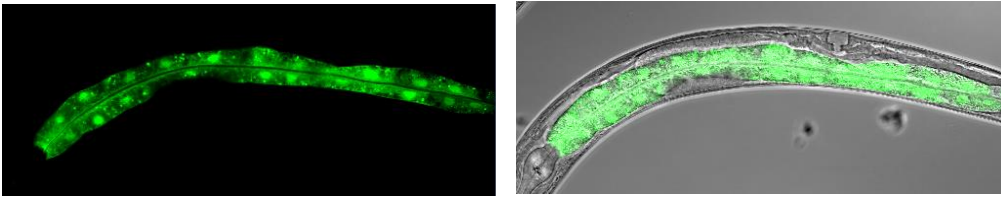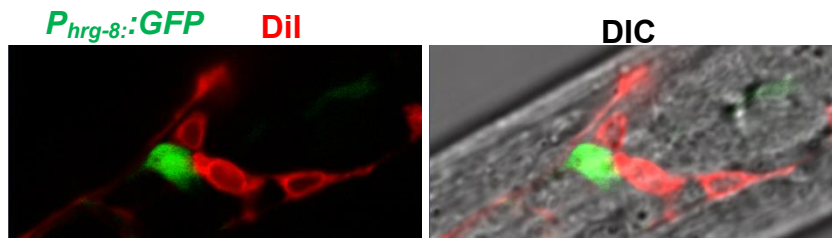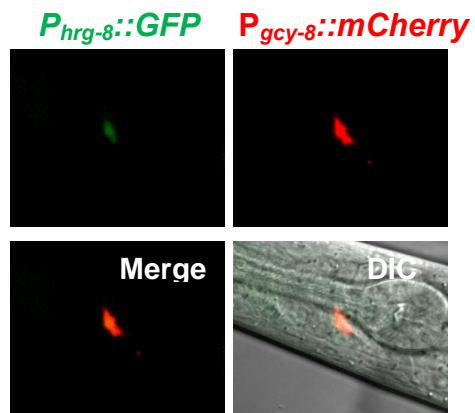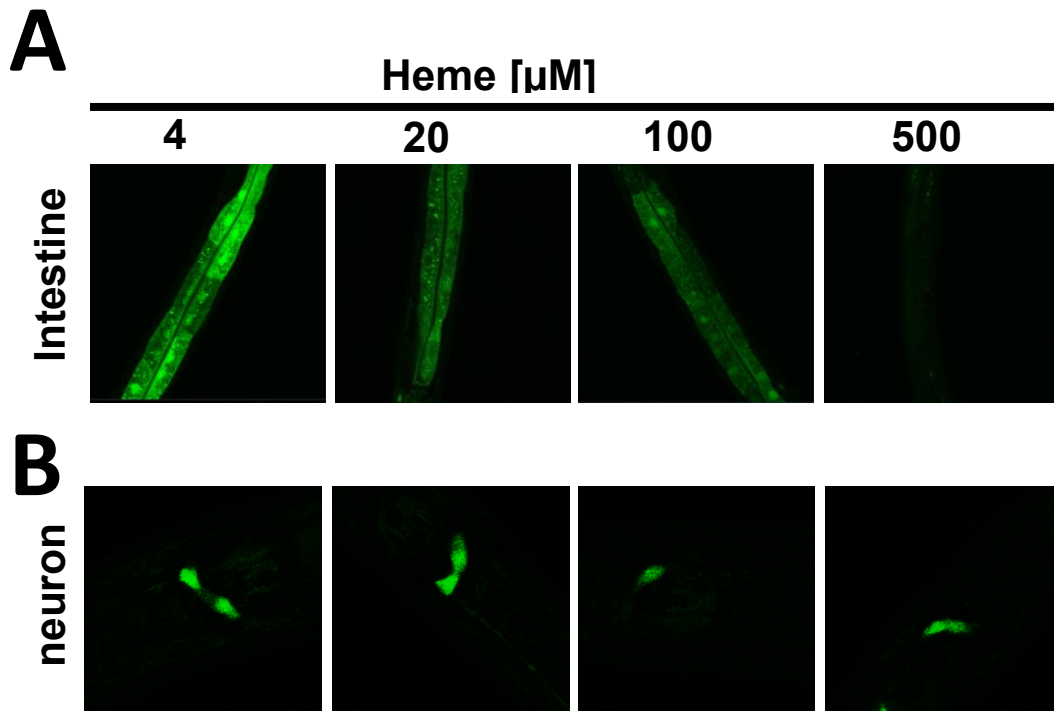
Figure 3.9: *hrg-8* expression is regulated by heme in the intestine but not in the

AFD neuron pair

GFP expression in strain IQ7801($P_{hrg-8}::GFP$) grown in 4, 20, 100, or 500 μM heme.

Images are 63 X. **A)** GFP in the intestine, which is strongest at 4 μM heme. **B)** GFP

in the AFD neuron pair, which is of equal intensity across heme concentrations.

HRG-7 and HRG-8 are secreted from the intestine and localize to neurons

Having established that *hrg-7* is exclusively expressed in low heme in the intestine and *hrg-8* is expressed in the intestine and AFD neuron pair over a broad range of heme concentrations, we next sought to uncover the localization of HRG-7 and HRG-8 by fusing their 5' flanking regions and coding sequences in frame with mCherry (strain IQ7777 and IQ7888, respectively). We expected three possible outcomes based on the localization of known A1 and C1 proteases in mammals and helminths: 1) lysosomal localization; 2) apical secretion into the gut lumen; 3) basolateral secretion into the pseudocoelom [147, 174-176]. For strain IQ7777 (P_{hrg-7}::*HRG-7::mCherry*), we observed weak mCherry fluorescence in the intestine but strong fluorescence in coelomocytes, macrophage like cells that take up substances non-specifically from the pseudocoelomic fluid and are used as a marker of secretion in *C. elegans* **(Figure 3.10A)** [177]. Therefore, the presence of HRG-7::mCherry in coelomocytes indicated that it was secreted from the basolateral membrane of the intestine into the body cavity. This localization was not likely due to ectopic expression because we did not observe fluorescence in coelomocytes at 20 µM heme, and we have previously demonstrated that the HERE motif is only active in the intestine [24]. Additionally, we observed mCherry fluorescence in distinct punctae in the anterior and posterior of the worm, suggesting that HRG-7 is specifically targeted after secretion (Figure 3.10B). To analyze HRG-8 localization, we crossed the transgene P_{hrg-8}::*HRG-8::mCherry* into IQ7801 to obtain the double transgenic strain IQ7880 (P_{hrg-8}::*GFP*, P_{hrg-8}::*HRG-8::mCherry*). IQ7880 showed GFP and mCherry in the intestine, but only mCherry fluorescence in coelomocytes, indicating that

Figure 3.10: Secreted HRG-7::mCherry localizes to coelomocytes and punctae in the anterior and posterior of the worm

mCherry expression in IQ7777 (P_{hrg-7}::*HRG-7::mCherry*). **A)** mCherry expression in coelomocytes. Intestine is indicated by yellow lines, the coelomocytes are indicated by a white arrow. Scale bar = 20 µm. **B)** mCherry expression in anterior and posterior of worm. Scale bar = 20 µm. Images are 63x.

A

P_{hrg-7}::HRG-7::mCherry::hrg-7 3' UTR

4 µM heme   **20 µM heme**

mCherry

DIC

B   **Anterior**   **Posterior**

mCherry

DIC
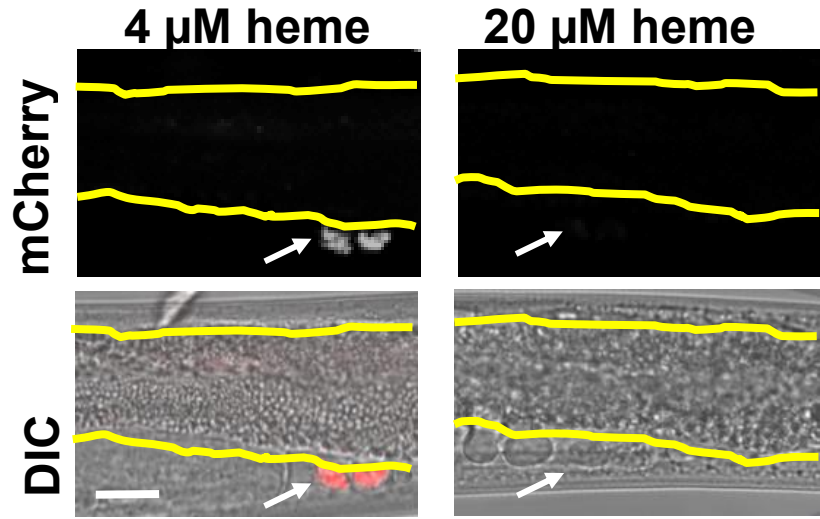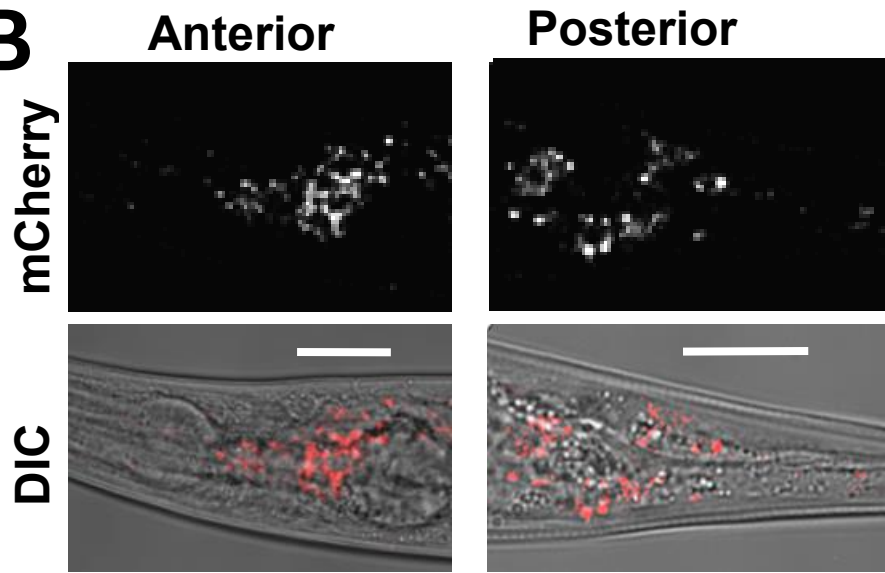
HRG-8 is also secreted from the basolateral membrane of the intestine (**Figure 3.11A**). HRG-8::mCherry was localized as punctae in the anterior of the worm, a portion of which was distinct from the AFD neuron pair (**Figure 3.11B**). To confirm that the observed localization patterns were not due to ectopic expression in extraintestinal tissue, we expressed HRG-7 and HRG-8 mCherry translational reporters from the intestine specific *vha-6* promoter [178]. In strains IQ7670 (P_{vha-6}*::HRG-7::mCherry*) and IQ7680 (P_{vha-6}*::HRG-7::mCherry*) we observed accumulation of mCherry in coelomocytes and distinct punctae in the anterior and posterior of the worm even though the protein was being specifically expressed from the intestine (**Figure 3.12A, B**). Next, we sought to clarify the specificity of this localization by analyzing two additional strains: IQ8333 (P_{vha-6}*::HRG-3::mCherry*) and IQ8630 (P_{vha-6}*::HRG-3SP-mCherry*). HRG-3, like HRG-7 and HRG-8, is secreted from the basolateral membrane of the intestine but localizes to developing oocytes and embryos [11]. The second strain, IQ8630, expresses mCherry with the amino terminal signal peptide of HRG-3, allowing mCherry to go through the secretory pathway. Expectedly, both these strains showed strong mCherry fluorescence in coelomocytes although neither recapitulated the fluorescence localization pattern of HRG-7::mCherry and HRG-8::mCherry (**Appendix IIIA, B**).

To determine the target tissue of HRG-7 and HRG-8, we crossed tissue specific GFP or YFP markers into IQ7670 and IQ7680. The markers used included P_{ceh-22}*::GFP* (pharyngeal muscle), P_{dpy-7}*::YFP* (hypodermis), P_{myo-2}*::GFP* (body wall muscle) and $P_{unc-119-2}$*::GFP* (neurons). For both HRG-7::mCherry and HRG-8::mCherry, we observed the strongest colocalization with $P_{unc-119}$*::GFP*

Figure 3.11: Secreted HRG-8::mCherry localizes to coelomocytes and punctae in the anterior of the worm

GFP and mCherry expression in IQ7880 ($P_{hrg-8}::GFP$, $P_{hrg-8}::HRG-8::mCherry$). **A)** GFP and mCherry expression in the intestine and coelomocytes. Only mCherry is detected in coelomocytes. **B)** GFP and mCherry expression in the anterior of the worm. mCherry is detected in tissue distinct from the AFD neuron pair, which is shown by the arrow. Images are 63x.

A

P_{vha-6}::HRG-7::mCherry::unc-54

coelomocyte | anterior | posterior

B

P_{vha-6}::HRG-8::mCherry::unc-54

coelomocyt | anterior | posterior
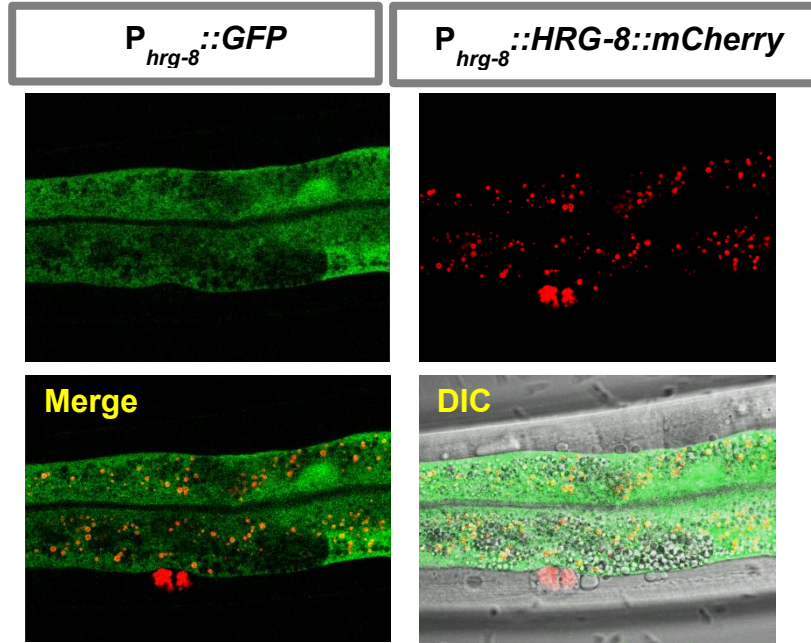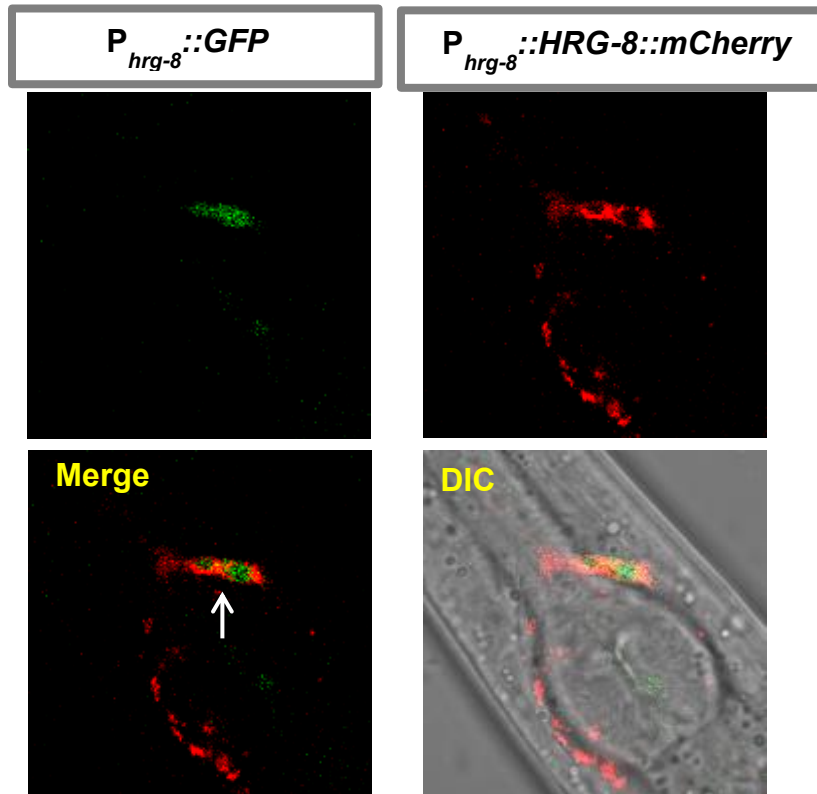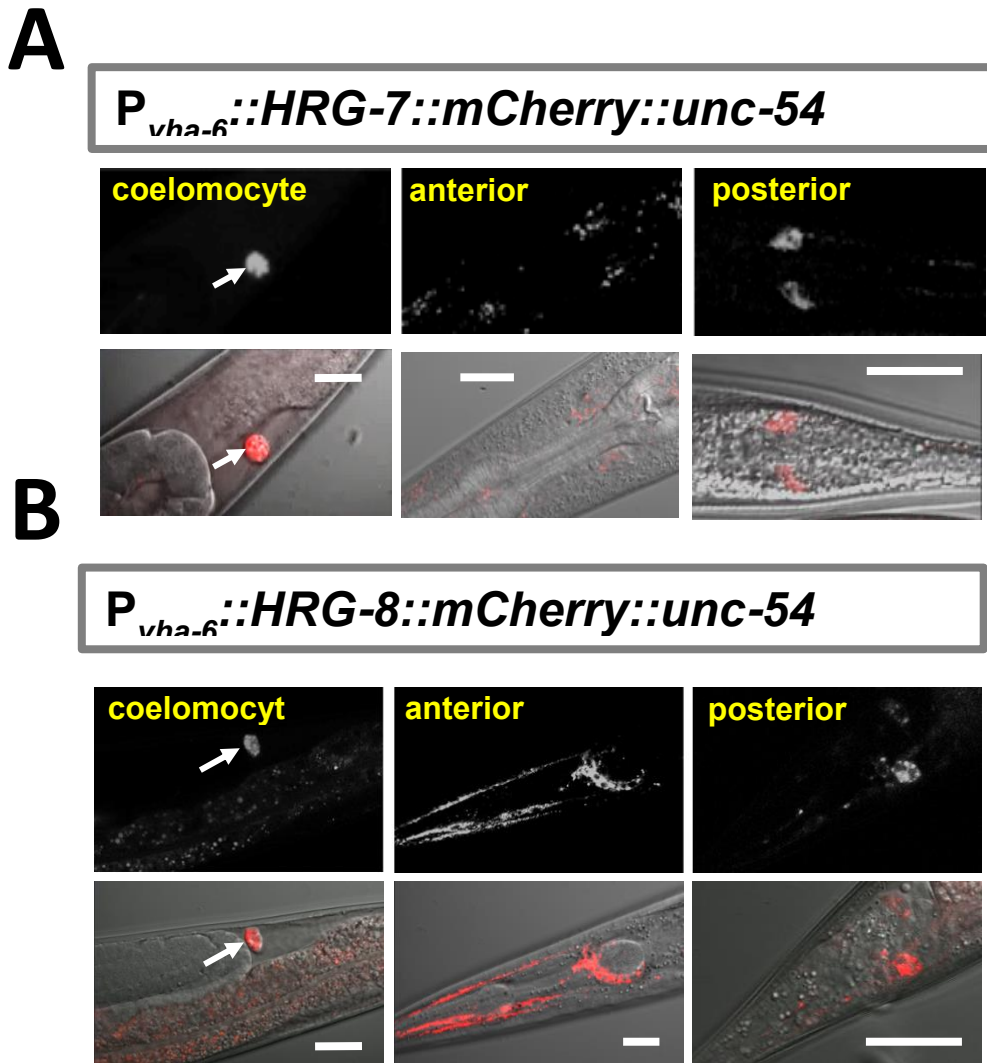
Figure 3.12: Intestinally driven HRG-7 and HRG-8 localize to coelomocytes and punctae in the anterior and posterior of the worm

A) mCherry expression in the coelomocytes, anterior and posterior of strain IQ7670 (P_{vha-6}:HRG-7:mCherry) B) mCherry expression in the intestine and coelomocytes, anterior and posterior of strain IQ7680 (P_{vha-6}:HRG-8::mCherry). White arrows indicate coelomocytes.   Images are 63x. Scale bar = 20 μm.

(Figure 3.13A, Appendix IV). Confocal microscopy at higher magnifications

revealed that HRG-7::mCherry and HRG-8::mCherry localized to neurons and that

these proteins may be internalized **(Figure 3.13B)**. Both fusion proteins appeared to

localize to a subset of neurons, with the strongest signal near the nerve ring. Amphid

sensory neurons, whose cell bodies are located posterior to the nerve ring, are

involved in nutrient homeostasis through signaling to the intestine to initiate lipolysis

[74]. To determine if HRG-7 and HRG-8 localized to sensory neurons, we pulsed

IQ7670 and IQ7680 with fluorescein isothiocyanate (FITC) for 3 hours. Similar to

DiI, amphid neurons take up FITC due to their direct contact with the external

environment. We observed HRG-7::mCherry and HRG-8::mCherry within the same

neurons that took up FITC, suggesting that HRG-7 and HRG-8 localize, at least in

part, to sensory neurons **(Figure 3.14A, B)**. Together, these data suggest that the

upregulation of *hrg-1::GFP* due to depletion of *hrg-7* and *hrg-8* may be in response

to a disruption in communication between the intestine and neurons to regulate

intestinal heme transport during heme deficiency.

Discussion

The nematode *C. elegans* is unable to synthesize heme and is therefore reliant upon

heme absorbed through the intestine to fulfill the heme requirement of all tissues. We

have previously shown that intestinal heme uptake is mediated by the permeases

Figure 3.13 HRG-7::mCherry and HRG-8::mCherry colocalize with GFP expressed in neurons

Expression of the pan-neuronal GFP marker $P_{unc-119}::GFP$ crossed into strains IQ7670 ($P_{vha-6}::HRG-7::mCherry$) and IQ7680 ($P_{vha-6}::HRG-8::mCherry$). A) 63X images, scale bar = 20µm. B) 100X images, scale bar = 10 µM. Yellow outline indicates nerve ring. White dotted circles indicate nerve ring nuclei.

A

| HRG-7::mCherrv | *unc119*::GFP | DIC | Merged 3D rendering |

| HRG-8::mCherrv | *unc119*::GFP | DIC | Merged 3D rendering |

B

| HRG-7::mCherry | Punc-119::GFP | Merge |

0.5µm sections

| HRG-8::mCherry | Punc-119::GFP | Merge |

A

HRG-7:mCherry FITC Merge DIC

B

HRG-8:mCherry FITC Merge DIC
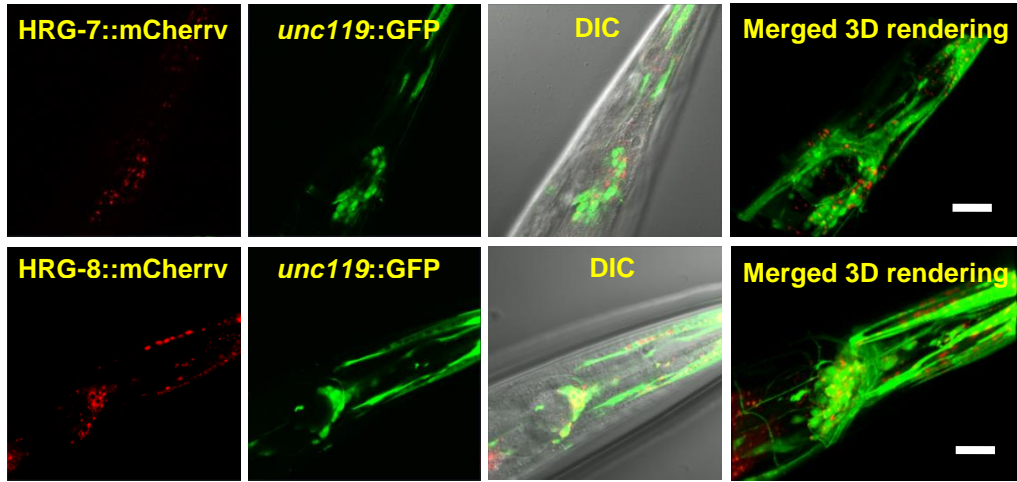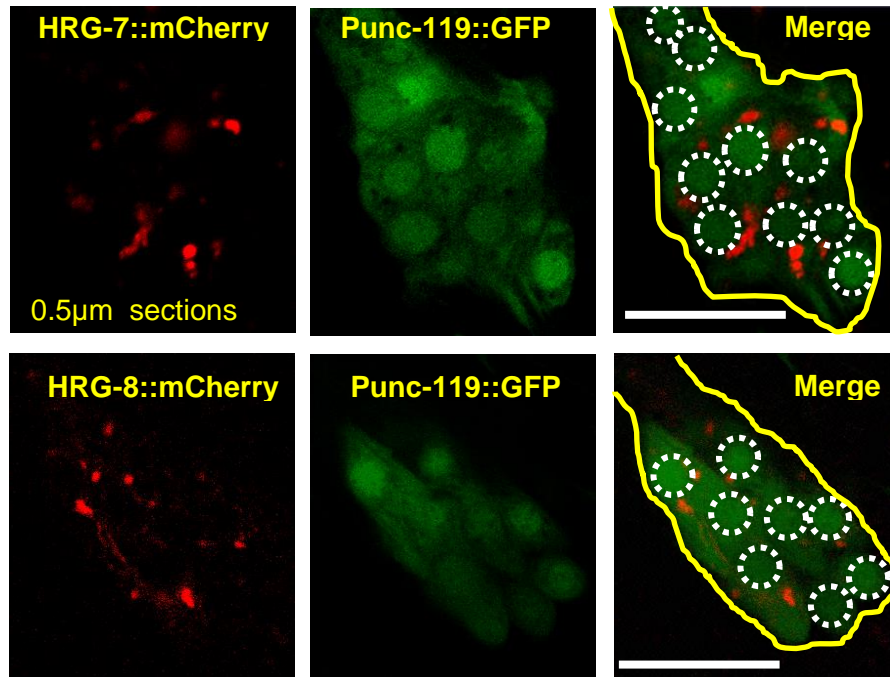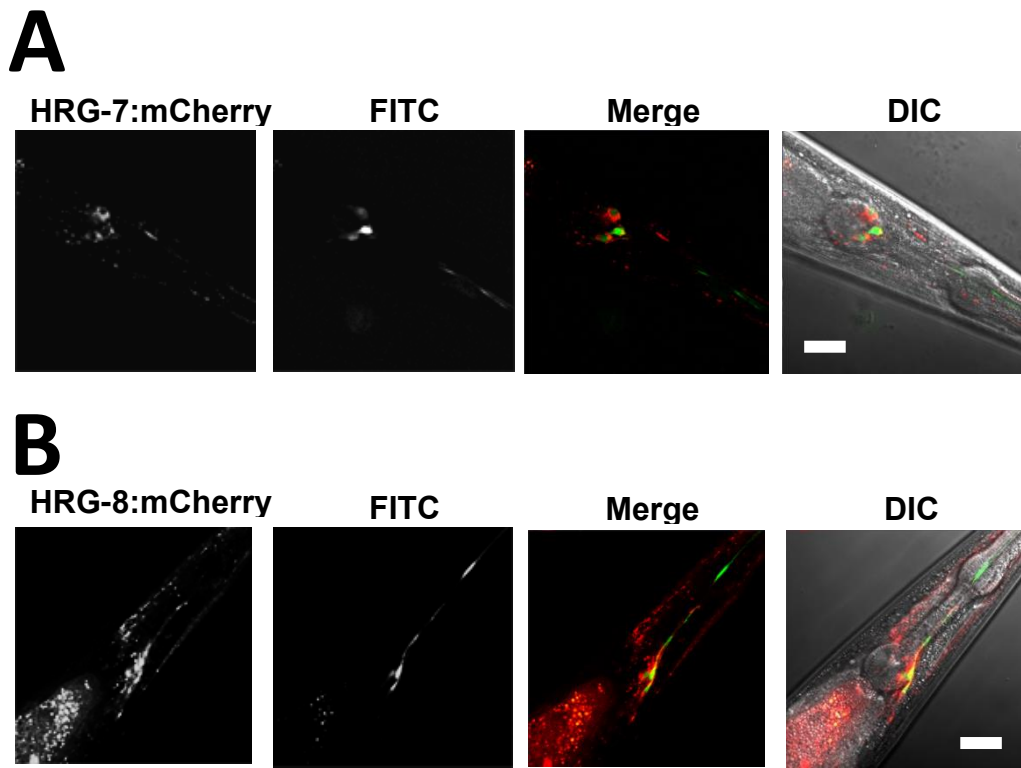
Figure 3.14: HRG-7::mCherry and HRG-8::mCherry localize to sensory neurons

IQ7670(P_{vha-6}::*HRG-7::mCherry*) and IQ7680 (P_{vha-6}::*HRG-8::mCherry*) were pulsed with 10 µg /ml FITC for 3 h, then analyzed by confocal microscopy. **A)** Representative image of anterior of IQ7670 adult. **B)** Representative image of anterior of IQ7680 adult. Images are 63x. Scale bar = 20 µM.

HRG-1 and HRG-4, while the ABC transporter MRP-5 exports heme from the basolateral membrane of the intestine into the pseudocoelom to be utilized by extraintestinal tissues [12, 13]. Surprisingly, depletion of *mrp-5* results in upregulation of GFP in the heme sensor strain IQ6011 despite resulting in intestinal heme accumulation. This suggests that the heme deficiency signal observed in the absence of MRP-5 is likely originating from extraintestinal tissues. Data from our genome-wide RNAi screen for modulators of heme homeostasis supported the existence of an intertissue communication network, as ~30% of the genes identified from the screen were not reported as being expressed in the intestine, despite regulating two intestinal heme reporters. Analyses of candidate genes with signal peptides uncovered the aspartic protease-like HRG-7 and the cysteine protease-like HRG-8 as potential secreted regulators of heme homeostasis. Further analyses revealed that HRG-7 and HRG-8 are upregulated by low heme in the intestine, are then secreted and, surprisingly, localize to neurons. Therefore, the communication between the intestine and extraintestinal tissues is likely bidirectional, and the communication between the gut and neurons may be of particular importance.

It is intuitive that extraintestinal signals, which rely on the intestine for heme, can direct the intestinal release of heme, but why does a signal also need to come from the intestine, the source of heme? In vertebrates, several nutrient receptors that are expressed on the tongue are also expressed in the intestinal EECs, including the sugar receptors T1R2 /T1R3 [179]. When these receptors are activated by sugars, the EECs secrete GLP-1 and GIP that target the brain and pancreas, resulting in altered feeding behavior and increased insulin secretion [76]. Similarly, intestinal iron

content is communicated to other tissues through BMP6 [180]. By probing the environment and its own nutrient content, the intestine is able to signal nutrient availability to extraintestinal tissues, allowing them to adapt accordingly. In this fashion, intestinal sensing and signaling through HRG-7 and HRG-8 may allow extraintestinal tissues to adapt to varying environmental heme availability.

It is noteworthy that promoters of only three genes, *hrg-1*, *mrp-5*, and *hrg-7,* contain the *cis* HERE motif. HRG-1 is involved in the release of heme stored in vesicles while MRP-5 allows heme to be exported from basolateral membrane of the intestine. HRG-7, meanwhile, may facilitate heme utilization in extraintestinal tissues. Therefore, each of the genes regulated by the HERE are interlinked; heme import, heme export, and integration of heme import and export with the rest of the body. Furthermore, our data indicate that the intestinal HERE can receive signals from distal tissues, giving these tissues input into control of intestinal heme levels. Together, this implicates that the HERE has an important role beyond the intestine.

Why do HRG-7 and HRG-8 localize to amphid sensory neurons? Interestingly, sensory neurons in *C. elegans* are unique in that they are the only cell types that are ciliated. Ciliated sensory neurons control systemic lipid homeostasis by regulating intestinal fat storage, which similarly to heme homeostasis likely requires bidirectional signaling between neurons and the intestine. This regulation is dependent on a protein called TUB-1, which is most strongly expressed in amphid and phasmid neurons, which are poised for sensing external and internal nutrient levels [74]. Furthermore, intact cilia are required for normal lipid homeostasis, and cilia mediated signaling is required for metabolic adaptations [181]. Thus sensory

neurons are uniquely adapted and have an emerging role in systemic nutrient homeostasis.

Although it is anticipated that pathways exist that allow the intertissue distribution of heme in a heme auxotroph such as *C. elegans*, several lines of evidence suggest that heme is also transported between cells in organisms that make heme. Disruptions to heme homeostasis or systemic iron homeostasis can result in anemia, so intertissue heme trafficking cannot substitute for heme synthesis. However, different tissue types have different heme requirements, and some tissues may rely more on heme uptake than others. Additionally, intertissue heme transport may be relevant during iron deficiency or pathological states [17, 182]. Taken together, our results indicate that an intertissue signaling network exists for maintenance of systemic heme homeostasis in *C. elegans*, and based on evidence supporting intertissue heme distribution in vertebrates, portions of this network may be conserved in mammals.

Chapter 4: Characterization of HRG-7 and HRG-8

Summary

Our genome-wide screen for modulators of systemic heme homeostasis revealed that the protease homologs HRG-7 and HRG-8 are secreted from the intestine and localize to neurons to mediate systemic heme homeostasis. Here, we show that although both genes are required for normal growth and reproduction, only the *hrg-7* growth defect can be rescued by heme supplementation. Moreover, ectopically expressed HRG-7 and HRG-8 regulate heme homeostasis only when expressed from the intestine, but not from the neuron or muscle. Intestinal secretion of HRG-7 is a prerequisite for proper function, as depletion of specific trafficking factors revealed that the secretion and maturation of HRG-7 require post-Golgi fusion events and low pH. Unlike other protease orthologs, cleavage of the HRG-7 propeptide requires a trans-acting protease and mutating the active site did not eliminate rescue of *hrg-1::GFP* upregulation in the intestine. These results reveal that, at least, a portion of the regulatory function of HRG-7 is independent of its proteolytic activity. Together, our data indicate that HRG-7 and HRG-8 must be secreted from the intestine to regulate *hrg-1::GFP*, and this regulation may be independent of proteolytic activity. Although proteases have been implicated in the breakdown of hemoglobin and therefore heme uptake in helminthic worms, the use of protease-like molecules to govern systemic homeostasis of a specific micronutrient is unprecedented.

Results

HRG-7 and HRG-8 are required for normal growth and reproduction

As previously mentioned, depletion of *hrg-7* in the RNAi hypersensitive strain VH624 results in embryonic lethality, which can be rescued by heme supplementation of bacterial RNAi cultures. This phenotype suggested that *hrg-7* was required for normal growth specifically in heme-limiting conditions. To further evaluate the correlation of *hrg-7* with organismal heme levels, we knocked down *hrg-7* by dsRNA injection in strain IQ6916, a double mutant for *hrg-1* and *hrg-4*. IQ6916 worms show a heme-dependent growth delay due to reduced intestinal heme import [19]. The F1 progeny from P0 worms injected with dsRNA were grown on heme synthesis deficient RP523 bacteria supplemented with 1 μM or 50 μM heme [166]. While worms injected with dsRNA against control vector at 1 μM heme showed minimal growth delay compared to worms grown at 50 μM heme, worms injected with dsRNA against *hrg-7* at 1 μM heme were severely growth retarded (**Figure 4.1A**). This phenotype was fully rescued by supplementation with 50 μM heme, confirming that *hrg-7* is required specifically when organismal heme levels are low.

Depletion of *hrg-8* in strain VH624 did not result in embryonic lethality. However, *hrg-8* depleted worms had a slight growth delay and appeared to produce less F1 progeny than worms fed dsRNA against vector control only. Therefore, we performed a brood size experiment to evaluate the effects of *hrg-8* on reproduction. Synchronized VH624 L1s were fed dsRNA against control vector or *hrg-8* for 72 hours, then transferred to fresh RNAi plates to determine brood size. We found that

Figure 4.1: HRG-7 and HRG-8 are required for normal growth and development

A) Growth analyses of IQ6916 (*hrg-1(tm3199)*, *hrg-4(tm2994)*) injected with dsRNA against control vector or *hrg-7* and supplemented with 1 µM or 50 µM heme. Images are 20x. **B)** F1 brood size analyses of strain VH624 (*nre-1*; *lin-15b*(*hd126*)) fed dsRNA against control vector or *hrg-8*. Graph is representative of 3 replicates, with 3 P0s per replicate. *P<0.05 (T-test).

A

IQ6916(Δ*hrg-1*; Δ*hrg-4*)

F1 progeny

vector

hrg-7

1 μM heme   **20 μM heme**
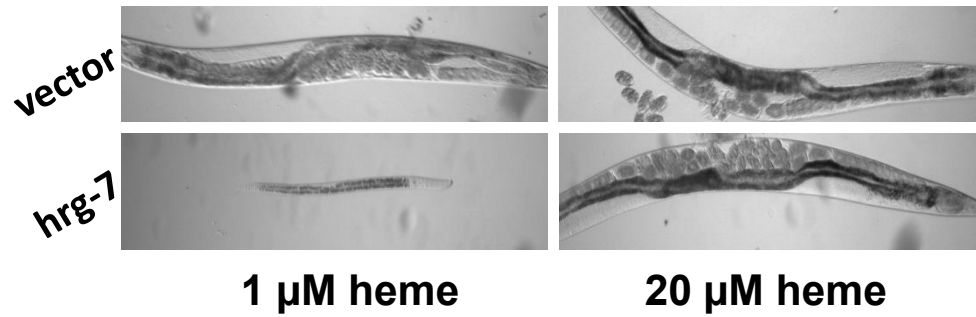
B
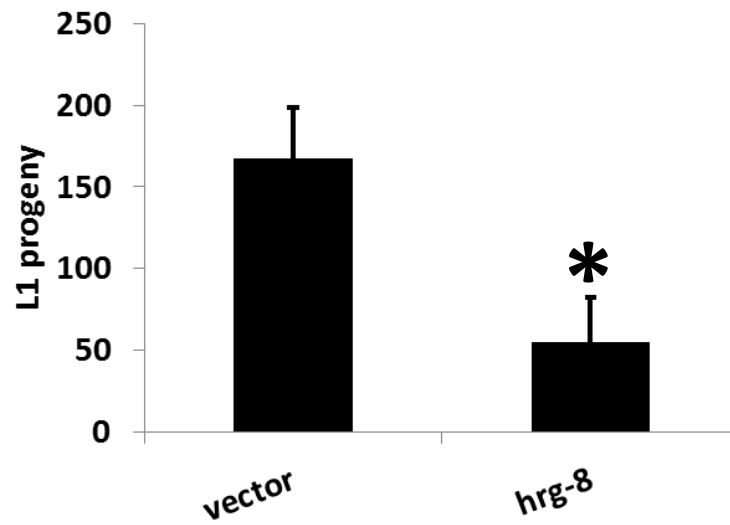
hrg-8 RNAi worms had a significantly reduced brood size **(Figure 4.1B)**. This reduction in brood size was independent of heme concentration. Notably, an *hrg-8* deletion allele (*ok2017*) is homozygous embryonic lethal, and neither excess heme nor ectopic expression of *hrg-8* rescued embryonic lethality.

Together, our data indicate that HRG-7 is crucial under low heme conditions, while HRG-8 appears to be required normal growth and reproduction across a wide-range of heme concentrations even though both genes are highly responsive under low heme.

HRG-7 and HRG-8 need to be secreted from the intestine to suppress intestinal expression of *hrg-1*

Our data had indicated that HRG-7 and HRG-8 are secreted from the intestine and localize to neurons. However, it was unclear whether HRG-7 and HRG-8 A) had to be expressed specifically in the intestine; B) was functional only after secretion, and; C) whether internalization into its cognate tissue was essential for function. In order to address these questions, we expressed HRG-7 and HRG-8 from various tissues or membrane anchored HRG-7 and HRG-8 to prevent its internalization into distal tissues **(Figure 4.2A)**. To test the functionality of these ectopically expressed transgenes we synthesized recoded *hrg-7* (*hrg-7^{PR}*) and recoded *hrg-8* (*hrg-8^{REC}*) by introducing silent mutations into the degenerate site of each codon **(Appendix V)**. These mutations result in the transgene being resistant to RNAi but not the endogenous *hrg-7* and *hrg-8*. Unlike *hrg-8*, recoding the entire sequence of *hrg-7* led to poor expression, so only the first 300 bp were recoded. We

Figure 4.2: Schematics for HRG-7^{PR} and HRG-8^{REC} secretion and membrane anchoring by transgenic expression

A) Model depicting HRG-7 and HRG-8 expressed transgenically in the intestine (endogenous tissue of origin), the muscle (ectopic expression) and neurons (target tissue), with and without tethering to the cell membrane. **B)** Schematic for generation of *C. elegans* strains to assay the localization requirements of HRG-7 and HRG-8.

A

Neuron

Muscle

Circulation

HRG-7/8

HRG-7/8

HRG-7/8

HRG-7/8

HRG-7/8

Intestine
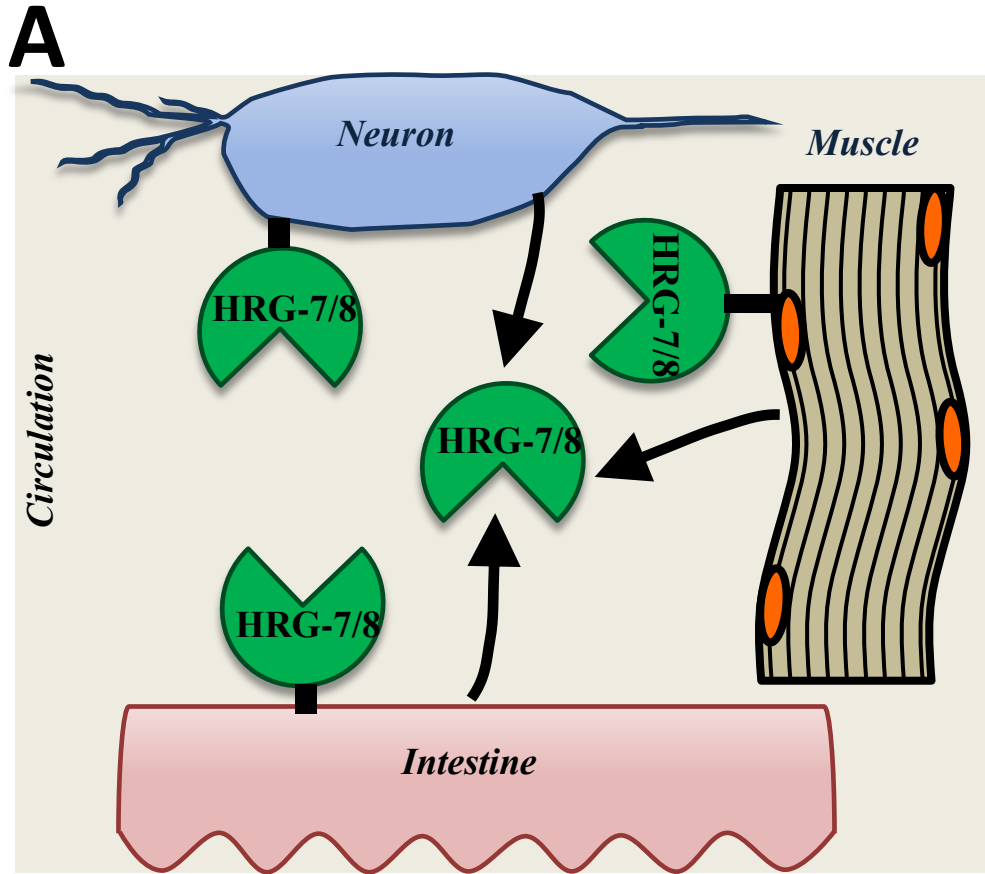
B

Recoded (RNAi resistant) rescue constructs

HRG-7$_{PR}^{PR}$::ICS::mCherry

HRG-7$_{PR}$::mCherry

HRG-7 ::mCherry-TM

intestine (*vha-6* promoter)

muscle (*myo-3* promoter)

neuron (*unc-119* promoter)

HRG-8$_{REC}^{REC}$::ICS::mCherry

HRG-8^{REC}::mCherry

HRG-8^{REC}::mCherry-TM

IQ6011 (*hrg-1::gfp*)
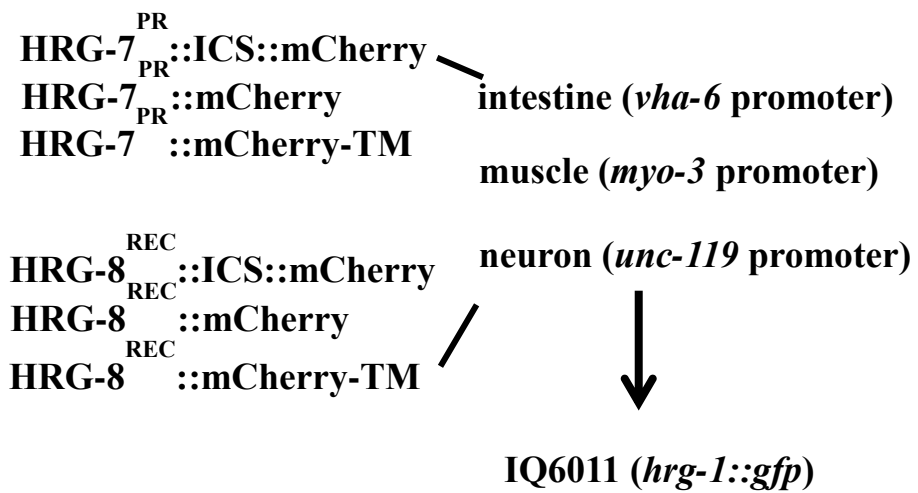
then generated a mCherry with or without a transmembrane domain on the carboxyl terminal. We chose the transmembrane domain from the Tac antigen, which is the alpha chain of the interleukin-2 receptor, or a GPI anchor . We speculated that incorporation of a transmembrane domain would anchor HRG-7^{PR} and HRG-8^{REC} to the cell surface with the protein facing the extracellular space, allowing contact with the pseudocoelom but preventing localization to distal tissues. In addition to the mCherry tag, we generated constructs with an intercistronic (ICS) SL2 sequence preceding mCherry, which enabled *hrg-7*^{PR} and *hrg-8*^{REC} to be translated independently from mCherry through a trans-splicing mechanism in the event that tagging the carboxyl terminus interfered with function [183]. All the RNAi resistant transgenes were then driven from three different promoters: the intestine (*vha-6*), the body wall muscle (*myo-3*), or neuron (*unc-119*). Finally, worms expressing each of these transgenes were crossed to IQ6011 to interrogate the consequences of these transgenes on intestinal *hrg-1* expression **(Figure 4.2B)**.

For functional studies of HRG-7^{PR}, we utilized two RNAi constructs: ds*hrg-7*^{300bp} and ds*hrg7*^{ORF}. The former sequence only targets the first 300 bp of *hrg-7*, and thus does not knock down *hrg-7*^{PR}, while the latter targets the entire *hrg-7* ORF and will therefore knockdown both endogenous *hrg-7* and *hrg-7*^{PR}. Indeed, western blots of non-transgenic worms and worms expressing *P$_{vha-6}$::HRG-7^{PR}::ICS::mCherry* confirmed that our transgenes were functioning as expected **(Figure 4.3A)**. By comparing *hrg-1::GFP* expression in double transgenic worms after knockdown of *hrg-7* with both RNAi clones, we determined the proportion of rescued animals as a

Figure 4.3: RNAi resistant HRG-7 driven from an intestinal promoter rescues

$P_{hrg-1}::GFP$ **expression**

A) Immunoblot analysis of HRG-7 and HRG-7^{PR} from IQ6011 ($P_{hrg-1}::GFP$) and

IQ7711 ($P_{vha-6}::HRG-7^{PR}:ICS::mCherry, P_{hrg-1}::GFP$) fed dsRNA against control

vector, $hrg-7^{300bp}$, and $hrg-7^{ORF}$. Membranes were probed with polyclonal anti-HRG-

7 antibody and then incubated with HRP-conjugated anti-rabbit secondary antibody. *

indicates pro-HRG-7. + indicates mature HRG-7. Arrowhead indicates tubulin **B)**

GFP fluorescence (120 worms per treatment) quantified from IQ6011 ($P_{hrg-1}::GFP$)

and IQ7711 ($P_{vha-6}::HRG-7^{PR}:ICS::mCherry, P_{hrg-1}::GFP$) fed dsRNA against control

vector, $hrg-7^{300bp}$, and $hrg-7^{ORF}$ at 10 µM heme. GFP was quantified using COPAS

BioSort. ***P<0.001 (one-way ANOVA). **C)** GFP fluorescence (120 worms per

treatment) quantified from IQ6011 ($P_{hrg-1}::GFP$) and IQ7771 ($P_{vha-6}::HRG-$

$7^{PR}::mCherry, P_{hrg-1}::GFP$) fed dsRNA against control vector, $hrg-7^{300bp}$, and $hrg-$

7^{ORF} at 10 µM heme. GFP was quantified using COPAS BioSort. ***P<0.001 (one-

way ANOVA).

A

vector   hrg-7^300bp   hrg-7^ORF   vector   hrg-7^300bp   hrg-7^ORF

*
+

◄

IQ6011   IQ7711

B

P_{hrg-1}::GFP

ns   ***

7
6
5
4
3
2
1
0

IQ6011   IQ7711

□ vector
■ hrg-7_300bp
▨ hrg-7_ORF

P_{vha-6}::hrg-7^{PR}::|ICS|::mCherry

C

P_{hrg-1}::GFP

ns   ***

8
7
6
5
4
3
2
1
0

IQ6011   IQ7771

□ vector
■ hrg-7_300bp
▨ hrg-7_ORF

P_{vha-6}::hrg-7^{PR}::mCherry
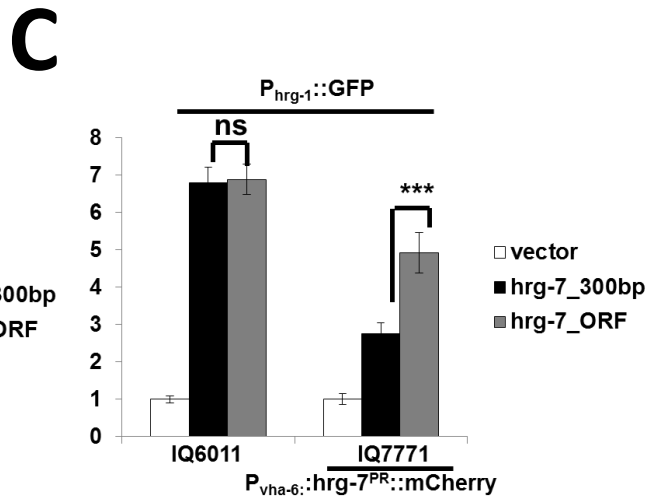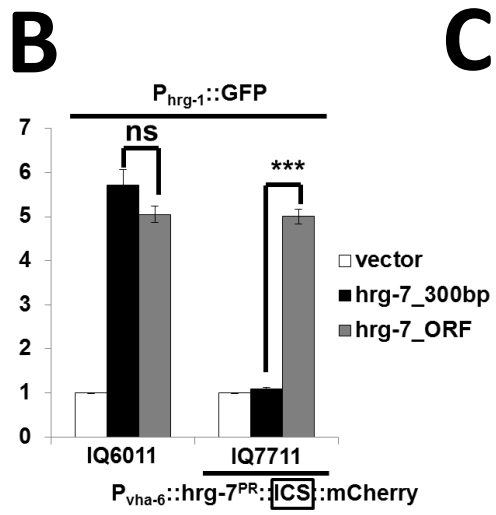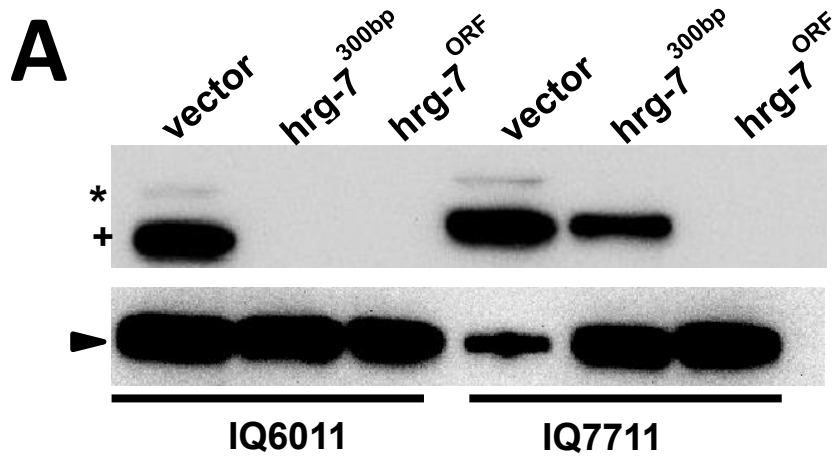
function of the transgene, HRG-7^{PR}. We found that expressing untagged HRG-7^{PR} in the intestine, when endogenous *hrg-7* is depleted with *dshrg-7*^{300bp}, was sufficient to restore *hrg-1::GFP* levels to that observed in worms fed vector only **(Figure 4.3B)**. This rescue is specific to *hrg-7^{PR}*, as knocking down both *hrg-7* and *hrg-7^{PR}* with *dshrg7*^{ORF} results in upregulation of *hrg-1::GFP* comparable to worms not expressing *hrg-7^{PR}*. Additionally, HRG-7^{PR} fused directly to mCherry showed significant rescue (P<0.001) **(Figure 4.3C)**, indicating the HRG-7 with a carboxyl terminus tag still retains significant function and that the observed localization of HRG- 7::mCherry is authentic. For HRG-8^{REC} with and without a mCherry tag, intestinal driven expression was sufficient to rescue *hrg-1::GFP* expression **(Figure 4.4A, B)**. Together these data demonstrate that *hrg-7^{PR}* and *hrg-8^{REC}* secreted from an intestinal specific promoter is functional in the IQ6011 strain.

We postulated that if HRG-7 and HRG-8 are involved in cell non-autonomous communication, it was possible that they would retain function when expressed ectopically from another tissue, such as the muscle or directly in the target tissue – neurons. However, we observed no rescue of *hrg-1::GFP* when endogenous *hrg-7* was depleted and *HRG-7^{PR}::ICS::mCherry* was expressed from the muscle or neuron **(Appendix VI A , neuron not shown)**. To ascertain whether mature HRG-7^{PR} was even made in these tissues, we knocked down endogenous *hrg-7* in strains ectopically expressing *hrg-7^{PR}* and immunoblotted for HRG-7. We observed that mature HRG-7 was only produced when expressed in the intestine **(Appendix VI B)**. The muscle expressed a higher molecular weight band that did not correlate with the mature HRG-7, and no HRG-7^{PR} was detected in neurons. Similarly, we observed no rescue
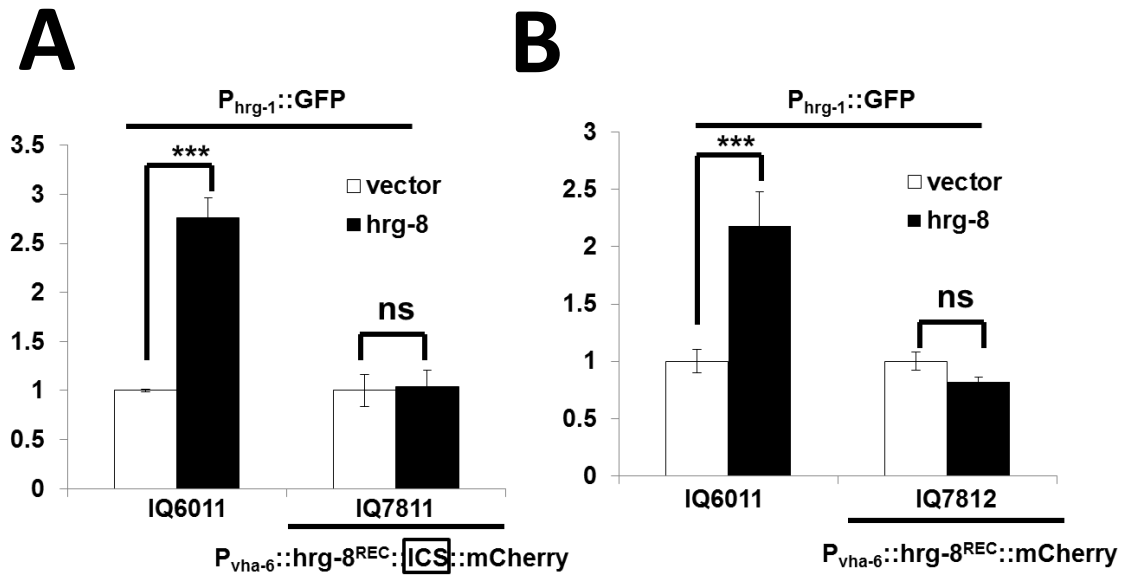
Figure 4.4: RNAi resistant HRG-8 driven from an intestinal promoter rescues

P_{hrg-1}*::GFP* **expression**

A) GFP fluorescence (120 worms per treatment) quantified from IQ6011 (P_{hrg-1}*::GFP*) and IQ7811 (P_{vha-6}*::HRG-8^{REC}:ICS::mCherry, P_{hrg-1}::GFP*) fed dsRNA against vector or *hrg-8* at 10 μM heme. GFP was quantified using COPAS BioSort. ***P<0.001 (one-way ANOVA). **B)** GFP fluorescence (120 worms per treatment) quantified from IQ6011 (P_{hrg-1}*::GFP*) and IQ7881 (P_{vha-6}*::HRG-8^{REC}::mCherry, P_{hrg-1}::GFP*) fed dsRNA against vector, *hrg-7^{300bp}*, and *hrg-7^{ORF}* at 10 μM heme. GFP was quantified using COPAS BioSort. ***P<0.001 (one-way ANOVA).

when $hrg8^{REC}$ was expressed from muscle or neuron (**Appendix VI C, neuron not shown**). Together, these results indicate that HRG-7 and HRG-8 have to be synthesized in the intestine for function.

HRG-7 secretion is required for function

Next, we asked if HRG-7 and HRG-8 retained function when anchored to the intestinal plasma membrane facing the extracellular space, or if they required contact with a distal tissue to function. However, attempts to anchor HRG-7^{PR} and HRG-8^{REC} to the plasma membrane proved unsuccessful. Although placing the Tac receptor transmembrane domain on the carboxyl terminus of HRG-7^{PR}::mCherry appeared to successfully membrane-anchor the chimeric protein, it was not localized to the plasma membrane. Rather, it seemed to accumulate in large vesicles within the intestine, and not accessible to pseudocoelom as we could have expected (**Appendix VII A**). Similar results were observed for HRG-8^{REC}::mCherry-Tac. A GPI anchor on the carboxyl terminus of HRG-8^{REC}::mCherry did inhibit secretion, and we did not observe any expression of HRG-7^{PR}::mCherry-GPI (**Appendix VII B, HRG-7 not shown**). We also attempted to anchor HRG-8^{REC} using the LDLR receptor transmembrane domain. However, similar to the Tac receptor, HRG-8$^{rec::}$mCherry-LDLR accumulated within intracellular vesicles in the intestine (**Appendix VII C**). Therefore, it remained inconclusive whether HRG-7 and HRG-8 required secretion and contact with distal tissues.

Due to the technical difficulties we encountered trying to express chimeric membrane anchored proteins for both HRG-7 and HRG-8, we decided to focus our

97

efforts on deciphering the function of HRG-7 because of the heme-dependent phenotype of *hrg-7* RNAi in worms. During protein maturation, HRG-7 temporarily has an endogenous transmembrane domain; the signal peptide tethers HRG-7 to the ER prior to proteolysis by a signal peptidase. Therefore, we mutated the signal peptidase cleavage site, A16-E17, to Y16-Y17 in HRG-7^{PR}::mCherry. A second possible cleavage site, Q20-F21, was also mutated to adjacent tyrosines. These mutations result in the signal peptide remaining as a transmembrane domain, similar to a signal-anchor sequence. (TM-HRG-7^{PR}::mCherry). Unlike previous attempts to membrane anchor HRG-7^{PR}, mutation of the signal peptide resulted in an even distribution of TM-HRG-7^{PR} throughout the intestine and prevented accumulation in extraintestinal tissues such as the coelomocytes, indicating that TM-HRG-7^{PR} was successfully membrane-anchored facing the luminal side of the secretory pathway **(Figure 4.5A)**. We then crossed *P$_{vha-6}$:: TM-HRG-7^{pr}::mCherry* into IQ6011 (strain IQ7712) and evaluated *hrg-1::GFP* rescue when endogenous *hrg-7* is knocked down. TM-HRG-7^{PR} had no effect on *hrg-1* expression suggesting that HRG-7 must be secreted form the intestine to elicit a biological response **(Figure 4.5B)**. This result confirms that the heme deficiency signal observed in the intestine is through cell non-autonomous mechanisms as HRG-7 accumulation within the intestine in the absence of secretion is unable to suppress intestinal *hrg-1* expression.

Figure 4.5: HRG-7 requires secretion from the intestine to function

A) mCherry fluorescence in worms expressing $P_{vha-6}::HRG-7^{PR}::mCherry$ or $P_{vha-6}::TM-HRG-7^{PR}::mCherry$. Arrows indicate coelomocytes. **B)** GFP fluorescence (120 worms per treatment) quantified from IQ6011 ($P_{hrg-1}::GFP$), IQ7771 ($P_{vha-6}::HRG-7^{PR}::mCherry, P_{hrg-1}::GFP$), and IQ7412 ($P_{vha-6}::TM-HRG-7^{PR}:ICS::mCherry, P_{hrg-1}::GFP$) fed dsRNA against vector, $hrg-7^{300bp}$, and $hrg-7^{ORF}$ at 10 µM heme. GFP was quantified using COPAS BioSort. ***P<0.001 (one-way ANOVA).

A

HRG-7 | TM-HRG-7

mCherry

DIC

B

$P_{hrg\text{-}1}::GFP$

☐ vector ■ hrg-7^{300bp} ☐ hrg-7^{ORF}

GFP

ns   ***   ns

HRG-7^{PR}::mCherry

TM-HRG-7^{PR}::mCherry
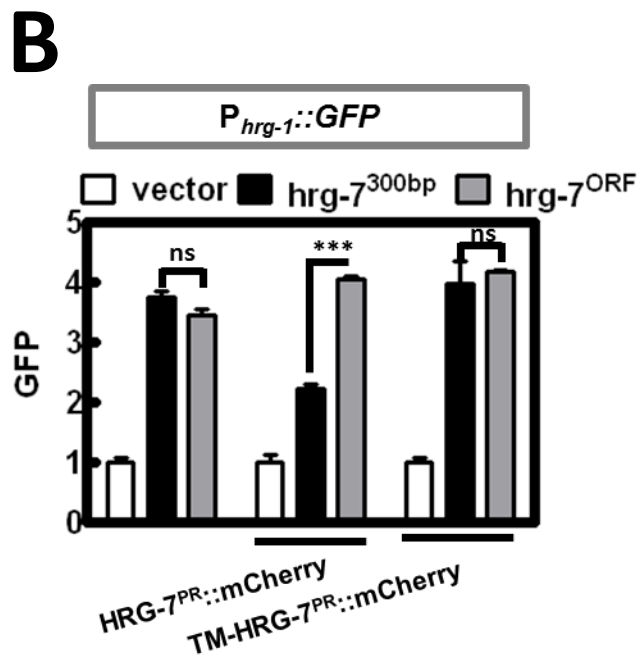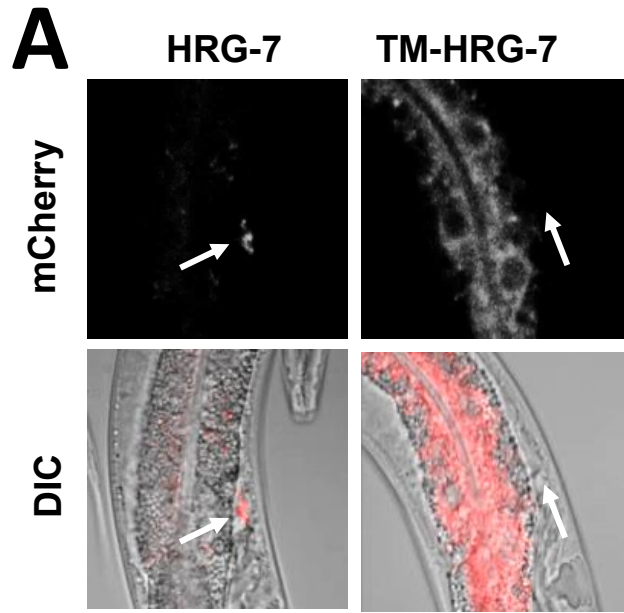
HRG-7 secretion and maturation requires specific trafficking factors

We found it intriguing that mature, functional HRG-7 could only be produced and secreted from the intestine, implying that there may be specific compartments or factors that aid in HRG-7 folding, maturation, and secretion. To gain a better understanding of HRG-7 secretion, we drove HRG-7::mCherry expression from the *hsp-16.2* promoter, which is active in several tissues including the intestine (IQ7170) [184]. Approximately 180 minutes after heat shock of IQ7170, mCherry fluorescence was clearly visible in the pseudocoelomic fluid (**Figure 4.6A**). After 360 minutes, strong fluorescence was observed in coelomocytes without accumulation in the intestine, suggesting that HRG-7 is secreted shortly after translation (**Figure 4.6B**). To uncover regulators of HRG-7 secretion, we knocked down 45 known trafficking genes in strain IQ7670 [185]. We observed that depletion of the SNARE protein SNAP-29 or components of the vacuolar ATPase resulted in accumulation of HRG-7::mCherry in the intestine (**Figure 4.7A**). Moreover, depletion of these genes results in accumulation of pro-HRG-7 (**Figure 4.7B**). Specific trafficking pathways are involved in the regulation of HRG-7 trafficking and maturation, as depletion of *sec-6*, a component of the exocyst complex, did not affect HRG-7. Together, these results suggest that HRG-7 maturation and secretion requires specific factors involved in post-Golgi fusion events and vesicular acidification. Additionally, we found that some of the factors that regulated HRG-7 did not regulate HRG-8 secretion and *vice versa* implying that even though there are commonalities to both proteins there are also differences in their membrane trafficking (**Table 4.1**). It has been demonstrated that the v-ATPase complex can regulate secretion independently of its role as a pH

101
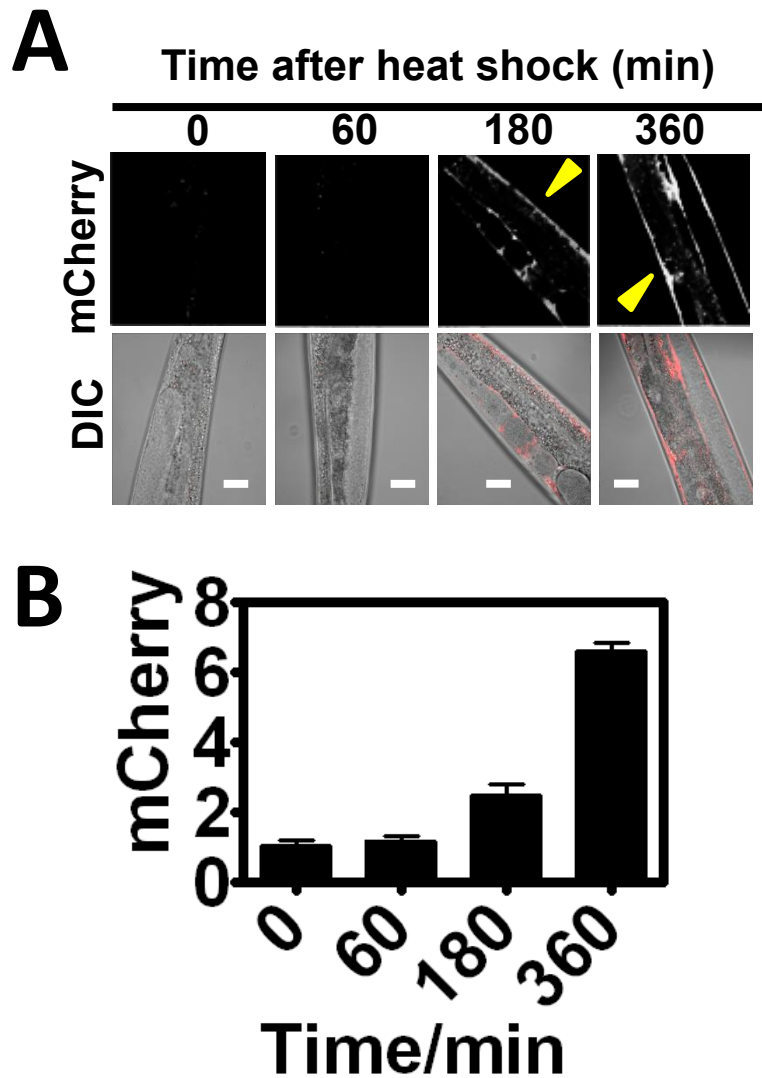
Figure 4.6: HRG-7 is quickly secreted from the intestine after translation

A) mCherry expression in strain IQ7170 ($P_{hsp\text{-}16.2}$::*HRG-7*::*mCherry*) placed in 37°C for 30 minutes, then 20°C for 60, 180, and 360 minutes. Arrowheads indicate pseudocoelom. Images are 63x. Scale bar = 20 µm. **B)** Quantification of coelomocytes using region of interest function on simple PCI software.
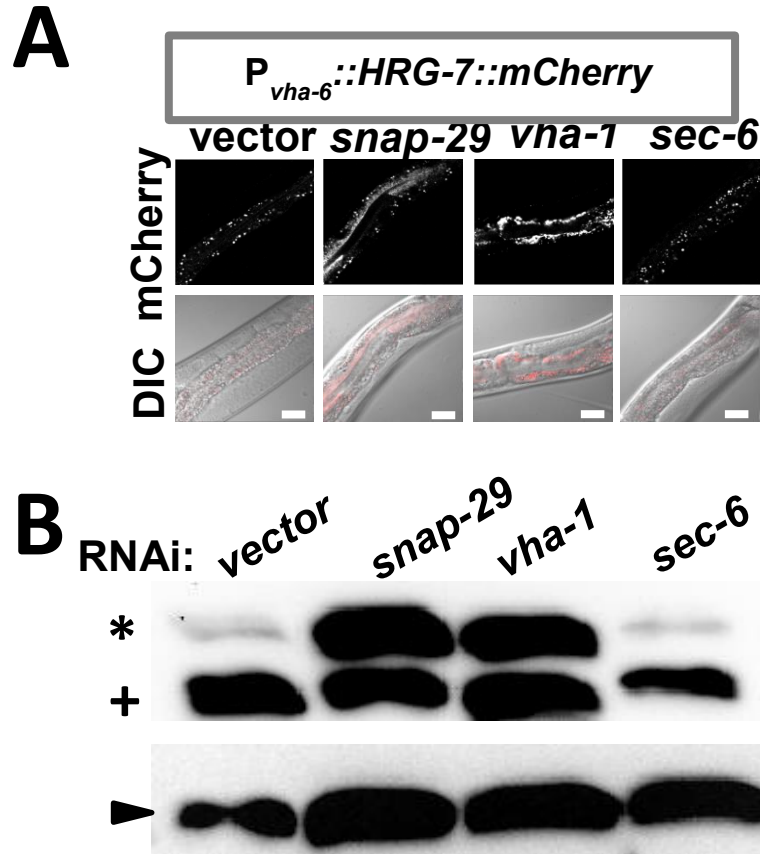
Figure 4.7: HRG-7 secretion and maturation is regulated by specific membrane trafficking factors

A) mCherry expression in strain IQ7670 (P_{vha-6}::HRG-7::mCherry) fed dsRNA against vector, *snap-29*, *vha-1*, and *sec-6*. Images are 63x. Scale bar = 20 μm. **B)** Immunoblot analysis of strain N2 fed dsRNA against vector, *snap-29*, *vha-1*, and *sec-6*. Membranes were probed with polyclonal anti-HRG-7 antibody and then incubated with HRP-conjugated anti-rabbit secondary antibody. * indicates pro-HRG-7. + indicates mature HRG-7. Arrowhead indicates tubulin.

Table 4.1: Specific regulators of the secretory pathway direct HRG-7 and HRG-8 trafficking and secretion from the intestine

Gene ID	HRG-7::mCherry		HRG-8::mCherry		Description
	Intestine	Circulation	Intestine	Circulation	
Y113G7A.3	Increased	nc	Increased	nc	vesicle coat complex COPII, subunit SEC23
F12F6.6	nc	nc	Increased	nc	encodes one of two C. elegans Sec24 homologs
K02D10.5	Increased	nc	nc	nc	SNAP-25 component of SNARE complex
T14G10.5	Increased	nc	Increased	nc	gamma subunit of the coatomer (COPI) complex
Y25C1A.5	Increased	nc	Increased	nc	beta subunit of the coatomer (COPI) complex
ZK180.4	nc	nc	Increased	nc	vesicle coat complex COPII, GTPase subunit SAR1
T20G5.1	Increased	nc	Increased	nc	vesicle coat protein clathrin, heavy chain
C01G8.5	Increased	Increased	nc	nc	ortholog of the ERM family of cytoskeletal linkers
R10E11.8	Increased	Increased	nc	Increased	16-kDa proteolipid of the vacuolar-type H+-ATPase
R10E11.2	nc	nc	Increased	nc	16-kDa proteolipid of the vacuolar-type H+-ATPase
T01H3.1	Increased	nc	Increased	nc	vacuolar H+-ATPase V0 sector, subunit c
C17H12.14	Increased	nc	Increased	nc	E subunit of a V-ATPase (vacuolar H+-ATPase)
ZK970.4	Increased	nc	Increased	nc	vacuolar H+-ATPase V1 sector, subunit F
Y49A3A.2	Increased	nc	Increased	nc	vacuolar H+-ATPase V1 sector, subunit A

Red lettering denotes factors specific to one protein but not the other.

regulator through proton transport [186]. Therefore, in order to further evaluate

whether pH influenced HRG-7 maturation, we analyzed lysate from *C. elegans*

expressing HRG-7::3xFLAG (strain IQ7370) at neutral or acidic pH. Immunoblots of

the 3xFLAG tagged HRG-7 show the presence of a discernible propeptide form of the

protein indicative of a slower maturation time. We capitalized on this aspect to study

the dynamics of HRG-7 maturation. While no HRG-7::3xFLAG propeptide

processing occurs in lysates at pH 7.2, maturation is quickly induced in lysate titrated

to pH 4, with over 90% of HRG-7-3xFLAG processed within 20 minutes **(Figure

4.8A)**. We exposed IQ7370 lysate to a pH gradient to determine the optimal pH for

processing and found that HRG-7::3xFLAG maturation was expedited as acidity

increased **(Figure 4.8B)**. These results confirm that HRG-7 requires trafficking

through acidic compartments where it is processed to the mature form. Because

aspartic proteases such as pepsin undergo autocatalysis of the propeptide when

exposed to acidic conditions, [187], while renin requires an unidentified trans-acting

protease for maturation [133], we interrogated whether HRG-7 requires the predicted

D90 D318 active site aspartic acid residues maturation. We mutated both D90 and

D318 to an alanine in HRG-7^{PR} to generate iHRG-7^{PR} **(Figure 4.9A)**. Mutation of the

aspartic acid residues did not result in accumulation of pro-HRG-7, suggesting that a

trans-acting protease must be responsible for pro-HRG-7 processing to the mature

form **(Figure 4.9B)**. We next crossed *Pvha-6::iHRG-7^{PR}::ICS::mCherry* into IQ6011

(strain IQ7712) to evaluate whether the predicted catalytic residues were involved in

heme signaling through regulation of *hrg-1*. Surprisingly, there was significant

A HRG-7-3xFLAG

20 min | 10 min | 15 min | 20 min

* pro-HRG-7-3xFLAG
+ ~50kD

pH = 7.2   pH = 4

B

% processed vs pH: 7.2 6.5 6 5.5 5 4.5 4

Time = 20 min
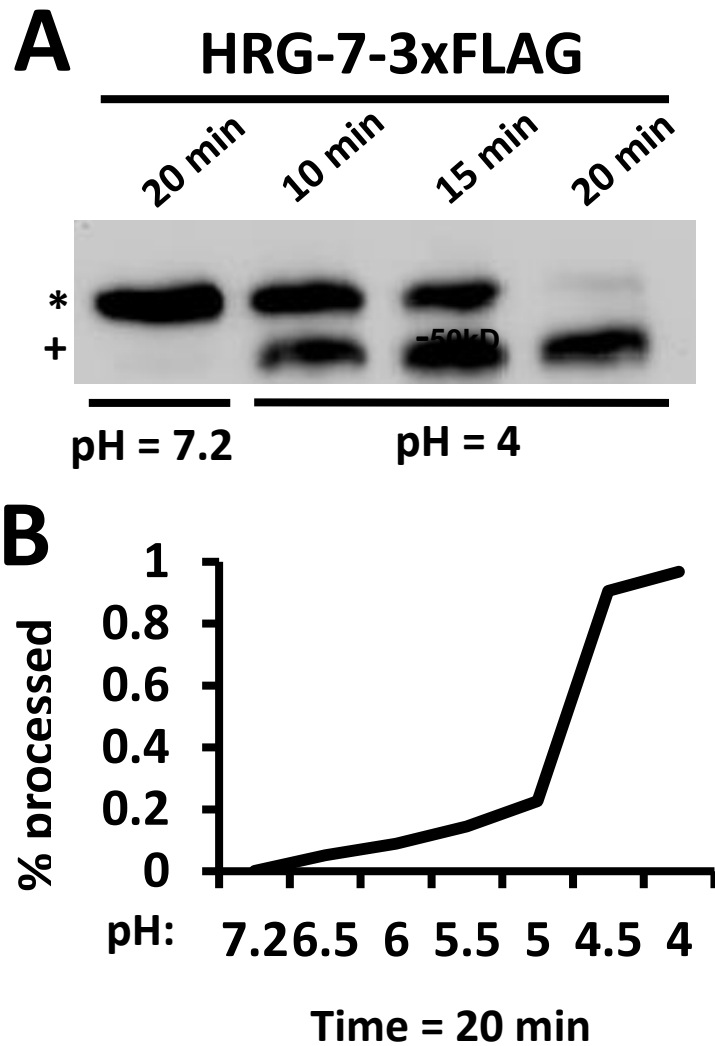
Figure 4.8: Acidic conditions facilitate HRG-7 maturation

A) Immunoblot analysis of lysate prepared from strain IQ7370 (P_{vha-6}::HRG-7::3xFLAG) at pH 7.2 and pH 4. Membranes were probed with monoclonal anti-FLAG antibody and then incubated with HRP-conjugated anti-mouse secondary antibody. * indicates pro-HRG-7-3xFLAG. + indicates mature HRG-7-3xFLAG. **B)** Quantification of immunoblot analyses of IQ7370 lysate and maintained at indicated pH values for 20 minutes. Quantification was performed with Chemidoc software.

Figure 4.9: HRG-7 does not require the predicted catalytic aspartates for maturation or regulation of *hrg-1::GFP*

A) Cartoon depicting mutation of the predicted catalytic aspartic acid residues D90 and D318 to alanines to make iHRG-7. **B)** Immunoblot analysis of lysate from N2, worms expressing P_{vha-6}::HRG-7::ICS::mCherry, and worms expressing P_{vha-6}::iHRG-7::ICS::mCherry. Membranes were probed with polyclonal anti-HRG-7 antibody and then incubated with HRP-conjugated anti-rabbit secondary antibody. **C)** GFP fluorescence (120 worms per treatment) quantified from IQ6011 (P_{hrg-1}::GFP), IQ7711 (P_{vha-6}::HRG-7^{PR}:ICS::mCherry, P_{hrg-1}::GFP), and IQ7712 (P_{vha-6}::iHRG-7^{PR}:ICS::mCherry, P_{hrg-1}::GFP) fed dsRNA against vector, $hrg-7^{300bp}$, and $hrg-7^{ORF}$ at 10 μM heme. GFP was quantified using COPAS BioSort. ***P<0.001 (one-way ANOVA).
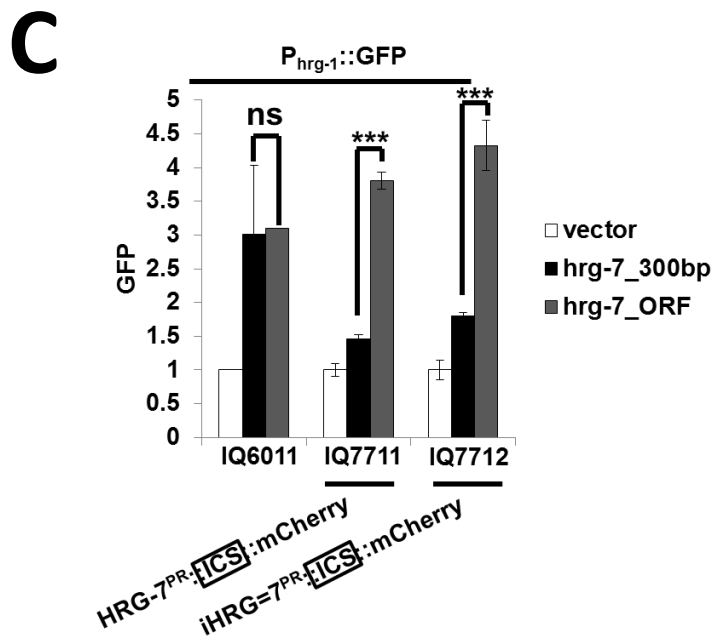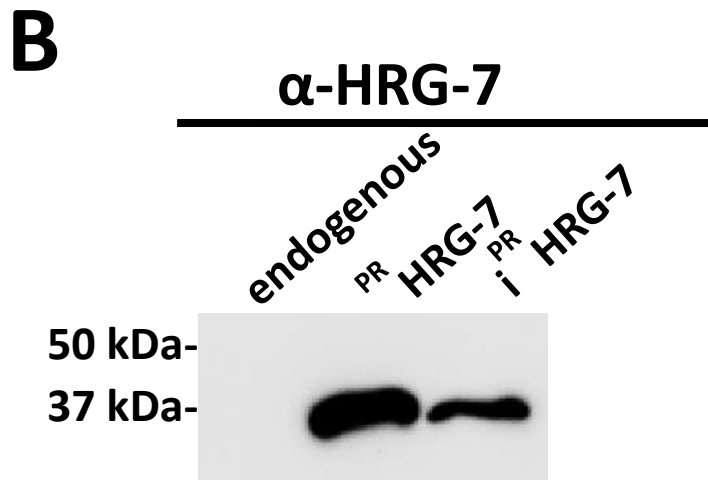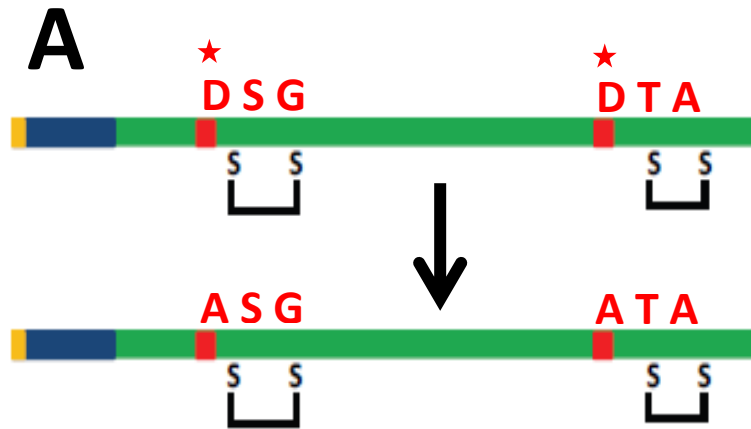
rescue of $P_{hrg-1}::GFP$ expression, indicating that HRG-7 function is, at least in part, independent of the predicted catalytic residues **(Figure 4.9C)**.

Discussion

We have demonstrated that functionally competent HRG-7 must be expressed from its native tissue of origin, the intestine, and secreted. Further analyses of HRG-7 through an RNAi screen of *C. elegans* trafficking factors reveal that maturation and secretion of HRG-7 requires acidification and post-Golgi fusion events. The *in silico* prediction of putative active sites for HRG-7 is not essential for maturation, suggesting that either a trans-acting protease in the intestine is required for activation of HRG-7 or the presence of other active site residues. Correspondingly, the predicted active site of HRG-7 was not required for *hrg-1* regulation suggesting that systemic heme homeostasis may be independent of the canonical aspartic protease activity of HRG-7.

Why do protease homologs, potentially devoid of catalytic activity, play such an important role in heme homeostasis? Proteases have several features that make them attractive candidates for signaling mechanisms. They are involved in interactions with their cognate substrates or inhibitors. Many are secreted or localize to the secretory pathway, so they have signal peptides. And, like many canonical signaling factors and hormones, they are inactive until removal of a propeptide, allowing a rapid cellular response to stimuli. It is becoming evident that proteases have expansive and essential roles in intercellular cell signaling [126]. Furthermore, there are over two hundred protease homologs in the human genome that do not have

a canonical active site and may be pseudoproteases. Currently the majority of

pseudoproteases have no ascribed function, although several have been shown to be

involved intercellular signaling [129]. Two secreted morphogens, HGF and sonic

hedgehog, are proteolytically inactive pseudoproteases of the serine and

metalloprotease families, respectively [143]. The Hedgehog morphogen has retained

the predicted catalytic residues, H134 and D176, similar to those seen in the M15

metalloprotease family, yet functions as a ligand through receptor binding rather than

as a protease [142]. Moreover, active proteases can have signaling function

independent of enzymatic activity. Renin, a hormone which mainly functions in

regulation of systemic blood pressure through processing of angiotensinogen, also has

a receptor that can activate downstream signaling independent of the proteolytic

active site [188]. Cathepsin D has been shown to act as a mitogen in tumor cells even

after the active site is abolished [189]. It is possible that, as in the previous examples,

HRG-7 and HRG-8 can continue to act as receptor ligands, independent of its

inherent catalytic activity.

Both secreted HRG-7::mCherry and HRG-8::mCherry are functional only

when secreted from the intestine. It is likely that HRG-7 and HRG-8 are regulated by

or interact with specific factors only expressed in the intestine for secretion,

activation, and other processes. HRG-7 secretion and maturation requires acidified

compartments, the snare protein SNAP-29, and likely a *trans*-activating protease for

propeptide removal. VHA-1 of the v-ATPase complex involved in vesicular

acidification has been reported as being enriched in the intestine, and SNAP-29 is not

expressed in muscle and only some neurons. [172, 190]. And, aside from individual

factors, whole compartments, such as the acidic "gut granules," autofluorescent lysosome-like organelles, are specific to the intestine [191]. Therefore, as a specialized organ, the intestine may have unique properties and factors that allow expression of competent HRG-7 and HRG-8.

Although HRG-7 and HRG-8 have several overlapping characteristics, HRG-7 expression is completely repressed by 20 μM and growth phenotypes associated with *hrg-7* depletion can be rescued by heme. This suggests that HRG-7 is highly specific to heme homeostasis. HRG-8, however, is expressed even at 500 μM heme and the growth and reproduction phenotype associated with HRG-8 depletion cannot be rescued by heme supplementation. Therefore, either HRG-8 is required for heme homeostasis over a broad range of heme concentrations or has functions that are independent of heme homeostasis. One possibility is that HRG-8 impacts several pathways and thus has several interactors, with each interactor conferring pathway specificity through receptor binding or some other mechanism. Along those lines, endogenous HRG-8 is produced in both the intestine and neurons, yet HRG-8 only functions in heme homeostasis when expressed from the intestine. This would suggest distinct functions for intestinal and neuronal HRG-8, possibly due to different interacting partners. Our preliminary results show that HRG-7 and HRG-8 do not interact with each other as immunoprecipitations did not precipitate the corresponding interactor and they have different phenotypes when depleted in strain VH624. Alternatively, rather than directly binding interacting partners or a receptor, HRG-8 may inhibit endogenous cysteine proteases. In this case, RNAi depletion of HRG-8 would result in several overactive cysteine proteases which could function in different

processes. Biochemical analyses of HRG-8 is required to gain a better understanding

of HRG-8 function.

Chapter 5: The neuron-gut axis is critical for systemic heme homeostasis

Summary

Based on our results, we postulated that *C. elegans* maintains systemic heme homeostasis through bidirectional signaling between the intestine and extraintestinal tissues. We have identified HRG-7 and HRG-8 as secreted proteins that are made in the intestine and localize to neurons. HRG-7 in particular is crucial for *C. elegans* adaptation to low heme conditions. The localization of HRG-7 and HRG-8 to neurons indicates that neurons may communicate back to the intestine. However, our genome-wide RNAi would have missed identifying these signals, as *C. elegans* neurons are refractory to RNAi. To circumvent this hurdle, we synthesized a neuronal RNAi-sensitive strain by crossing a *lin-15b* mutation into IQ6011 (IQ6015). Systematically knocking down 127 known morphogens and neuropeptides in *C. elegans* led to the identification of DBL-1 as an important mediator of neuron to intestine heme signaling. Importantly, intestinal response to DBL-1 is dependent upon the transcription factor SMA-9, and disruption of this pathway results heme-dependent growth impairment. Depletion of both *dbl-1* and *hrg-7* results in a synthetic growth phenotype which is suppressed by environmental heme. Together, these data implicate a bidirectional signaling system between the intestine and the nervous system to control systemic heme homeostasis.

Results

Identification of the DBl-1 / SMA-9 signaling axis as a regulator of heme homeostasis

Our results suggest that neurons may play an important role in systemic heme homeostasis and intestinal heme uptake. However, because neurons are refractory to RNAi in *C. elegans*, it is unlikely that neuronal signaling factors would have been depleted to result in a phenotype in our RNAi screen. Therefore, we generated strain IQ6015, a neuronal RNAi hypersensitive strain, by introducing a *lin-15b* mutation (*n744*) into the IQ6011 heme sensor strain. Mutations in *lin-15b* allow enhanced RNAi efficiency in neurons [192]. We then knocked down 127 genes (~83 percent) known to encode morphogens and neuropeptides in both IQ6011 and IQ6015. We were interested in genes that, when depleted, caused an enhanced GFP phenotype specifically in IQ6015 as this would be indicative of gene knockdown in neurons. We uncovered four genes for which RNAi depletion resulted in significantly higher GFP expression in IQ6015 compared to IQ6011: the TGF beta-like *dbl-1*, the insulin-like *ins-21* and *ins-32*, and the neuropeptide-like *nlp-12* (**Figure 5.1A**). All four genes have been reported as being expressed in the nervous system [193-195]. Next, we cross-referenced the known physical and genetic interactors of each gene with candidates from our genome-wide screen to evaluate inter-tissue pathway connections. Interestingly, we found a pathway connection between *dbl-1* and *sma-9*, genes previously been shown to genetically interact to regulate body size (**Figure 5.1B**) [196]. DBL-1 and SMA-9 are homologous to the human TGF beta superfamily member, bone morphogenic protein 5 (BMP-5), and the SHN

Figure 5.1: The DBL-1 / SMA-9 signaling axis regulates *hrg-1* expression

A) GFP quantification of strain IQ6011 (P_{hrg-1}*::GFP*) and strain IQ6015 (P_{hrg-1}*::GFP; lin-15b(n744))* after knockdown of morphogens and neuropeptides. Red data points are significant outliers in a regression curve as determined by SAS software. 120 worms were analyzed for each treatment. GFP is fold change compared to worms fed control vector only **B)** geneMANIA genetic / physical interaction network of *dbl-1*.

A
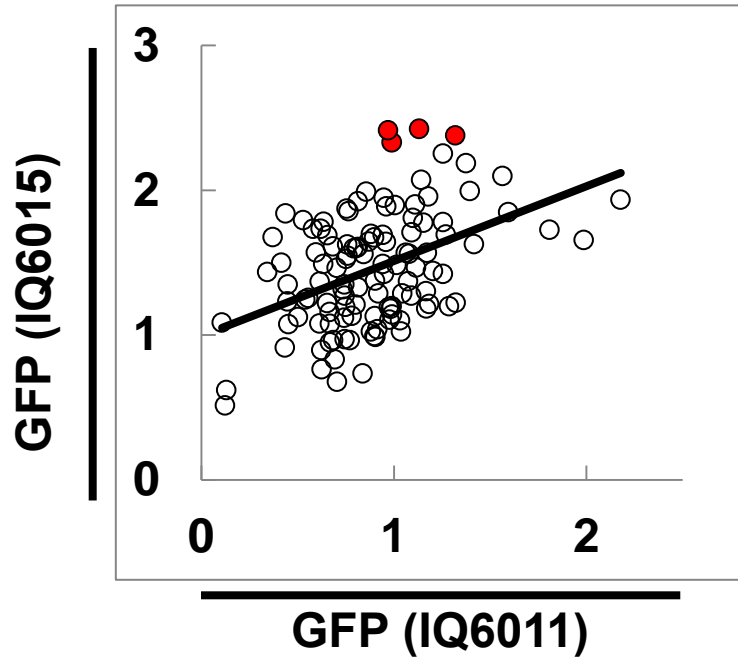
B
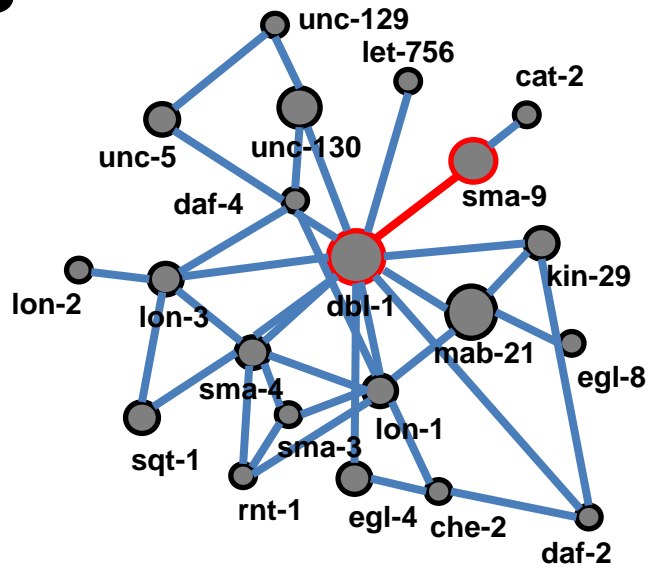
transcription factors, respectively. No physical or genetic interactions were identified for *ins-32* and *nlp-12* (**Appendix VIII**).

To delineate the role of DBL-1 in heme homeostasis, we analyzed transcriptional reporter fusions for *dbl-1*and *sma-9.* Interestingly, *dbl::GFP* was predominately expressed in neurons, while *sma-9::HIS-24::mCherry* was expressed in most somatic tissue, including the intestine (**Figure 5.2A, B**) [193, 196]. This indicates that the heme deficiency signal generated by depletion of DBL-1may be transmitted to the intestine through SMA-9. In order to demonstrate that *sma-9* was functioning in the same pathway as *dbl-1* to regulate *hrg-1*, we knocked down *sma-9* in IQ6011 and the *dbl-1* null mutant strain IQ6311 (*dbl-1(nk3);P$_{hrg-1}$::GFP;*). While knockdown of *sma-9* results in significant increase of GFP in IQ6011 control worms, GFP levels were unaltered in *dbl-1 (nk3)* mutants, suggesting *hrg-1* repression is dependent on *dbl-1* via *sma-9* (**Figure 5.3A**). Interestingly, published microarray data indicate that ~10% of heme-responsive genes are also regulated by *dbl-1*, half of which have intestinal expression (**Figure 5.3B, Table 5.1**) [197]. Together, this data suggests that the DBL-1/ SMA-9 signaling axis has a strong influence on heme homeostasis, and in particular neuron to intestinal signaling.

DBL-1 function is dose-dependent and is required for normal growth in low heme

DBL-1 has been shown to affect body size in a dose-dependent manner [193]; *dbl-1(nk3)* mutants are small, while overexpression of *GFP::DBL-1* results in long worms. In order to evaluate whether DBL-1 has a dose-dependent effect on heme
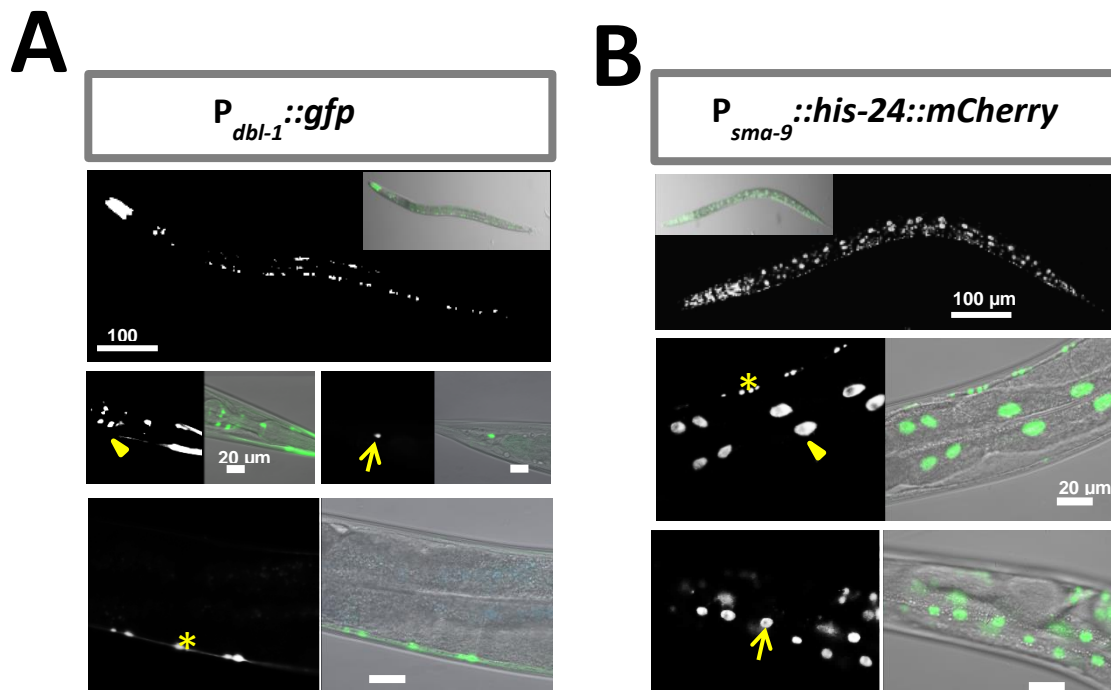
Figure 5.2: Tissue specific expression of *dbl-1*and s*ma-9*

A) GFP expression in strain BW1946 (*P$_{dbl-1}$::GFP*). Images are 63 x. Arrowhead indicates head neurons. Arrow indicates tail neurons. * indicates body neuron. **B)** mCherry expression in strain RW10745 (*P$_{sma-9}$::HIS-24::mCherry*). Images are 63 x. Arrowhead indicates intestinal nuclei. * indicates body neurons. Arrow indicates hypodermal nuclei.
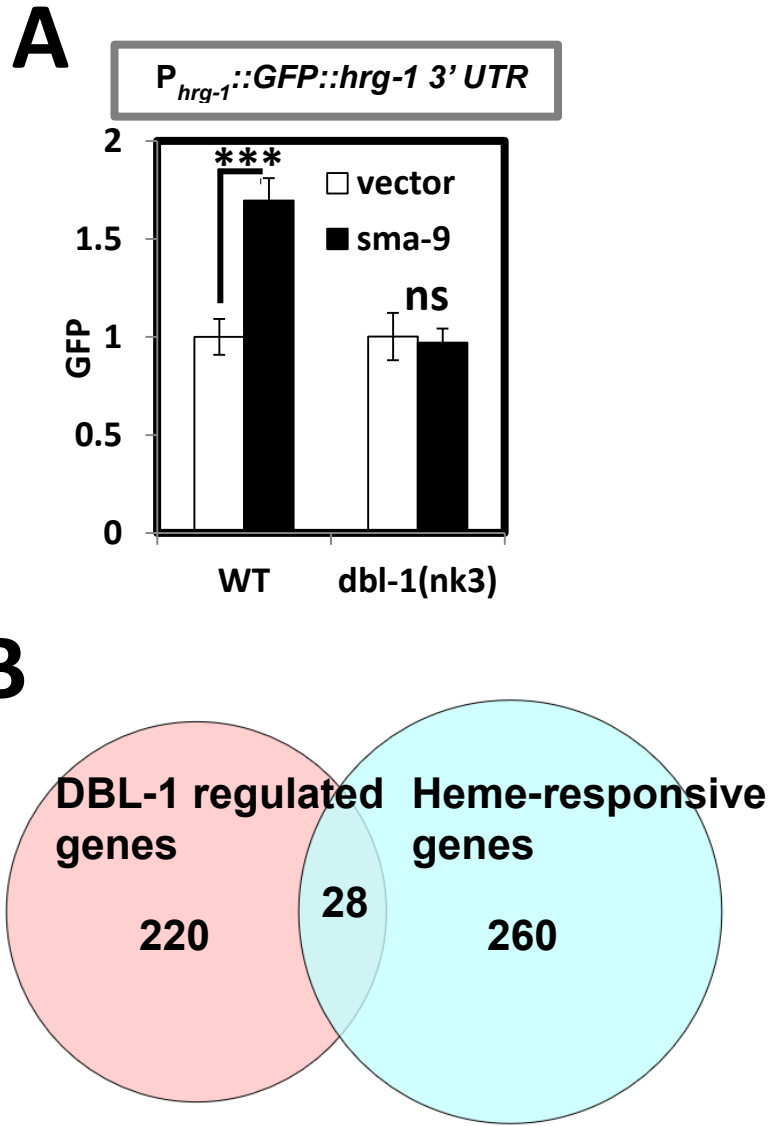
Figure 5.3: DBL-1 and SMA-9 coordinate to regulate neuron to intestine heme signaling

A) GFP fluorescence (120 worms per treatment) quantified from IQ6011 ($P_{hrg-1}::GFP$) and IQ6311 ($P_{hrg-1}::GFP$; *dbl-1(nk3)*) fed dsRNA against vector or *sma-9* at 10 μM heme. GFP was quantified using COPAS BioSort. ***P<0.001 (t-test). **B)** Venn diagram depicting overlap of heme-responsive genes and genes regulated by *dbl-1 / sma-9*.

Table 5.1 Heme-responsive genes regulated by DBL-1

Sequence	Gene	Intestinal expression	Short Description
B0218.8	clec-52	Yes	
C03H5.1	clec-10	Yes	
C04F6.1	vit-5	Yes	vit-5 encodes a vitellogenin.
C05C10.4	pho-11		
C15C8.3	hrg-7	Yes	
F09G2.3	pitr-5		
F15E11.12	pud-4	Yes	
F35C5.9	clec-66	Yes	
F59D8.2	vit-4	Yes	
H23N18.1	ugt-13		
K01A2.3		Yes	
K01A2.4			
K01D12.14	hrg-2		
K07H8.6	vit-6	Yes	vit-6 encodes a vitellogenin precursor.
K08E7.9	pgp-1	Yes	pgp-1 is a member of the ABC transporter superfamily.
K10C2.3	asp-14		
M02D8.4	asns-2	Yes	
M02H5.4	nhr-202		
R02E12.6	hrg-1	Yes	hrg-1 encodes a heme transporter.
T05E12.6			
T08A9.8	spp-4	Yes	
T24B8.5			T24B8.5 encodes an ShK-like toxin peptide.
W03G1.7	asm-3		
W08A12.3			
Y19D10B.7	pud-1.2	Yes	
Y38E10A.5	clec-4		
ZC443.5	ugt-18		
ZK970.7			

homeostasis, we crossed overexpressed *GFP:DBL-1* into IQ6211 to generate IQ6312 ($P_{hrg-1}::GFP;P_{dbl-1}::GFP::DBL-1;$ *dbl-1(nk3)).* We grew each of the three strains, wild type *dbl-1*, *dbl-1(nk3)* null mutants, or *GFP::DBL-1* overexpressors over a range over of heme concentrations and evaluated intestinal *hrg-1::GFP* expression **(Figure 5.4A, B)**. Worms lacking *dbl-1* phenocopied RNAi knockdown, leading to the upregulation of *hrg-1::GFP* at all heme concentrations tested when compared to WT worms, confirming that DBL-1 is a repressor of *hrg-1* **(Figure 5.4C)**. Conversely, *hrg-1::GFP* expression was reduced in worms overexpressing *GFP::DBL-1* compared to WT worms, confirming a dose-dependent effect of DBL-1. Together, these results indicate that neuronal

expression of DBL-1 strongly influences intestinal *hrg-1* expression. Next, we grew IQ6011 and IQ6311 worms lacking *dbl-1* on RP523 bacteria food supplemented with 1 or 50 μM heme. Worms lacking *dbl-1* and grown on low heme were growth delayed, a phenotype suppressed by 50 μM heme **(Figure 5.5)**. This result suggested that DBL-1 is necessary for normal growth under low heme conditions. Together, our data indicate that DBL-1 is an important regulator of heme homeostasis.

DBL-1 and HRG-7 synergistically regulate heme homeostasis

We have shown that both HRG-7 and DBL-1 are secreted signals involved in long-range signaling to promote heme homeostasis. Depletion of either *dbl-1* or *hrg-7* result in overlapping heme-dependent phenotypes, despite being expressed in different tissues. It is noteworthy that published microarray results show that *hrg-7* mRNA is upregulated in *dbl-1* mutant worms [197]. This is not surprising given that

Figure 5.4: DBL-1 regulates *hrg-1::GFP* in a dose-dependent manner

A) Schematic for genotyping *dbl-1*, *dbl-1(nk3)*, and transgenic *GFP::DBL-1*. Primer

sequences are in appendix II. **B)** Single worm PCR of IQ6011, IQ6311 ($P_{hrg-1}::GFP$;

dbl-1(nk3)), and IQ6312 ($P_{hrg-1}::GFP\ P_{dbl-1}::GFP$; *dbl-1(nk3)*) worms with primers

from panel A. **C)** Fluorescence images and GFP quantification from IQ6011,

IQ6311, and IQ6312 grown on 0P50 supplemented with indicated heme

concentrations. Images are 63x. Scale bar = 20 µm. GFP fluorescence (100 worms

per treatment) was quantified using COPAS BioSort.

A

7 kbp (1 kbp in nk3 deletion)

A →   ← B

dbl-1

C →   ← D

740

nk3 deletion

Rescue transgene   GFP

E →   ← F

750

B

A+B   C+D   E+F

1000bp
800bp
650bp

dbl-1(nk3); GFP::DBL-1
dbl-1(nk3)
WT
H20
dbl-1(nk3); GFP::DBL-1
dbl-1(nk3)
WT
H20
dbl-1(nk3); GFP::DBL-1
dbl-1(nk3)
WT
H20

C

$P_{hrg-1}::GFP$

dbl-1(nk3)

WT

dbl-1(nk3); GFP::DBL-1

123
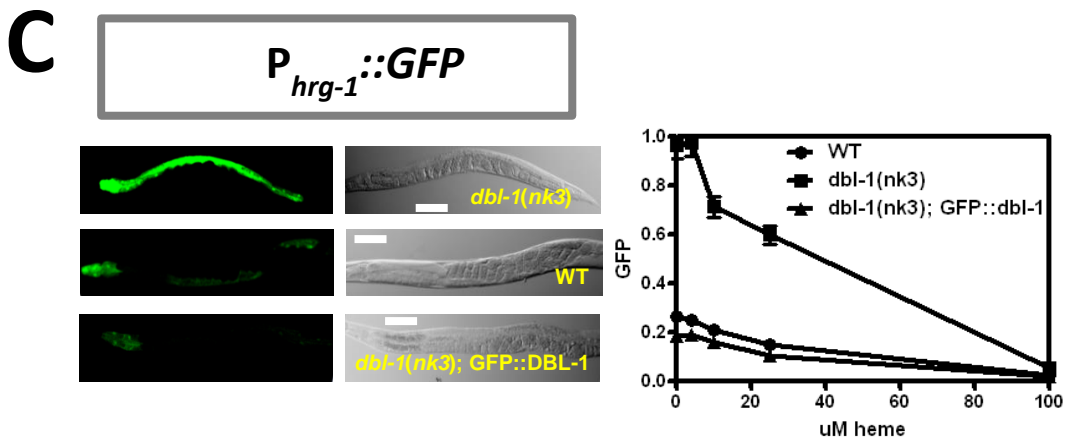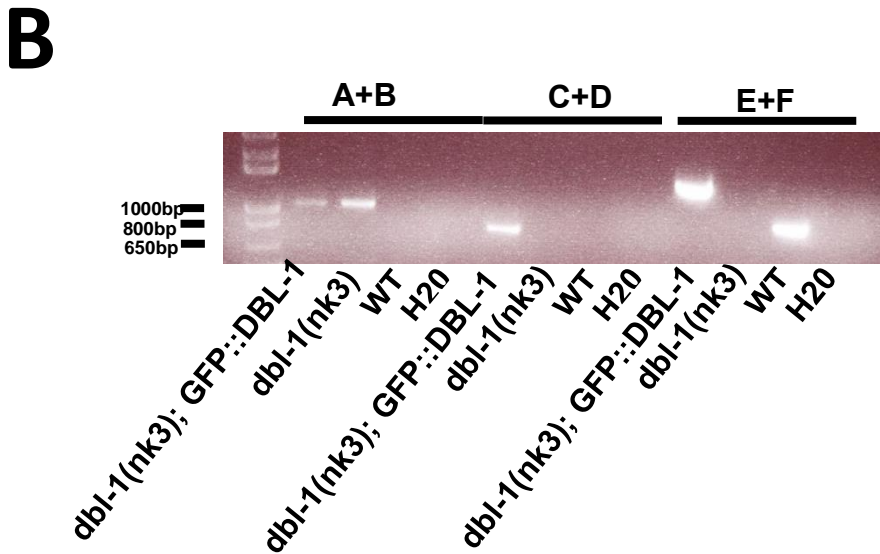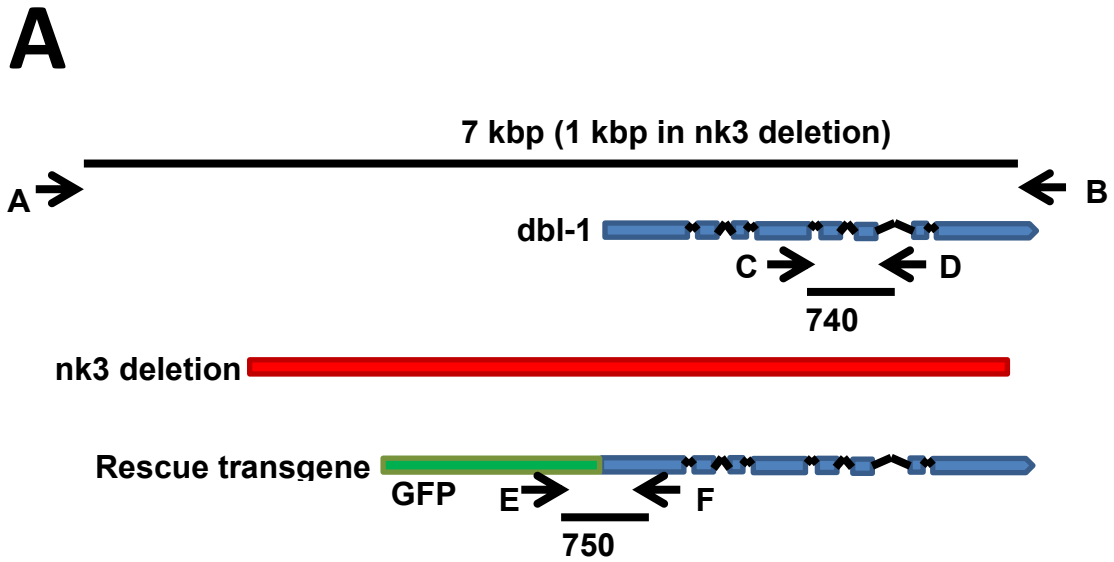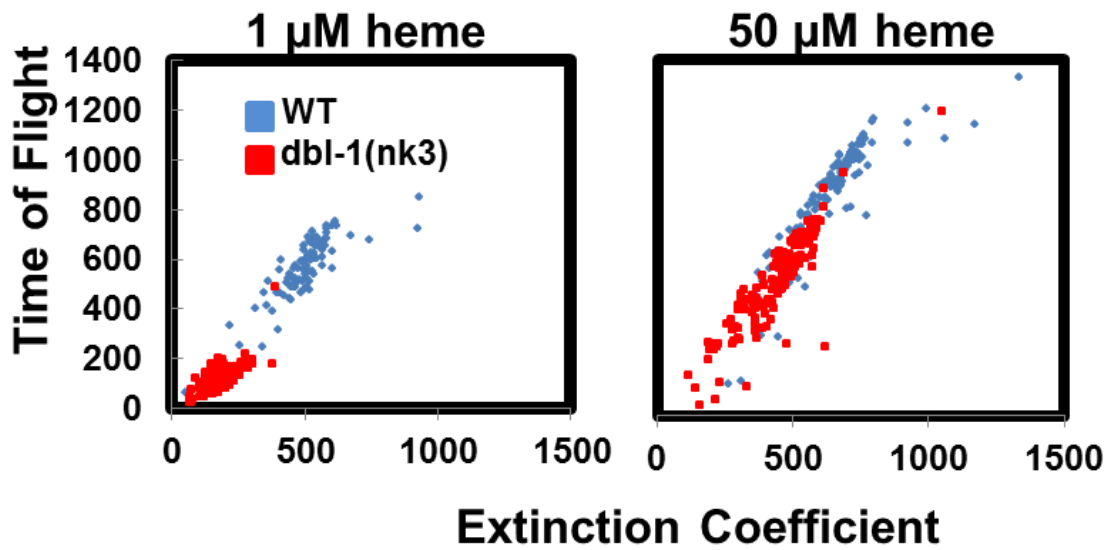
Figure 5.5: DBL-1 is required for normal growth in low heme

Size analyses (200-300 worms per treatment) quantified from IQ6011 ($P_{hrg-1}::GFP$)
and IQ6311 ($P_{hrg-1}::GFP$; *dbl-1(nk3)*) fed RP523 *E. coli* grown in l µM or 50 µM
heme for 96 or 72 hours, respectively. Size was analyzed using COPAS BioSort.

DBL-1 is a regulator of *hrg-1*, and both *hrg-1* and *hrg-7* contain HERE motifs for heme-responsiveness. To evaluate whether HRG-7 was also upregulated in the absence of *dbl-1*, we analyzed HRG-7 protein levels in strains IQ6011 (*Phrg-1::GFP*) and IQ6311 (*Phrg-1::GFP; dbl-1(nk3)*). Unexpectedly, total HRG-7 was markedly decreased in worms lacking *dbl-1*. Intriguingly, only the mature form was decreased, while the pro-form was slightly upregulated **(Figure 5.6A)**. This suggests that mature HRG-7 is not stable in the absence of DBL-1. To evaluate whether the posttranslational regulation of HRG-7 by DBL-1 was dependent on *sma-9*, we analyzed HRG-7 expression in VH624 hypersensitive strain. In contrast to *dbl-1*mutants, RNAi of *sma-9* resulted in increased mature HRG-7 **(Figure 5.6B)**. These results suggest that the DBL-1/SMA-9 pathway regulates *hrg-7* at the transcriptional level, but DBL-1 may also have a *sma-9* independent role in the post-translational regulation of HRG-7.

To determine whether HRG-7 regulated DBL-1 expression, we knocked down *hrg-7* in the DBL-1 translational reporter VC1478 (*dbl-1(nk3)*; P_{dbl-1}::*GFP::DBL-1*). The depletion of *hrg-7* did not result in any detectable changes in GFP::DBL-1 expression **(Figure 5.7A)**. Our previous results had suggested HRG-7 preferentially localized to sensory neurons. To evaluate whether these neurons also expressed *dbl-1*, we generated the double transgenic strain IQ7671(P_{vha-6}::*HRG-7::mCherry*; P_{dbl-1}::*GFP*). GFP and mCherry were not present in the same neurons in this strain **(Figure 5.7B)**. Based on these experiments, we hypothesized that DBl-1 is a regulator of HRG-7 but HRG-7 is not a regulator of DBL-1 expression. However, we have not ruled out the possibility that HRG-7 regulates DBL-1 post-translationally.
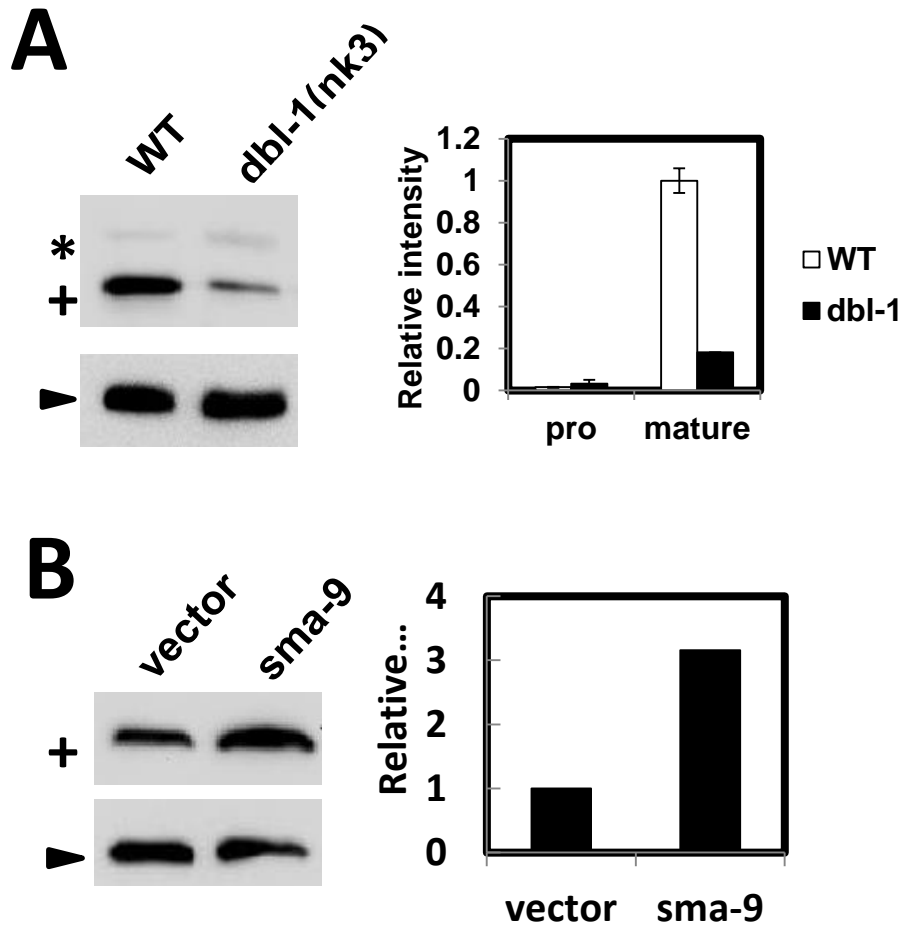
Figure 5.6: DBl-1 regulates HRG-7 levels post-translationally independent of SMA-9.

A) Immunoblot analysis of HRG-7 expression in IQ6011 (P_{hrg-1}::*GFP*) and IQ6311 (P_{hrg-1}::*GFP* ; *dbl-1(nk3)*). Membranes were probed with polyclonal anti-HRG-7 antibody and then incubated with HRP-conjugated anti-rabbit secondary antibody. * indicates pro-HRG-7. + indicates mature HRG-7. Arrowhead indicates tubulin. B) Immunoblot analysis of HRG-7 expression in VH624 fed dsRNA against vector or *sma-9*. + indicates mature HRG-7. Arrowhead indicates tubulin. Blots were quantified with Chemidoc software. N=5000 worms per treatment. Images and quantification are representative of two experiments.
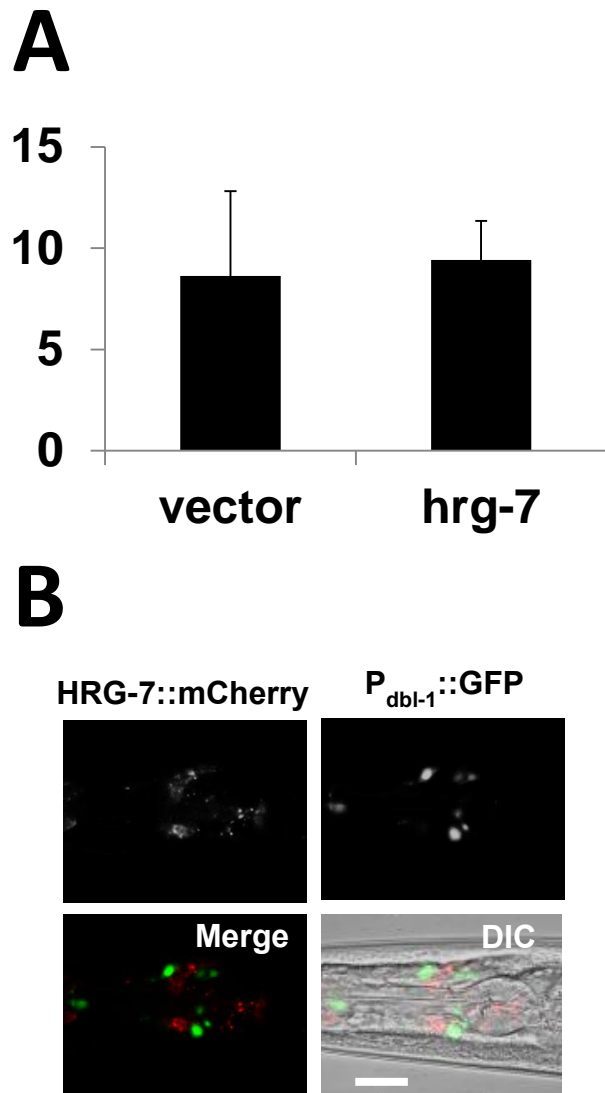
Figure 5.7: HRG-7 does not regulate DBL-1 expression

A) GFP fluorescence in neurons (20 worms each treatment) of VC1478 (*dbl-1(nk3);*

Pdbl-1::DBL-1GFP) fed ds RNA against control vector only or *hrg-7*. Neurons were

quantified using the Region of Interest function in simple PCI. Graph is

representative of two experiments. **B)** GFP and mCherry expression in strain

IQ7671(P_{vha-6}::*HRG-7::mCherry*; P_{dbl-1}::*GFP*). Scale bar =20 μm. Image is 63x.

To evaluate whether DBL-1 and HRG-7 regulated *hrg-1* through the same pathway or independently of one another, we knocked down *dbl-1*, *sma-9*, and *hrg-7* either singly or together in IQ6015. As expected, RNAi of *dbl-1* and *sma-9* simultaneously did not result in any further upregulation of GFP **(Figure 5.8A)**. However, knockdown of *dbl-1* and *hrg-7* simultaneously lead to significantly enhanced upregulation of GFP. Similar results were observed when *hrg-7* and *sma-9* were knocked down simultaneously. To validate these results, we knocked down *hrg-7* in IQ6011, IQ6311 *dbl-1*null mutants and IQ6312 *GFP::DBL-1* overexpressors. While *hrg-1* upregulation was dampened in *dbl-1*null worms compared to WT worms and worms overexpressing *GFP::DBL-1*, we observed significant GFP upregulation compared to worms fed control vector **(Figure 5.8B)**. Next, we knocked down *hrg-7* in these three strains and grew worms with or without 200 μM heme. Although *hrg-7* knockdown resulted in a growth delay in IQ6011, this phenotype is dramatically enhanced in the *dbl-1(nk3)* background **(Figure 5.9A, B)**. This growth delay can either be rescued partially by the DBL-1 transgene or fully rescued by heme supplementation. Together, our data suggests that DBL-1 and HRG-7 function synergistically to regulate heme homeostasis.

Discussion

Our results reveal that intestinal heme transport is regulated by retrograde signaling from the neurons by DBL-1, which acts on the gut by regulating *hrg-1* via SMA-9. This neuron to gut communication is necessary for the normal growth of *C.*
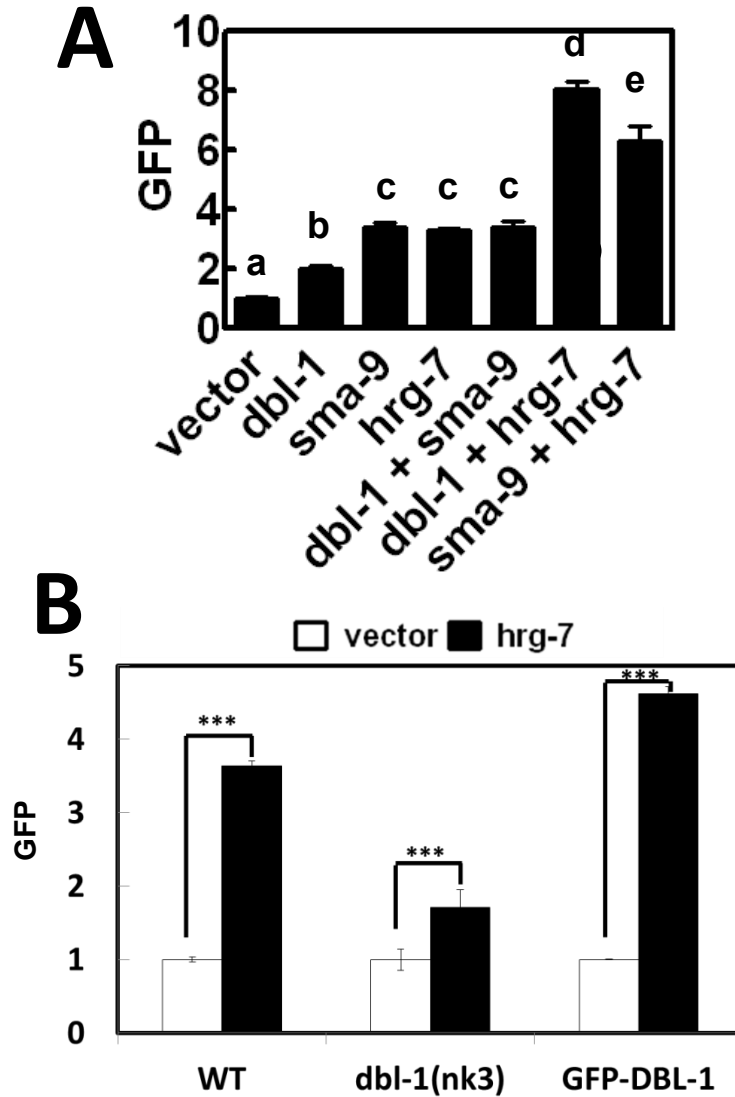
Figure 5.8: HRG-7 and DBl-1 independently regulate *hrg-1::GFP*

A) GFP fluorescence (120 worms per treatment) quantified from IQ6015 (l*in-15b(nk3);P_{hrg-1}::GFP*) fed dsRNA against control vector, *dbl-1*, *sma-9*, and *hrg-7* at 10 μM heme alone or in combination. GFP was quantified using COPAS BioSort. P<0.01 (one way ANOVA). **B)** GFP fluorescence (120 worms per treatment) quantified from of IQ6011, IQ6311 (*P_{hrg-1}::GFP* ; *dbl-1(nk3)*), and IQ6312 (*P_{hrg-1}::GFP P_{dbl-1}::GFP* ; *GFP*) fed dsRNA against control vector or *hrg-7* at 10 μM heme. GFP was quantified using COPAS BioSort. P<0.001 (t-test)
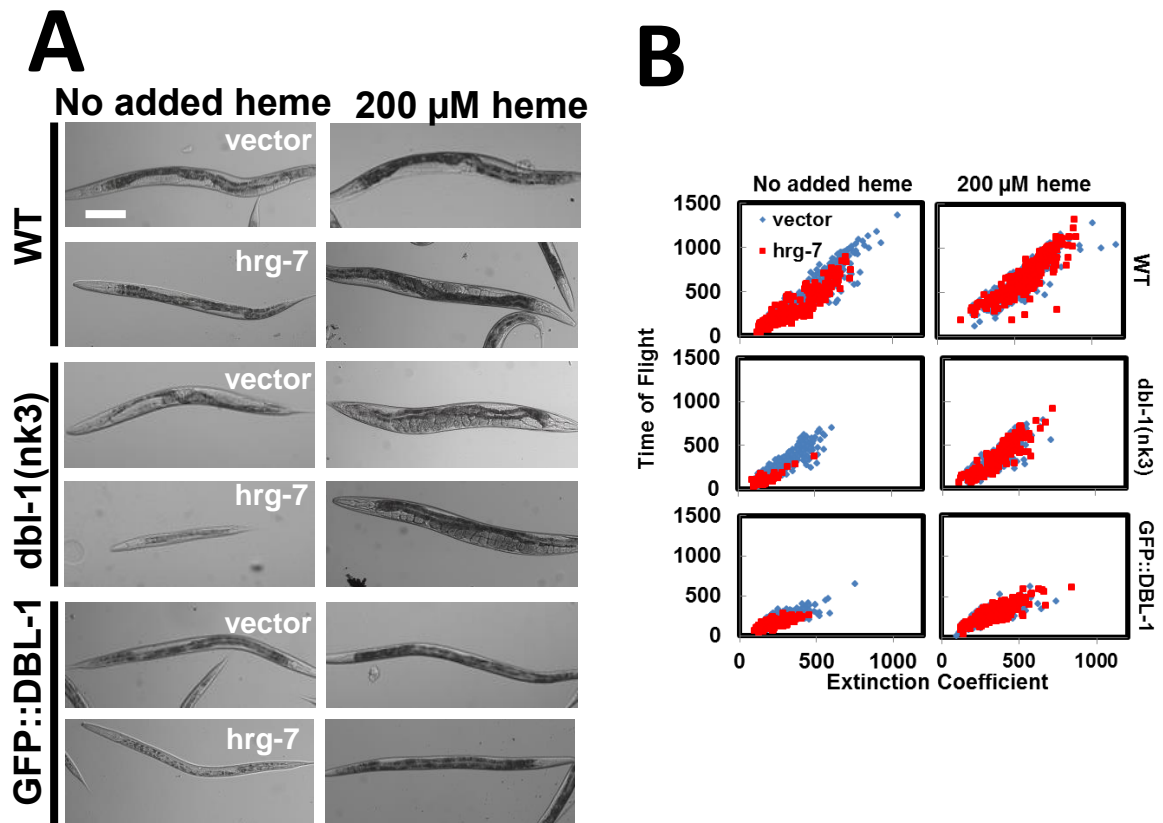
Figure 5.9: HRG-7 and DBL-1 synergistically regulate heme homeostasis

A) Representative images of IQ6011, IQ6311 ($P_{hrg-1}::GFP$; *dbl-1(nk3)*), and IQ6312 ($P_{hrg-1}::GFP$; *GFP::DBL-1*; *dbl-1(nk3)*) fed dsRNA against control vector or *hrg-7* with no added heme or 200 µM heme. **B)** Quantification of worms from panel A (200-300 worms per treatment) using COPAS BioSort. Graph is representative of three experiments.

elegans at low heme, and this pathway functions in context with anterograde intestine to neuron signaling through HRG-7 to regulate systemic heme homeostasis. Depletion of either pathway results in a heme-dependent growth delay, but interrupting both pathways simultaneously results in a severe growth defect. Together, this suggests that the bidirectional signaling at the neural-intestinal axis in *C. elegans* is critical for ensuring the worm can physiologically respond to low nutritional heme (**Figure 5.10**).

Our results indicate that *hrg-7* is repressed by the DBL-1 /SMA-9 pathway, but DBL-1 may also have a role in HRG-7 protein stability that is independent of SMA-9 transcriptional regulation. Conversely, HRG-7 does not appear to modulate *DBL-1::GFP* expression. Importantly, depletion of DBL-1 and HRG-7 simultaneously results in enhanced GFP and growth defects, indicating that, at least partially, the two proteins may function independent of each other to regulate heme homeostasis.

In addition to understanding intertissue heme trafficking, the discovery of bidirectional signaling between the neurons and gut to regulate heme homeostasis may be informative as a paradigm for other micronutrients, an accepted concept for macronutrients such as glucose and lipids.

Despite the advances in understanding systemic iron homeostasis, the role of the central nervous system in regulation of tissue iron availability and even regulation of iron levels within the central nervous system itself have not been well studied. The central nervous system is an important mediator of metabolism and micronutrient levels in the brain must be extremely well regulated [198]. Interestingly, it has been
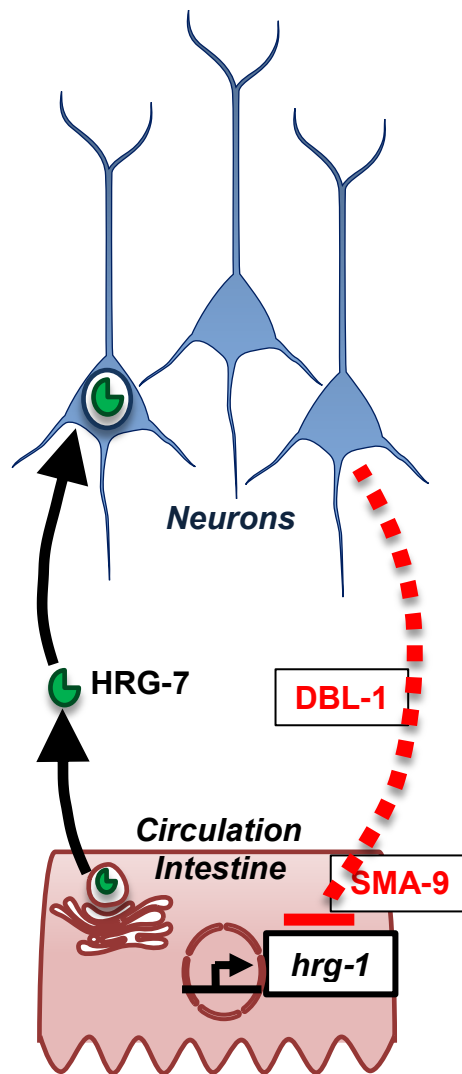
Figure 5.10: Systemic heme homeostasis is maintained by the neuron-gut axis

In low heme conditions, HRG-7 is secreted from the intestine and localizes to sensory

neurons to regulate *hrg-1*. In conjunction, neurons can regulate *hrg-1* by signaling to

the intestine through DBL-1 /SMA-9. Together, this bidirectional long-range

signaling between intestine and neurons allow systemic heme homeostasis to be

maintained.

shown that pica behavior, or a desire to eat non-food items, is linked to anemia and can be treated with iron supplementation [199-201]. This suggests that micronutrient deficiency influences foraging behavior. It has also been shown that although the liver secretes hepcidin, signaling is initiated from the intestine [180]. We postulate that the brain-gut axis plays a role in mammalian systemic micronutrient homeostasis.

Chapter 6: Overall conclusions

Heme is an iron containing tetrapyrrole that is required by all cells for incorporation into hemoproteins. The current paradigm states that cellular requirements for heme are fulfilled by the cell's internal capacity to synthesize and degrade its own heme, *i.e.* cell autonomous regulation. While evidence suggests that there is also cell non-autonomous regulation of cellular heme levels, the mechanisms involved in this latter form of regulation have been difficult to uncover due to interference from heme synthesis. The goal of this project was to take advantage of the obligate heme auxotroph, *C. elegans*, to understand how tissues communicate to direct interorgan heme transport and maintain heme homeostasis on a systemic level. The major findings of these studies are outlined below.

1) Knockdown of the intestinal heme exporter, *mrp-5*, results in upregulation of intestinal GFP in the heme sensor strain IQ6011 ($P_{hrg-1}::GFP$). This indicates a heme deficiency signal, despite the intestine accumulating heme in the intestine when *mrp-5* is depleted. A genome-wide RNAi screen for modulators of heme homeostasis confirmed that >30% of genes were extraintestinal and that interorgan communication may contribute to the regulation of *hrg-1*.

2) The genome-wide RNAi screen revealed two protease homologs, HRG-7 and HRG-8, as mediators of heme homeostasis. The catalytic dyad of aspartic proteases, which consists of two aspartic acid residues, is conserved in HRG-7, while HRG-8

lacks both catalytic residues found in typical cysteine proteases. Depletion by RNAi of either gene results in upregulation of GFP in IQ6011 and growth retardation phenotypes. For *hrg-7* RNAi the growth phenotype was reversible by heme supplementation but not for *hrg-8* RNAi. Additionally, HRG-7 and HRG-8 are both upregulated by low heme; HRG-7 is not expressed beyond 20 µM heme while HRG-8 is expressed at $\geq$ 500 µM heme. This suggests that HRG-7 is specifically required during heme limitation, while HRG-8 may have additional functions that may be independent of heme levels.

3) Translational fusions show that HRG-7 and HRG-8 are secreted from intestine and then internalized into sensory neurons. This suggests that the heme deficiency signal observed during HRG-7 and HRG-8 depletion could be a result of signaling from the target tissue. In support of this, the intestinal heme deficiency signal is rescued by secretion of HRG-7 but not if HRG-7 is membrane tethered to the intestine. These results predict the intestine responds to a HRG-7 dependent signal which originates from sensory neurons.

4) The heme-response of *hrg-7*, *hrg-1*, and presumably *mrp-5* is mediated by the HERE and surrounding GATA *cis*-elements. HRG-1 and MRP-5 are involved in heme transport into and from the intestine, while HRG-7 seems to be necessary for the sensation of heme deficiency by extraintestinal tissues in response to intestinal heme status. Taken together, these results suggest that under heme limiting

conditions, extraintestinal tissues signal to the intestine through the HERE to upregulate genes required for heme acquisition for systemic homeostasis.

5) HRG-7 is secretly shortly after translation and this secretion is essential for function. Of the 45 known trafficking factors, we show that the snare protein SNAP-29 and components of the vacuolar ATPase were required for HRG-7 secretion. Moreover, depletion of these genes by RNAi resulted in the accumulation of pro-HRG-7. Together, our data suggest that HRG-7 matures in an acidified compartment and is secreted after post-Golgi fusion events which rely on SNARE proteins. It is possible some of the trafficking components are intestinal-specific, as we could not express functionally competent HRG-7 from muscle or neuron.

6) HRG-7 propeptide removal requires acidic conditions typical of aspartic proteases. In most aspartic proteases this is often through autocatalysis which require the active site aspartic acids. However, mutating D90 and D318 in HRG-7 did not prevent propeptide cleavage, indicating that a *trans*-acting protease may serve to cleave HRG-7. Surprisingly, this "inactive" HRG-7 could suppress the heme deficiency signal suggesting that either the predicted catalytic residues are not required for this function or there are other residues that may serve as active site ligands. Whether HRG-7 is a protease at all *in vivo* or *in vitro* has not been determined.

7) HRG-7 and HRG-8 localized to neurons, leading us to postulate that neurons could regulate systemic heme homeostasis by signaling to the intestine. Because neurons

are refractory to RNAi in *C. elegans*, we generated a neuronal RNAi sensitive heme sensor strain, IQ6015, by introducing a *lin-15b* mutation into the heme sensor strain, IQ6011. RNAi knockdown of 127 known morphogens and neuropeptides led to the discovery that of *dbl-1*, a bone morphogenic protein homolog, which is expressed in neurons. Depletion of *dbl-1* and *sma-9*, a transcription factor, recapitulate *hrg-7* deficiency by upregulating *hrg-1*.

8) To gain a better understanding of how DBL-1 functions in heme homeostasis, we crossed either a *dbl-1* null (*nk3*) or GFP::DBL-1 overexpressing worms into IQ6011. Worms lacking *dbl-1* showed increased *hrg-1*, while those with overexpressed DBl-1 showed *hrg-1* even lower than WT worms. This indicated that DBL-1 regulated *hrg-1* in a dose-dependent manner. Worms lacking *dbl-1* were growth retarded in low heme, a phenotype that was reversible in the presence of heme supplementation. Together, our data indicate that neurons, through DBL-1, are important mediators of systemic heme homeostasis.

9) Microarray data and our RNAi experiments show that *hrg-7* is upregulated when *dbl-1* is depleted [197]. However, a *dbl-1*null mutant showed lower levels of mature HRG-7 and elevated amounts of pro-HRG-7, suggesting that *dbl-1* mutants have a defect in posttranslational control of HRG-7 protein maturation. SMA-9 does not play a role in this regulation of HRG-7 as RNAi depletion of *sma-9* resulted in upregulation of HRG-7 both transcriptionally and at the protein level. Together, these

results posit that the DBL-1 / SMA-9 pathway is a genetic repressor of *hrg-7,* while DBL-1 may have an additional regulatory role on HRG-7 protein levels.

10) Depletion of both *dbl-1* and *hrg-7* simultaneously show an enhanced synthetic effect; these worms are severely growth retarded, but growth is restored by heme supplementation. These results reveal that neurons and the intestine act cooperatively through two secreted factors, HRG-7 and DBL-1, to maintain systemic heme homeostasis.

Future Directions

Identification of HRG- 7 and HRG-8 substrates and interacting partners

Our genetic assays suggest that HRG-7 does not require the canonical active site. To evaluate whether HRG-7 has retained any protease activity, we are currently performing expression analyses of HRG-7-6xHIS in the methanotrophic yeast, *Pichia pastoris*. Expression of secreted proteins in *Pichia* offers several advantages, including large scale protein purification and secretion directly into the media, bypassing cell lysis [202]. Once we purify sufficient amounts of HRG-7-6xHIS using a nickel column, we will utilize a peptide library to determine if HRG-7 has proteolytic activity and if so, its substrate preference [203]. If we can identify peptide substrates of HRG-7 *in vitro*, we can build a position weight matrix of cleavage specificity, and scan the *C. elegans* genome to find potential endogenous substrates. This will be done in collaboration with the laboratory of Dr. Charles Craik at the

University of California, San Francisco. If successful, we will knockdown candidates in IQ6011 and VH624 to evaluate which genes, when depleted, phenocopy *hrg-7* knockdown. It is also possible that HRG-7 does not have any proteolytic activity but functions as either a morphogen or a heme chaperone. We will use the purified HRG-7 from *Pichia* in conjunction with hemin-agarose columns to analyze the heme-binding capabilities of HRG-7. To isolate an HRG-7 receptor or binding partners we will use Multi Dimensional Protein Identification Technology (MuDPIT). MuDPIT couples immunoprecipitation with mass spectrometry analyses to identify the interacting partners of a bait protein. This is being done in collaboration with the laboratory of Dr. James Wohlschlegel at the University of California, Los Angeles. We are currently utilizing this technique for both HRG-7-3xFLAG and HRG-8-3xFLAG. We have also generated a secreted negative control: HRG-3SP-mCherry-3xFLAG. The immunoprecipitation has been optimized and we have already obtained preliminary results **(Figure 6.1A, B)**. We plan to repeat this experiment to identify a list of HRG-7 and HRG-8 candidates that repeatedly CO-IP with HRG-7 and HRG-8 but not secreted mCherry. Candidates can then be knocked down by RNAi in IQ6011 and VH624 to analyze if they can phenocopy HRG-7 or HRG-8 depletion. If candidates are validated by RNAi, reciprocal CO-IPs will be performed. Together, this will provide strong evidence for genuine interacting partners. These experiments will be necessary in order to understand how HRG-7 and HRG-8 function mechanistically.

Figure 6.1: HRG-7 and HRG-8 MuDPIT reveals potential interacting partners

A) Silver stain analyses of immunoprecipitation eluates. Lysate from worms

expressing HRG-7-3xFLAG, HRG-8-3x-FLAG, and HRG-3SP-3xFLAG were

incubated overnight with anti-FLAG antibody conjugated to agarose beads. The

beads were washed and bound proteins were eluted off with 3xFLAG peptide.

Eluates were run on an SDS-PAGE gel and analyzed by silver stain. * indicates

eluted target protein B) Venn diagram depicting the number of unique and

overlapping proteins between samples after immunoprecipitation and MuDPIT

analysis.

A

HRG-7-3XFLAG　　HRG-8-3XFLAG　　HRG-3SP-mCherry-3XFLAG

50kD>

37kD>

25kD>

Eluate 1　Eluate 2　Eluate 1　Eluate 2　Eluate 1　Eluate 2

B

HRG-7　　　　　　　　HRG-8

79　　39　　44

38

5

Secreted mCherry
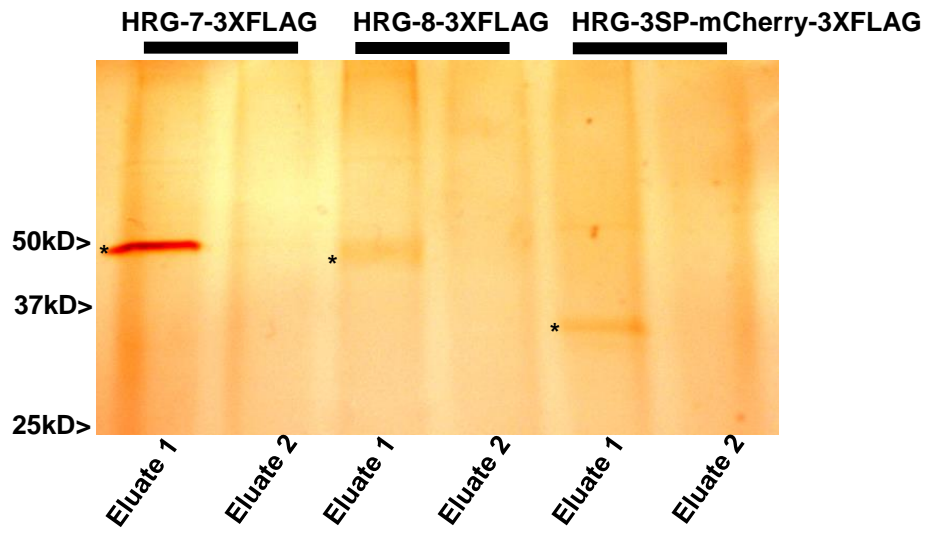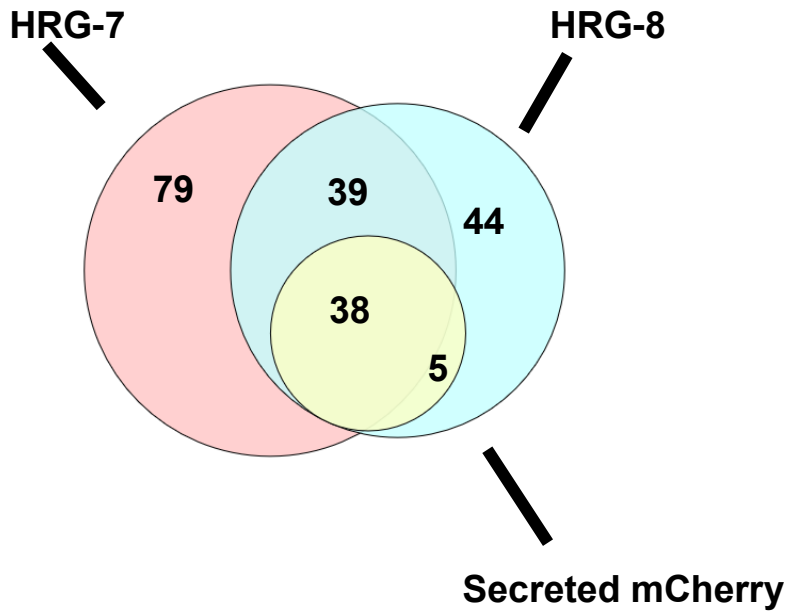
HRG-7 and HRG-8 structure function analysis

We have already shown that the predicted catalytic residues of HRG-7 are not required, at least, for intestinal regulation of *hrg-1*. Moreover, HRG-8 altogether lacks obvious active site domains catalytic residues. Therefore, we will perform a structure / function analyses of HRG-7 and HRG-8 to determine which residues are critical for function. Within the active site pocket, there are conserved non-catalytic residues for both HRG-7 and HRG-8 (**Figure 6.2A, B**). Although Hedgehog and HGF do not require the catalytic residues of the active site for function, they still require residues in the vicinity of the active site, suggesting that the binding pocket is important. Therefore, we will mutate the conserved residues near the canonical catalytic centers in HRG-7^{PR} and HRG-8^{PR}. These transgenes can be crossed into IQ6011 for functional evaluation of *hrg-1* responsiveness. Interestingly, HRG-7 has a unique insert of 40 amino acids that is predicted to form a cysteine rich alpha helix. In addition to protein stability, cysteines are important for metal coordination and redox sensing [204, 205]. We will delete this entire region to evaluate whether it is required for function. To analyze whether HRG-7 and HRG-8 require autocatalytic activation for function, we will mutate the residues of the predicted propeptide cleavage site.

Identification of downstream regulators of HRG-7 signaling

HRG-7 and DBL-1 appear to regulate *hrg-1* through separate pathways. Therefore, the feedback mechanism functioning downstream of HRG-7 has yet to be uncovered.

Figure 6.2: Conserved residues of HRG-7 and HRG-8

A) ClustalW alignment of HRG-7 with Cathepsin E. Black shading indicates

identical residues. Gray shading indicates similar residues. Red asterisk indicate

catalytic residues. Green line indicates residues unique to HRG-7. B) ClustalW

alignment of HRG-8 with Cathepsin B. Black shading indicates identical residues.

Gray shading indicates similar residues. Red asterisk indicate catalytic residues

(absence in HRG-8).

A

```
HRG-7         1 MKTFTALIALLTVV---SAEVHQFNIGYRPNVRQRVNAKGKLAEYEKERNE---LLSKKS
CathepsinE    1 MKTLILLLLVLLELGEAQGSIHRVPIRRHPSLKKKIRARSQLSEDWKSHNLDMIQFIESC

HRG-7        55 LQLASSSSPVIDYEDMAYMVQISIGSPAQNFVLFIDSGSSNLWVPDITCAGGKDATC
                                                              _____
CathepsinE   61 SMDQSAKEPIINYLDMEYFGTISIGSPPQNETVIFDTGSSNLWVPSVYCT-------
                                                        *

                 _____
HRG-7       112 GSYCKSTPYDACLTFCQEECCTKTVEGVKVLSTTDACQSKHRFNSSLSSSYVTNGQ
CathepsinE  111 --------------------------------SPACKTHSRFCPSQSSTYSQPGQ

HRG-7       168 KFDYTYNTGEVKGFFGVDTFCFTNTSVCATGGVFGQATT-IGEABAKQPEDGIIGL
CathepsinE  134 SFSIQYGTGSLSGIIGADQVSVEG--ITVVGQQFGESVTEPGQTFVDAEFDGILGL

HRG-7       223 GWPALAVNQQTPPLFNNMNQGKLDQPYFVVYLANIGPTSQINGGAFTVGGLDTTHC
CathepsinE  188 GYPSLAVGGVTPVFDNYMAQNLVDLPMFSVYYS--SNPEGGAGSELIFGGYDHSHF

HRG-7       279 SSNVDWVPLSTQTFWQFKLGGVSSGSYSQAPNSGWQAAADTAASFTGAPKSVVTSL
CathepsinE  242 SGSINWVPVTKQAYWQIALDNIQVGGTVMFCSEGCQAIVDTGTSLITGPSDKIKQL
                                                        *

HRG-7       335 AKAVGATYVPLTGAFFMDCDAVVPDIVFTINGKTYNMPSTSEVYSAGPGPCMEAFY
CathepsinE  298 QNAIGAAPVDGEYAVECANLNVMPDVTFTINGVPYTLSPTAYTLLDFVDGMQECSS

HRG-7       391 ELTAGGFYP----AWYLGPPEYRAYCHVHDMKSGRIGLAKVL- 428
CathepsinE  354 GFQCLDIHPPAGPLWILGDVFIRQYYSVFDRGNNRVGLAPAVP 396
```

B

```
HRG-8         1 MLEIFLSFLLPLFICTPLHSSVTYQSSISSEAIKLSGSDLTSYVNKKQKLWKAETSRMTF
CathepsinB    1 -MWQLWASLCCLLVLANARSRPSFHP--------LS-DELVNYVNKRNTTWQAGHNFYNV

HRG-8        61 QEKMARAKSIKFIKSNDEVSEKTGNDNVLVDIESSFDSRQKWPSCSQIGAVRDQSDCGSA
CathepsinB   51 DMSYLKRLCGTFLGGPKPPQRVMFTED--IKLPASFDAREQWPQCPTIKEIRDQGSCGSC
                                                                             *

HRG-8       121 AHLVAVEIASDRTCIASNGTFNWPLSAQDPLSCCVGLMSICGDGWGCDGSWEKDIL
CathepsinB  109 WAFGAVEAISDRICIHTNAHVSVEVSAEDLLTCCG---SMCGD--GCNGGYPAEAW

HRG-8       177 KWWQTHGICTGGNYNDQFGCKPYSIYPCDKKYANGTTSVPCPG-YHTPTCEEHCTS
CathepsinB  160 NFWTRKGLVSGGLYESHVGCRPYSIPPCEH-HVNGSR-PPCTGEGDTPKCSKICEP

HRG-8       232 NITWPIAYKQDKHFGKAHYNVGKKMTDIQIEIMTNGPVIASFIIYDDFWDYKTGIY
CathepsinB  214 --GYSPTYKQDKHYGYNSYSVSNSEKDIMAEIYKNGPVEGAFSVYSDFLLYKSGVY

HRG-8       288 VHTAGDQEGGMDTKIIGWGVDNGVPYWICVHQWGTDFGENGFVRFLRGVNEVNIEH
CathepsinB  268 QHVTGEMMGGHAIRILGWGVENGTPYWIVANSWNTDWGDNGFFKILRGQDHCGIES
                              *                       *

HRG-8       344 QVLAALPDSEKHN--- 356
CathepsinB  324 EVVAGIPRTDQYWEKI 339
```

Identification of direct interactors through MuDPIT will facilitate the discovery of this pathway, but in conjunction with biochemical studies it would be useful to identify genes that are differentially regulated in the absence of HRG-7. Currently there are no strains harboring deletions in the coding region of *hrg-7*, but CRISPR / Cas9 technology has made it possible to engineer deletions into specific regions of the genome with relative ease. Therefore, we can generate a *hrg-7* deletion strain in the lab and perform RNAseq to evaluate changes in the transcriptome in the absence of HRG-7. We can genetically dissect pathways by knocking down candidate genes in conjunction with *hrg-7* RNAi in IQ6015 *(lin-15b (n744); P$_{hrg-1}$::GFP)*.

Functional dissection of HRG-7 and DBL-1 with tissue specific heme sensors
Depletion of *hrg-7*, *hrg-8*, or *dbl-1* results in a heme deficiency signal. We hypothesize that sensory neurons can signal to the intestine when HRG-7 is depleted, but the pathway may be indirect. Perhaps neurons integrate heme deficiency signals from other tissues prior to signaling to the intestine, the primary organ for heme uptake. We also hypothesize that depletion of *dbl-1* leads to SMA-9 depression in the intestine and therefore upregulation of *hrg-1*. However, this does not explain why there is a heme-dependent phenotype associated loss of DBL-1. Is heme availability compromised in specific tissues in the absence of HRG-7, HRG-8, and DBL-1? The lab is currently developing tissue specific heme sensors that will assist in understanding the origin of heme deficiency signals in the absence of specific genes. These sensors will be expressed from tissues-specific promoters and based on the enzymatic activity of horseradish peroxidase and ascorbate peroxidase, which require

145

a heme moiety for enzymatic function. Substrate can be added to lysate from these heme sensor strains grown under different RNAi conditions to evaluate specific tissues that might be heme deficient under a given condition.

Significance

Mammalian cells can regulate heme levels autonomously by coordinating heme synthesis and heme degradation. Although there is mounting evidence that heme levels can be regulated through intertissue heme trafficking, this regulation is difficult to separate from cell autonomous regulation. The lab has previously demonstrated that *C. elegans* is on obligate auxotroph, and must acquire dietary heme from the environment for incorporation into hemoproteins. Consequently, all heme must pass through the intestine before being distributed to extracellular tissue such as neurons, muscle, hypodermis, and the germline. Therefore, *C. elegans* is an ideal model in which to study intercellular heme trafficking. We speculate that peripheral tissues must be able to communicate heme status to the intestine to ensure that the balance between adequate heme availability and toxicity is maintained. In support of this hypothesis, depletion of the intestinal heme exporter MRP-5 simultaneously results in heme accumulation in the intestine and an intestinal heme deficiency signal. Additionally, analyses of candidate genes from our genome-wide screen indicated that knockdown of genes in peripheral tissues could result in an intestinal heme deficiency signal. One such signaling factor is DBL-1, which is secreted by neurons and acts on the intestine via SMA-9. Moreover, we show that this signaling is

bidirectional, as intestinal secreted HRG-7 and HRG-8 localizes to for maintaining proper heme homeostasis.

Our findings are highly reminiscent of macronutrient signaling in mammals, which relies on the coordinated actions of the brain-gut axis, the pancreas, and the liver to maintain blood glucose levels. Although the systemic coordination of micronutrients such as iron and copper is to be expected [206, 207], the contribution of the brain-gut axis to micronutrient homeostasis has not been established. It has been proposed that the brain can regulate iron levels independently of systemic iron status because in models of hemochromatosis the brain remains unaffected [208]. However, brain uptake of radioactive iron injected into mice was increased after being fed an iron deficient diet, and it is therefore likely that brain has an influence on the release of iron stores when iron deprived [63]. Additionally, pica behavior is associated with severe iron deficiency anemia and can be treated by iron supplementation, suggesting the brain can produce a satiety signal for iron [199-201]. Remarkably, the intestine has been proposed to be the main regulator of systemic iron homeostasis through the iron induced expression of BMP6, which will results lowering of available iron, systemically [180]. Our discovery of a neuron-gut regulatory axis for heme homeostasis is novel and may be highly relevant to mammalian heme and iron metabolism.

The majority of systemic iron will be utilized for heme. Therefore, either cells rely completely on the aforementioned systemic iron regulation for heme synthesis, or separate pathways exist that allow cells to supplement heme synthesis with heme import from distal tissues. The intestine and macrophages express HRG1

and MRP5, and a portion of absorbed heme can be transported out of these cell types *in toto* [58-60]. Therefore, heme transporters are expressed in tissues that would allow uptake and intertissue transfer of heme. Additionally, the brain expresses FLVCR1, MRP5, and HRG1 and neurons can take up exogenous heme, suggesting that heme can be imported and exported within the nervous system [13, 209, 210]. Are such pathways relevant? Interestingly, suboptimal neonatal iron levels are associated with higher placental LRP1 levels, suggesting that during limiting iron conditions there may be compensation by direct heme transport from mother to fetus [182]. This also hints at the possibility that the placenta can receive iron or heme dependent signals from the fetus or elsewhere. Altogether, we speculated that these data suggest that there are likely pathways for direct heme transfer between tissues. These pathways may be important compensatory mechanisms during iron deficiency, heme synthesis deficiency, or pathogenesis. Additionally, specific tissues may rely on heme uptake more than others. Generation of tissue specific knockout animals and genetic chimeras will help uncouple heme synthesis from intercellular trafficking in mammalians.

We have identified two secreted factors involved in long-range signaling that are essential for systemic heme homeostasis in *C. elegans*: HRG-7 and DBL-1. Both proteins have potential homologs in humans. The closest human homolog to HRG-7 is cathepsin E, which is most highly expressed in early erythroid cells. It has been proposed that cathepsin E is associated with inner leaflet of the plasma membrane in erythrocytes, but its function remains unclear [104]. Interestingly, erythrocyte secretion of several factors, including metalloproteases, appear to play a significant

role in the regulation of normal hematopoiesis [211, 212]. Additionally, it has recently been shown that erythroblast signaling influences systemic iron homeostasis in response to blood loss [213]. Taken together, it is possible that a portion of cathepsin E is secreted from these cells, or has a role in normal or pathological erythrocyte physiology. Further studies, such as phenotype analyses of iron deficient CTSE$^{-/-}$ mice will be required to understand the role of cathepsin E in mammalian iron / heme homeostasis.

The bone morphogenic protein BMP6 has a well-defined role in mammalian iron homeostasis through the regulation of hepcidin [214]. Although BMP2, BMP4, and BMP9 are also upregulated in the intestine in response to iron and loss of BMP6, iron homeostasis is not restored likely because these BMPs are not potent regulators of hepcidin [180]. The downstream targets of intestinal, iron-induced BMP2, BMP4, and BMP9 have not been uncovered. It is noteworthy that BMP2 and BMP4 are close homologs of DBL-1. This opens up the intriguing possibility that a DBL-1 like pathway may regulate systemic iron and heme metabolism.

Appendix I

Worm strains used in this study

Strain	Background	Transgene	Source
N2			CGC
IQ6011	N2	*Phrg-1::GFP::unc-54 3' UTR; rol-6 marker*	[13].
IQ8031	N2	*Phrg-1::GFP::unc-54 3' UTR; rol-6 marker*	[11].
VH624	*nre-1(hd20); lin-15B(hd126)*	rhIs13	CGC
IQ7380	*unc-119(ed3)*	P_{vha-6}*::HRG-8::3xFLAG::ICS::GFP::unc-54; unc-119(+)*	This study
IQ6916	*hrg-1(tm3199); hrg-4(tm2994)*		[19]
IQ7701	*unc-119(ed3)*	P_{hrg-7}*::GFP::unc-54 3' UTR; unc-119(+)*	This study
IQ7702	*unc-119(ed3)*	P_{hrg-7}^{mut}*::GFP::unc-54 3' UTR; unc-119(+)*	This study
IQ7801	*unc-119(ed3)*	P_{hrg-8}*::GFP::unc-54 3' UTR ; unc-119(+)*	This study
IQ7777	*unc-119(ed3)*	P_{hrg-7}*::HRG-7::mCherry::hrg-7 3' UTR; unc-119(+)*	This study
IQ7880	*unc-119(ed3)*	P_{hrg-8}*::GFP::unc-54 3'UTR ; unc-119(+)* P_{hrg-8}*::HRG-8::mCherry::hrg-8 3' UTR; unc-119(+)*	This study
IQ7670	*unc-119(ed3)*	P_{vha-6}*:HRG-7::mCherry::unc-54 3'UTR; unc-119(+)*	This study
IQ7680	*unc-119(ed3)*	P_{vha-6}*::HRG-8::mCherry::unc-54 3'UTR; unc-119(+)*	This study
IQ8333	*unc-119(ed3)*	P_{vha-6}*::HRG-3::mCherry::hrg-3 3'UTR; unc-119(+)*	
IQ7711	*unc-119(ed3)*	P_{vha-6}*::HRG-7$^{PR:}$ICS::mCherry:: unc-54 3'UTR* P_{hrg-1}*::GFP::unc-54 3'UTR; unc-119(+)*	This study
IQ7811	*unc-119(ed3)*	P_{vha-6}*::HRG-8^{REC}:ICS::mCherry::unc-54 3'UTR* P_{hrg-1}*::GFP::unc-54 3'UTR; unc-119(+)*	This study
IQ7812	*unc-119(ed3)*	P_{vha-6}*::HRG-8^{REC}:ICS::mCherry::unc-54 3'UTR* P_{hrg-1}*::GFP::unc-54 3'UTR; unc-119(+)*	This study
IQ7170	*unc-119(ed3)*	$P_{hsp-16.2}$*::HRG-7::mCherry::unc-54 3'UTR; unc-119(+)*	This study
IQ7370	*unc-119(ed3)*	P_{vha-6}*::HRG-8-3::XFLAG::ICS::GFP::unc-54; unc-119(+)*	This study
IQ7712	*unc-119(ed3)*	P_{vha-6}*::iHRG-7^{PR}:ICS::mCherry:: unc-54 3'UTR; unc-119(+)*	This study
IQ7771	*unc-119(ed3)*	P_{vha-6}*::HRG-7^{PR}::mCherry:: unc-54 3'UTR* P_{hrg-1}*::GFP:: unc-54 3'UTR; unc-119(+)*	This study
IQ7412	*unc-119(ed3)*	P_{vha-6}*::TM-HRG-7^{PR}:ICS::mCherry:: unc-54 3'UTR,* P_{hrg-1}*::GFP:: unc-54 3'UTR; unc-119(+)*	This study
IQ6015	*lin-15b(n744)*	P_{hrg-1}*::GFP; unc-54 3'UTR*	This study
BW1946	*unc-42(e270)*	ctIs43[pDP#MM016B, pNY+nls, pMY-nls (dbl-1::GFP)	CGC
RW10745	*unc-119(ed3)*	zuIs178 [his-72(1kb 5' UTR)::his-72::SRPVAT::GFP::his-72 (1KB 3' UTR) + 5.7 kb XbaI - HindIII unc-119(+)]. stIs10024 [pie-1::H2B::GFP::pie-1 3' UTR + unc-119(+)]. stIs10698 [sma-9.k::H1-wCherry + unc-119(+)].	CGC
IQ8330	*unc-119(ed3)*	P_{vha-6}*::HRG-7::mCherry::unc-54 3'UTR; unc-119(+)*	This Study
IQ6311	*dbl-1(nk3)*	P_{hrg-1}*::GFP:: unc-54 3'UTR*	This study
IQ6312	*dbl-1(nk3)*	P_{hrg-1}*::GFP:: unc-54 3'UTR:: P_{dbl-1}::GFP::DBL-1*	This study
ZC1478	*dbl-1(nk3)*	P_{dbl-1}*::GFP::DBL-1*	[215]

Appendix II

Oligonucleotides used in this study

Purpose	Name	Sequence
hrg-7 promoter amplification	5' PRM	AAGCTTTCCAACGGTCAAACG
	3' PRM	GGATCCTGGCTTCCAACTTTTTTCC
hrg-8 promoter amplification	5' PRM	GCC TTG TAA GAG CAG TTG AAG ACG
	3' PRM	AAGTTAAAAATTGAAATTTTATGAATTGATCAGGAAGAACC
hrg-7 coding region amplification	5' CDS	ATGAAGACGTTTATTGCATTG
	3' CDS	GAGAACCTTTGCAAGGCCAAG
hrg-8 coding region amplification	5' CDS	ATGCTCTTCATATTTCTATCATTTTTGTTACC
	3' CDS	CATCAGGATCCTTAGTTATGCTTTTCCGAATCTGGAAGCG
hrg-7 3' UTR amplification	5' 3'UTR	ATCCAATGAATCTCACATCAACG
	3' 3'UTR	TTGATTGTAAAGTTTTTATTAAATTTTAGGGGGACAACTTTGTATAATAAAGTTG
hrg-8 3' UTR amplification	5' 3'UTR	CACTTATTCACTTTCAATTTACAAATTTTGTTTGAATTGC
	3' 3'UTR	GGGGACAACTTTGTATAATAAAGTTGCAAGCTAGACGGCGATACCTGG
dbl-1(nk3) genotyping	5' internal (C)	CTTCATCGATTTGCCGGAAGATGTG
	3' internal (D)	CAGTAGGCACACAGCAAGGTG
	5' flanking (A)	CATGGACAAACATCGGGGA
	3' flanking (B)	CGTGTACACAAATCTGTTCG
	5' GFP (E)	CTGGGATTACACATGGCATGGATG
	3' *dbl-1* (F)	CGGATAATAGTGTCTGACCCAGTCGAC
lin-15b(n744) genotyping	5' l*in-15b(n744)*	CACAAACCTGGAGATCGCTCGAG
	3' *lin-15b(n744)*	CGACAATGGATTGCACATCTCGATCAG

Appendix III

HRG-3::mCherry and HRG-3-SP::mCherry do not localize to punctae in the anterior of the worm

A) mCherry expression in the intestine, coelomocytes, and anterior of strain IQ8330 (P_{vha-6}::*HRG-3SP-mCherry*). In the anterior of the worm, mCherry is non-specifically diffused throughout the pseudocoelomic fluid. **B)** mCherry expression in the gonad and coelomocytes of IQ8333 (P_{vha-6}::*HRG-3::mCherry*). No mCherry is observed in the anterior of the worm. Images are 63 x, scale bar =20µm.

A

P*vha-6*::HRG-3SP-mCherry
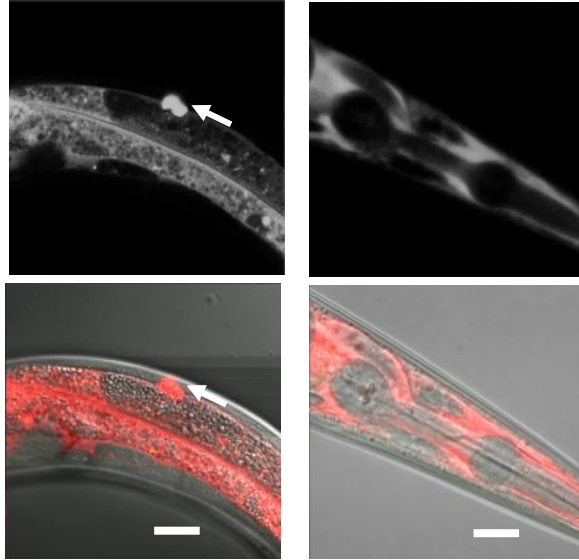
B

P*vha-6*::HRG-3::mCherry
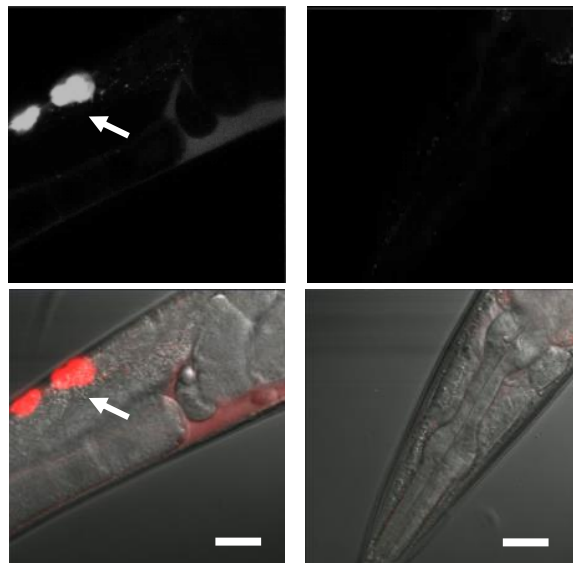
Appendix IV

HRG-7::mCherry and HRG-8::mCherry do not colocalize with GFP expressed in hypodermis, pharyngeal muscle, or body wall muscle

Representative images of expression of tissue specific GFP / YFP markers $P_{ceh-22}::GFP$ (pharyngeal muscle), $P_{dpy-7}::YFP$ (hypodermis), and $P_{myo-2}::GFP$ (body wall muscle) crossed into strains IQ7670 ($P_{vha-6}::HRG-7::mCherry$) and IQ7680 ($P_{vha-6}::HRG-8::mCherry$).* indicates body wall muscle (BWM). Arrow indicates pharyngeal muscle (PM). Arrowhead indicates hypodermis (H). Images are 63 x, scale bar =20µm.

| | GFP | mCherry | Merge | DIC |
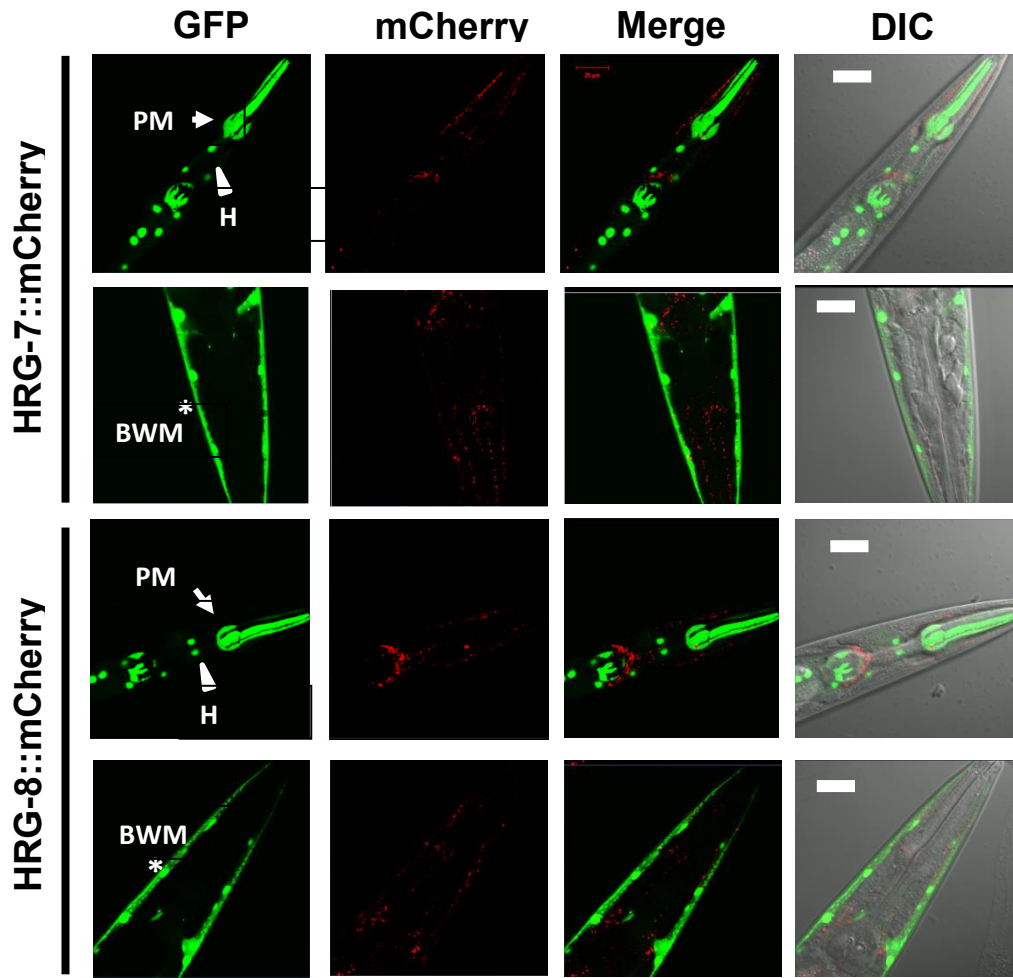
Appendix V

Recoded *hrg-7*

```
ATGAAAACCTTCATCGCCCTTCTTGCCCTTCTTACCGTTGTTTCCGCTGAGGTTCATCAGTTCAACATCGGATATC
GCCCAAATATGCGCCAGCGCATGAACGCTAAGGGAAAGCTTGCTGAGTACGAGAAAGAGCGTAACGAGCTCCTTTC
CAAAAAGTCGCTCCAACTTGCTTCTTCTTCCTCTCCAGTCATCGACTACGAAGACATGGCTTATATGGTCCAAATC
TCTCTTGGATCTCCAGCCCAAAACTTCGTCCTCTTCATCGACTCCGGATCCTCCAACCTTTGGGTTCCAGACATCA
CTTGCGCCGGAGGTAAGgtaagtttaaacatatatatactaactaaccctgattatttaaattttcagGACGCTAC
CTGCGGATCTTATTGCAAGTCCACCCCATACGACGCCTGCCTTACCTTTTGCCAGGAAGAGTGTTGCACTAAGACT
GTCGAGGGAGTCAAGGTCCTCTCCACAACCGATGCCTGCCAATCCAAGCACCGCTTCAACTCTTCCCTTAGTTCTT
CTTACGTTACTAACGGACAGAAGTTCGACATGACCTACAATACCGGAGAGGTTAAAGgtaagtttaaacagttcgg
tactaactaaccatacatatttaaattttcagGTTTCTTCGGAGTCGACACCTTCTGCTTTACCAATACCTCTGTT
TGCGCTACCGGACAAGTCTTTGGACAGGCTACTACCATTGGAGAGGCCTTCGCTAAGCAACCTGAGGACGGAATTA
TCGGACTCGGTTGGCCAGCCCTTGCTGTTAATCAACAGACCCCTCCACTTTTCAACCTTATGAACCAGGGAAAGCT
CGACCAGCCATATTTCGTTGTTTACCTCGCTAATATCGGACCAACCTCTCAGATTAACGGAGGTGCTTTTACTGTC
GGAGGACTTGACACCACCCACTGCTCTTCCAACGTGGATTGGGTCCCACTTTCTACCCAGACCTTTTGGCAATTCA
AACTTGGAGGTGTTTCTTCCGGATCTTACTCTCAAGCCCCTAATAGCGGTTGGCAGGCTGCCGCCGACACCGCCGC
TTCTTTCATTGGTGCTCCAAAATCGGTCGTCACTTCCCTCGCTAAGgtaagtttaaacatgattttactaactaac
taatctgatttaaattttcagGCTGTCGGAGCTACCTACGTCCCACTCACCGGAGCTTTCTTTATGGACTGCGATG
CCGTCGTTCCAGACATCGTTTTCACTATCAATGGAAAGACTTACAACATGCCTTCTACCTCCTTTGTCGTTTCCGC
CGGACCAGGACCTTGTATGTTCGCTTTCTACGAACTTACCGCCGGAGGTTTTTACCCTGCCTGGATGCTTGGTCCT
CCATTCATGCGCGCTTACTGCCATGTTCACGATATGAAATCTGGACGTCTCGGACTCGCCAAGGTCCTT
```

Recoded *hrg-8*

```
ATGTTGTTTATCTTCCTTTCCTTCCTTCTTCCACTTTTCATCTGCACCCCACTTCACTCTTCCGTCACTTATCAGT
CTTCTATCTCCTCGGAGGCTATTAAGCTCTCCGGTTCCGACTTAACCAGTTACGTTAACAAGAAGCAAAAGCTTTG
GAAGGCTGAGACATCTCGTATGACTTTCCAGGAAAAGATGGCTCGCGCTAAGTCCATTAAGTTCATCAAATCTAAC
GACGAGGTTAGCGAAAAGgtaagtttaaacatatatatactaactaaccctgattatttaaattttcagACCGGAA
ACGACAACGTCCTCGTTGATATCCCATCTTCTTTCGACTCTCGCCAAAAGTGGCCATCTTGCTCCCAGATCGGAGC
TGTCCGCGACCAATCAGACTGCGGATCCGCTGCCCATCTTGTCGCTGTCGAGATCGCTAGCGACCGTACCTGCATC
GCTTCTAACGGAACTTTCAACTGGCCGCTTTCCGCTCAGGACCCACTCTCCTGCTGCGTCGGACTTATGTCCATCT
GCGGAGACGGTTGGGGTTGCGATGGATCGTGGCCTAAGGgtaagtttaaacagttcggtactaactaaccatacat
atttaaattttcagACATCCTTAAATGGTGGCAGACTCACGGACTTTGCACCGGAGGAAACTACAACGACCAGTTC
GGTTGCAAGCCATACTCCATCTACCCATGCGACAAAAAGTACGCTAACGGAACTACCTCCGTTCCATGCCCAGGAT
ACCACACCCCAACTTGCGAAGAGCACTGCACCTCCAATATCACTTGGCCAATCGCTTACAAGCAGGACAAGCACTT
CGGAAAGGCTCACTACAACGTCGGAAAGgtaagtttaaacatgattttactaactaactaatctgatttaaatttt
cagAAAATGACTGATATCCAGATCGAGATTATGACTAACGGACCAGTTATCGCTTCCTTCATCATCTACGATGACT
TCTGGGACTACAAGACCGGAATTTACGTTCACACCGCTGGAGACCAGGAGGGAGGTATGGATACTAAGATCATCGG
TTGGGGTGTCGATAACGGAGTTCCCTACTGGCTCTGTGTCCACCAGTGGGGAACTGACTTCGGAGAAAACGGATTC
GTCCGTTTCCTTCGAGGAGTTAATGAAGTTAACATTGAGCACCAGGTCCTTGCTGCTCTCCCAGACTCTGAGAAAC
ACAAT
```

Capital letters denote coding sequence. Lower-case letters denote introns.

Appendix VI

Competent HRG-7 and HRG-8 cannot be expressed from muscle or neurons

A) Representative image of GFP fluorescence in worms expressing P_{hrg-1}::GFP alone

or with P_{vha-6}::HRG-7^{PR}:ICS::mCherry or P_{myo-3}::HRG-7^{PR}:ICS::mCherry and fed

dsRNA against vector, hrg-7^{300bp}, and hrg-7^{ORF} at 10 μM heme. **B)** Immunoblot

analyses of worms expressing P_{vha-6}::HRG-7^{PR}:ICS::mCherry , P_{myo-3}::HRG-

7^{PR}:ICS::mCherry, $P_{unc-119}$::HRG-7^{PR}:ICS::mCherry or WT worms fed dsRNA

against, hrg-7^{300bp}. Membranes were probed with polyclonal anti-HRG-7 antibody

and then incubated with HRP-conjugated anti-rabbit secondary antibody. * indicates

pro-HRG-7. + indicates mature HRG-7. **C)** Representative image of GFP

fluorescence in IQ6011 expressing P_{hrg-1}::GFP alone or with P_{vha-6}::HRG-

8^{REC}:ICS::mCherry or P_{myo-3}::HRG-8^{REC}:ICS::mCherry and fed dsRNA against

vector, hrg-7^{300bp}, and hrg-7^{ORF} at 10 μM heme.

A

P_{hrg-1}:GFP

P_{vha-6}:HRG-7^{PR} P_{myo-3}:HRG-7^{PR}

RNAi

vector

hrg-7$^{300\ bp}$

hrg-7^{ORF}

B

α-HRG-7

vha-6p   myo-3p   unc-119p   WT

*
+

C

P_{hrg-1}:GFP

P_{vha-6}:HRG-8^{REC} P_{myo-3}:HRG-8^{REC}

RNAi

vector
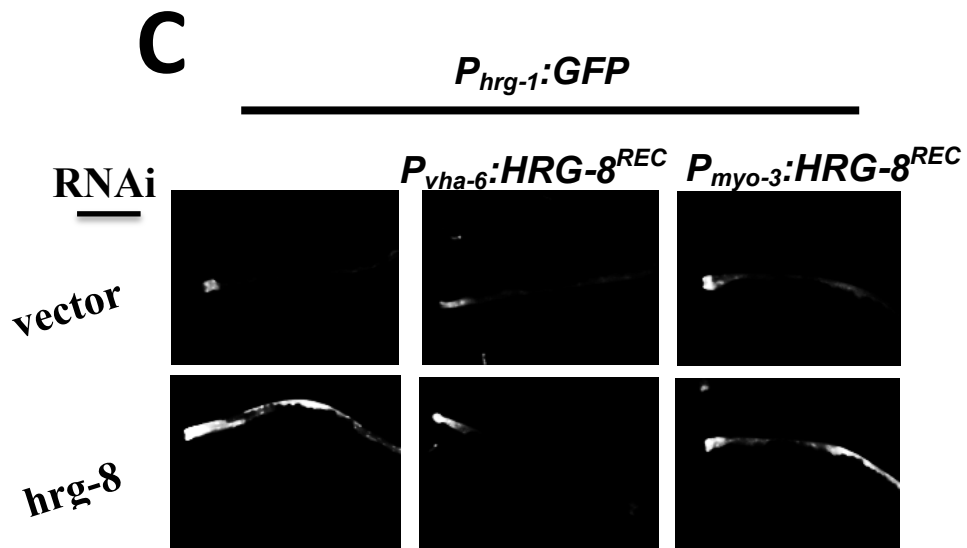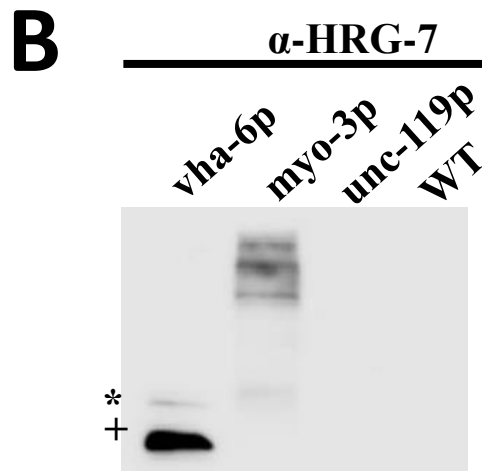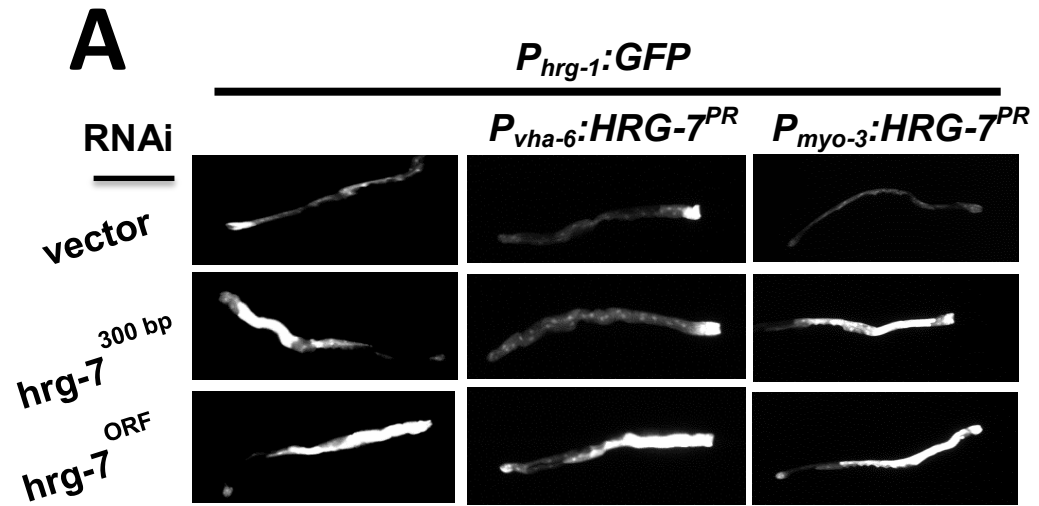
hrg-8

Appendix VII

HRG-7 and HRG-8 cannot be tethered to the intestinal basolateral membrane

A) mCherry expression in the intestine of a worm expressing P_{vha-6}*::HRG-7^{PR}::mCherry-TAC* **B)** mCherry expression in the coelomocytes of a worm expressing (P_{vha-6}*::HRG-8^{REC}::mCherry-GPI*). Arrow indicates coelomocyte. **C)** mCherry expression in the intestine of a worm expressing P_{vha-6}*::HRG-8^{REC}::mCherry-LDLR*. Images are 63x.

A

P*vha-6*::HRG-7*PR*::mCherry-Tac
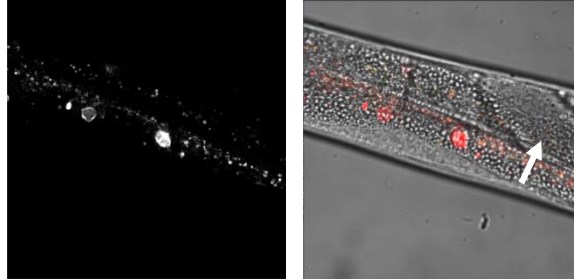
B

P*vha-6*::HRG-8*REC*::mCherry-GPI
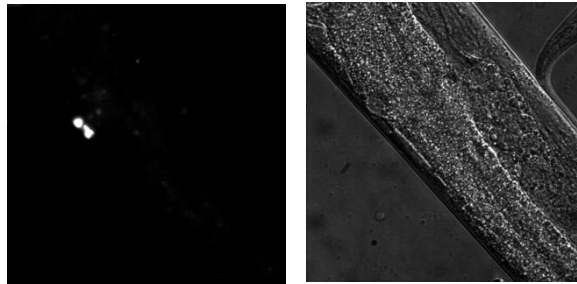
C

P*vha-6*::HRG-8*REC*::mCherry-LDLR
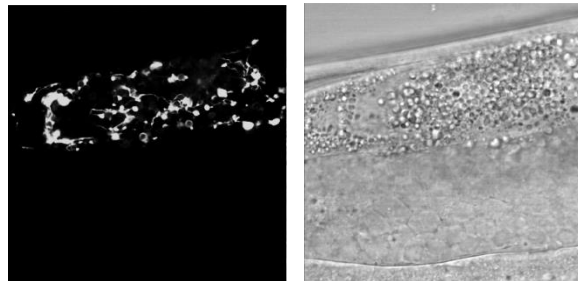
Appendix VIII

Genetic / physical interaction network of ins-21 using geneMANIA.
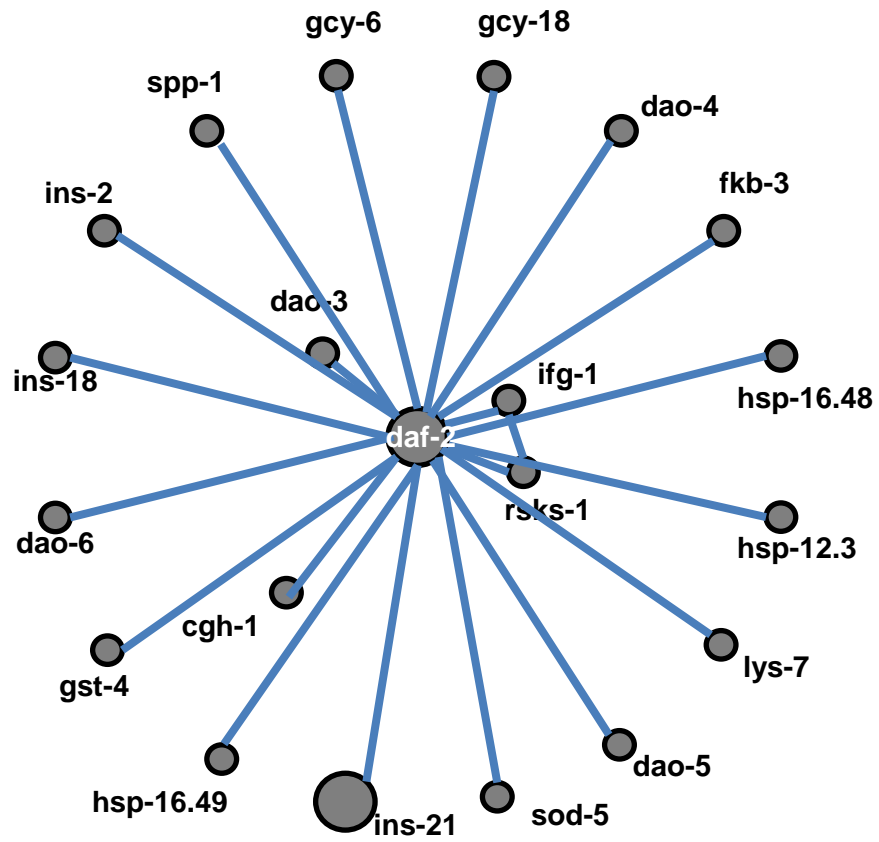
References

1.   Severance, S. and I. Hamza, *Trafficking of heme and porphyrins in metazoa.* Chem Rev, 2009. **109**(10): p. 4596-616.

2.   Ponka, P., *Cell biology of heme.* Am J Med Sci, 1999. **318**(4): p. 241-56.

3.   Monsen, E.R., et al., *Estimation of available dietary iron.* Am J Clin Nutr, 1978. **31**(1): p. 134-41.

4.   Roughead, Z.K. and J.R. Hunt, *Adaptation in iron absorption: iron supplementation reduces nonheme-iron but not heme-iron absorption from food.* Am J Clin Nutr, 2000. **72**(4): p. 982-9.

5.   Carpenter, C.E. and A.W. Mahoney, *Contributions of Heme and Nonheme Iron to Human-Nutrition.* Critical Reviews in Food Science and Nutrition, 1992. **31**(4): p. 333-367.

6.   Knutson, M. and M. Wessling-Resnick, *Iron metabolism in the reticuloendothelial system.* Crit Rev Biochem Mol Biol, 2003. **38**(1): p. 61-88.

7.   Balla, G., et al., *Exposure of endothelial cells to free heme potentiates damage mediated by granulocytes and toxic oxygen species.* Lab Invest, 1991. **64**(5): p. 648-55.

8.   Sassa, S., *The porphyrias.* Photodermatol Photoimmunol Photomed, 2002. **18**(2): p. 56-67.

9.   Vincent, S.H., *Oxidative effects of heme and porphyrins on proteins and lipids.* Semin Hematol, 1989. **26**(2): p. 105-13.

10.   Rao, A.U., et al., *Lack of heme synthesis in a free-living eukaryote.* Proc Natl Acad Sci U S A, 2005. **102**(12): p. 4270-5.

11.   Chen, C., et al., *An Intercellular Heme-Trafficking Protein Delivers Maternal Heme to the Embryo during Development in C. elegans.* Cell, 2011. **145**(5): p. 720-31.

12.   Korolnek, T., et al., *Control of metazoan heme homeostasis by a conserved multidrug resistance protein.* Cell Metab, 2014. **19**(6): p. 1008-19.

13.   Rajagopal, A., et al., *Haem homeostasis is regulated by the conserved and concerted functions of HRG-1 proteins.* Nature, 2008. **453**(7198): p. 1127-31.

14.   Keel, S.B., et al., *A heme export protein is required for red blood cell differentiation and iron homeostasis.* Science, 2008. **319**(5864): p. 825-8.

15.   Cao, C. and K.O. O'Brien, *Pregnancy and iron homeostasis: an update.* Nutr Rev, 2013. **71**(1): p. 35-51.

16.   Yang, Z., et al., *Kinetics and specificity of feline leukemia virus subgroup C receptor (FLVCR) export function and its dependence on hemopexin.* J Biol Chem, 2010. **285**(37): p. 28874-82.

17.   Haldar, M., et al., *Heme-mediated SPI-C induction promotes monocyte differentiation into iron-recycling macrophages.* Cell, 2014. **156**(6): p. 1223-34.

18.   *Genome sequence of the nematode C. elegans: a platform for investigating biology.* Science, 1998. **282**(5396): p. 2012-8.

19.   Yuan, X., et al., *Topologically conserved residues direct heme transport in HRG-1-related proteins.* J Biol Chem, 2012. **287**(7): p. 4914-24.

20.   Severance, S., et al., *Genome-wide analysis reveals novel genes essential for heme homeostasis in Caenorhabditis elegans.* PLoS Genet, 2010. **6**(7): p. e1001044.

21.   Goodwin, D.C., S.W. Rowlinson, and L.J. Marnett, *Substitution of tyrosine for the proximal histidine ligand to the heme of prostaglandin endoperoxide synthase 2: implications for the mechanism of cyclooxygenase activation and catalysis.* Biochemistry, 2000. **39**(18): p. 5422-32.

22.   Liu, Y., et al., *Replacement of the proximal histidine iron ligand by a cysteine or tyrosine converts heme oxygenase to an oxidase.* Biochemistry, 1999. **38**(12): p. 3733-43.

23.   Hawkins, M.G. and J.D. McGhee, *elt-2, a second GATA factor from the nematode Caenorhabditis elegans.* J Biol Chem, 1995. **270**(24): p. 14666-71.

24.   Sinclair, J. and I. Hamza, *A novel heme response element mediates transcriptional regulation in Caenorhabditis elegans.* J Biol Chem, 2010.

25.   Chen, C., et al., *Heme utilization in the Caenorhabditis elegans hypodermal cells is facilitated by heme-responsive gene-2.* J Biol Chem, 2012. **287**(12): p. 9601-12.

26.   McKie, A.T., et al., *A novel duodenal iron-regulated transporter, IREG1, implicated in the basolateral transfer of iron to the circulation.* Mol Cell, 2000. **5**(2): p. 299-309.

27.   Ohgami, R.S., et al., *Identification of a ferrireductase required for efficient transferrin-dependent iron uptake in erythroid cells.* Nat Genet, 2005. **37**(11): p. 1264-9.

28.   Eckel-Mahan, K. and P. Sassone-Corsi, *Metabolism and the circadian clock converge.* Physiol Rev, 2013. **93**(1): p. 107-35.

29.   van der Linden, A.M., et al., *Genome-wide analysis of light- and temperature-entrained circadian transcripts in Caenorhabditis elegans.* PLoS Biol, 2010. **8**(10): p. e1000503.

30.   Yang, J., et al., *A novel heme-regulatory motif mediates heme-dependent degradation of the circadian factor period 2.* Mol Cell Biol, 2008. **28**(15): p. 4697-711.

31.   Raghuram, S., et al., *Identification of heme as the ligand for the orphan nuclear receptors REV-ERBalpha and REV-ERBbeta.* Nat Struct Mol Biol, 2007.

32.   Kaasik, K. and C. Chi Lee, *Reciprocal regulation of haem biosynthesis and the circadian clock in mammals.* Nature, 2004. **430**(6998): p. 467-471.

33.   Srivastava, G., et al., *Regulation of 5-aminolevulinate synthase mRNA in different rat tissues.* J Biol Chem, 1988. **263**(11): p. 5202-9.

34.   Cox, T.C., et al., *Human erythroid 5-aminolevulinate synthase: promoter analysis and identification of an iron-responsive element in the mRNA.* EMBO J, 1991. **10**(7): p. 1891-902.

35.   Bishop, T.R., et al., *Genetic regulation of delta-aminolevulinate dehydratase during erythropoiesis.* Nucleic Acids Res, 1996. **24**(13): p. 2511-8.

36.   Chretien, S., et al., *Alternative transcription and splicing of the human porphobilinogen deaminase gene result either in tissue-specific or in housekeeping expression.* Proc Natl Acad Sci U S A, 1988. **85**(1): p. 6-10.

37.   Romeo, P.H., et al., *Molecular cloning and nucleotide sequence of a complete human uroporphyrinogen decarboxylase cDNA*. J Biol Chem, 1986. **261**(21): p. 9825-31.

38.   Takahashi, S., et al., *Differential regulation of coproporphyrinogen oxidase gene between erythroid and nonerythroid cells*. Blood, 1998. **92**(9): p. 3436-44.

39.   Tugores, A., S.T. Magness, and D.A. Brenner, *A single promoter directs both housekeeping and erythroid preferential expression of the human ferrochelatase gene*. J Biol Chem, 1994. **269**(49): p. 30789-97.

40.   Sun, J., et al., *Hemoprotein Bach1 regulates enhancer availability of heme oxygenase-1 gene*. EMBO J, 2002. **21**(19): p. 5216-24.

41.   Ogawa, K., et al., *Heme mediates derepression of Maf recognition element through direct binding to transcription repressor Bach1*. Embo J, 2001. **20**(11): p. 2835-43.

42.   Suzuki, H., et al., *Heme regulates gene expression by triggering Crm1-dependent nuclear export of Bach1*. EMBO J, 2004. **23**(13): p. 2544-53.

43.   Tahara, T., et al., *Heme-dependent up-regulation of the alpha-globin gene expression by transcriptional repressor Bach1 in erythroid cells*. Biochem Biophys Res Commun, 2004. **324**(1): p. 77-85.

44.   White, C., et al., *HRG1 is essential for heme transport from the phagolysosome of macrophages during erythrophagocytosis*. Cell Metab, 2013. **17**(2): p. 261-70.

45.   Warnatz, H.J., et al., *The BTB and CNC homology 1 (BACH1) target genes are involved in the oxidative stress response and in control of the cell cycle.* J Biol Chem, 2011. **286**(26): p. 23521-32.

46.   Quigley, J.G., et al., *Identification of a human heme exporter that is essential for erythropoiesis.* Cell, 2004. **118**(6): p. 757-66.

47.   Chiabrando, D., et al., *The mitochondrial heme exporter FLVCR1b mediates erythroid differentiation.* J Clin Invest, 2012. **122**(12): p. 4569-79.

48.   Wejman, J.C., et al., *Structure of haptoglobin and the haptoglobin-hemoglobin complex by electron microscopy.* J Mol Biol, 1984. **174**(2): p. 319-41.

49.   Okazaki, T., Y. Yanagisawa, and T. Nagai, *Analysis of the affinity of each haptoglobin polymer for hemoglobin by two-dimensional affinity electrophoresis.* Clin Chim Acta, 1997. **258**(2): p. 137-44.

50.   Graversen, J.H., M. Madsen, and S.K. Moestrup, *CD163: a signal receptor scavenging haptoglobin-hemoglobin complexes from plasma.* Int J Biochem Cell Biol, 2002. **34**(4): p. 309-14.

51.   Delaby, C., et al., *Sequential regulation of ferroportin expression after erythrophagocytosis in murine macrophages: early mRNA induction by haem, followed by iron-dependent protein expression.* Biochem J, 2008. **411**(1): p. 123-31.

52.   Bratosin, D., et al., *Cellular and molecular mechanisms of senescent erythrocyte phagocytosis by macrophages. A review.* Biochimie, 1998. **80**(2): p. 173-95.

53.   Hrkal, Z., Z. Vodrazka, and I. Kalousek, *Transfer of heme from ferrihemoglobin and ferrihemoglobin isolated chains to hemopexin.* Eur J Biochem, 1974. **43**(1): p. 73-8.

54.   Hvidberg, V., et al., *Identification of the receptor scavenging hemopexin-heme complexes.* Blood, 2005. **106**(7): p. 2572-9.

55.   Vinchi, F., et al., *Hemopexin prevents endothelial damage and liver congestion in a mouse model of heme overload.* Am J Pathol, 2008. **173**(1): p. 289-99.

56.   Knutson, M., et al., *Iron release from macrophages after erythrophagocytosis is up-regulated by ferroportin 1 overexpression and down-regulated by hepcidin.* Proc. Natl. Acad. Sci. U.S.A., 2005. **102**(5): p. 1324-8.

57.   Bonkovsky, H.L., et al., *Intravenous heme-albumin in acute intermittent porphyria: evidence for repletion of hepatic hemoproteins and regulatory heme pools.* Am J Gastroenterol, 1991. **86**(8): p. 1050-6.

58.   Turnbull, A., F. Cleton, and C.A. Finch, *Iron absorption. IV. The absorption of hemoglobin iron.* J Clin Invest, 1962. **41**: p. 1897-907.

59.   Wheby, M.S., G.E. Suttle, and K.T. Ford, 3rd, *Intestinal absorption of hemoglobin iron.* Gastroenterology, 1970. **58**(5): p. 647-54.

60.   Brown, E.B., et al., *Absorption of radiation-labeled hemoglobin by dogs.* J Lab Clin Med, 1968. **72**(1): p. 58-64.

61.   Uc, A., J.B. Stokes, and B.E. Britigan, *Heme transport exhibits polarity in Caco-2 cells: evidence for an active and membrane protein-mediated process.* Am J Physiol Gastrointest Liver Physiol, 2004. **287**(6): p. G1150-7.

62.   Dooley, K.A., et al., *montalcino, A zebrafish model for variegate porphyria.* Exp Hematol, 2008. **36**(9): p. 1132-42.

63.   Smith, A.G., E.L. Raven, and T. Chernova, *The regulatory role of heme in neurons.* Metallomics, 2011. **3**(10): p. 955-62.

64.   Whetsell, W.O., Jr., et al., *Studies on porphyrin-heme biosynthesis in organotypic cultures of chick dorsal root ganglion. I. Observations on neuronal and non-neuronal elements.* J Neuropathol Exp Neurol, 1978. **37**(5): p. 497-507.

65.   Chernova, T., P. Nicotera, and A.G. Smith, *Heme deficiency is associated with senescence and causes suppression of N-methyl-D-aspartate receptor subunits expression in primary cortical neurons.* Mol Pharmacol, 2006. **69**(3): p. 697-705.

66.   Morris, C.M., et al., *Evidence for the localization of haemopexin immunoreactivity in neurones in the human brain.* Neurosci Lett, 1993. **149**(2): p. 141-4.

67.   Wagner, K.R., et al., *Heme and iron metabolism: role in cerebral hemorrhage.* J Cereb Blood Flow Metab, 2003. **23**(6): p. 629-52.

68.   Tolosano, E., et al., *Specific expression in brain and liver driven by the hemopexin promoter in transgenic mice.* Biochem Biophys Res Commun, 1996. **218**(3): p. 694-703.

69.   Mayer, E.A., *Gut feelings: the emerging biology of gut-brain communication.* Nat Rev Neurosci, 2011. **12**(8): p. 453-66.

70.   Miguel-Aliaga, I., *Nerveless and gutsy: intestinal nutrient sensing from invertebrates to humans.* Semin Cell Dev Biol, 2012. **23**(6): p. 614-20.

71.   Lam, T.K., *Neuronal regulation of homeostasis by nutrient sensing.* Nat Med, 2010. **16**(4): p. 392-5.

72.   Durieux, J., S. Wolff, and A. Dillin, *The cell-non-autonomous nature of electron transport chain-mediated longevity.* Cell, 2011. **144**(1): p. 79-91.

73.   Hung, W.L., et al., *A Caenorhabditis elegans developmental decision requires insulin signaling-mediated neuron-intestine communication.* Development, 2014. **141**(8): p. 1767-79.

74.   Mak, H.Y., et al., *Polygenic control of Caenorhabditis elegans fat storage.* Nat Genet, 2006. **38**(3): p. 363-8.

75.   Taylor, R.C. and A. Dillin, *XBP-1 is a cell-nonautonomous regulator of stress resistance and longevity.* Cell, 2013. **153**(7): p. 1435-47.

76.   Miyamoto, T., G. Wright, and H. Amrein, *Nutrient sensors.* Curr Biol, 2013. **23**(9): p. R369-73.

77.   Wang, H., et al., *Neuropeptide secreted from a pacemaker activates neurons to control a rhythmic behavior.* Curr Biol, 2013. **23**(9): p. 746-54.

78.   Robinson, B., *The Gut and the Pelvic Brain.* 1907: Nabu Press.

79.   Ganfornina, M.D., D. Sanchez, and M.J. Bastiani, *Embryonic development of the enteric nervous system of the grasshopper Schistocerca americana.* J Comp Neurol, 1996. **372**(4): p. 581-96.

80.   Goldstein, A.M., R.M. Hofstra, and A.J. Burns, *Building a brain in the gut: development of the enteric nervous system.* Clin Genet, 2013. **83**(4): p. 307-16.

81.   Clerc, N. and J.B. Furness, *Intrinsic primary afferent neurones of the digestive tract.* Neurogastroenterol Motil, 2004. **16 Suppl 1**: p. 24-7.

82.   Li, Y. and C. Owyang, *Musings on the wanderer: what's new in our understanding of vago-vagal reflexes? V. Remodeling of vagus and enteric neural circuitry after vagal injury.* Am J Physiol Gastrointest Liver Physiol, 2003. **285**(3): p. G461-9.

83.   Parisi, M.A., *Hirschsprung Disease Overview.* 1993.

84.   Puri, P. and T. Shinkai, *Pathogenesis of Hirschsprung's disease and its variants: recent progress.* Semin Pediatr Surg, 2004. **13**(1): p. 18-24.

85.   Yang, J., et al., *Exome sequencing identified NRG3 as a novel susceptible gene of Hirschsprung's disease in a Chinese population.* Mol Neurobiol, 2013. **47**(3): p. 957-66.

86.   Goodall, J., *Acute intermittent porphyria and Hirschsprung's disease.* Proc R Soc Med, 1967. **60**(10): p. 1001-3.

87.   Hadary, A., et al., *Acute intermittent porphyria associated with hypoganglionosis in a young adult.* Gut, 2006. **55**(4): p. 581-2.

88.   Chen, Y., et al., *Distribution of carbon monoxide-producing neurons in human colon and in Hirschsprung's disease patients.* Hum Pathol, 2002. **33**(10): p. 1030-6.

89.   Piotrowska, A.P., et al., *Immunocolocalization of the heme oxygenase-2 and interstitial cells of Cajal in normal and aganglionic colon.* J Pediatr Surg, 2003. **38**(1): p. 73-7.

90.   Kurokawa, K., et al., *Comparative metagenomics revealed commonly enriched gene sets in human gut microbiomes.* DNA Res, 2007. **14**(4): p. 169-81.

91.   Borre, Y.E., et al., *Microbiota and neurodevelopmental windows: implications for brain disorders.* Trends Mol Med, 2014. **20**(9): p. 509-518.

92.   Keita, A.V. and J.D. Soderholm, *The intestinal barrier and its regulation by neuroimmune factors.* Neurogastroenterol Motil, 2010. **22**(7): p. 718-33.

93.   Artis, D., *Epithelial-cell recognition of commensal bacteria and maintenance of immune homeostasis in the gut.* Nat Rev Immunol, 2008. **8**(6): p. 411-20.

94.   Barbara, G., et al., *Mast cell-dependent excitation of visceral-nociceptive sensory neurons in irritable bowel syndrome.* Gastroenterology, 2007. **132**(1): p. 26-37.

95.   Borre, Y.E., et al., *Microbiota and neurodevelopmental windows: implications for brain disorders.* Trends Mol Med, 2014.

96.   Martinez, V. and Y. Tache, *CRF1 receptors as a therapeutic target for irritable bowel syndrome.* Curr Pharm Des, 2006. **12**(31): p. 4071-88.

97.   Almy, T.P., F. Kern, Jr., and M. Tulin, *Alterations in colonic function in man under stress; experimental production of sigmoid spasm in healthy persons.* Gastroenterology, 1949. **12**(3): p. 425-36.

98.   *Focus on neural control of feeding.* Nat Neurosci, 2012. **15**(10): p. 1321.

99.   Seo, S., et al., *Acute effects of glucagon-like peptide-1 on hypothalamic neuropeptide and AMP activated kinase expression in fasted rats.* Endocr J, 2008. **55**(5): p. 867-74.

100.   Meister, B., *Control of food intake via leptin receptors in the hypothalamus.* Vitam Horm, 2000. **59**: p. 265-304.

101.   Barrett, A.J., N.D. Rawlings, and E.A. O'Brien, *The MEROPS database as a protease information system.* J Struct Biol, 2001. **134**(2-3): p. 95-102.

102.   Erez, E., D. Fass, and E. Bibi, *How intramembrane proteases bury hydrolytic reactions in the membrane.* Nature, 2009. **459**(7245): p. 371-8.

103.   De Strooper, B., *Loss-of-function presenilin mutations in Alzheimer disease. Talking Point on the role of presenilin mutations in Alzheimer disease.* EMBO Rep, 2007. **8**(2): p. 141-6.

104.   Yamamoto, K., M. Yamada, and Y. Kato, *Age-related and phenylhydrazine-induced activation of the membrane-associated cathepsin E in human erythrocytes.* J Biochem, 1989. **105**(1): p. 114-9.

105.   Fruitier, I., I. Garreau, and J.-M. Piot, *Cathepsin D Is a Good Candidate for the Specific Release of a Stable Hemorphin from HemoglobinIn Vivo:VV-Hemorphin-7.* Biochemical and Biophysical Research Communications, 1998. **246**(3): p. 719-724.

106.   Nowotny, P., et al., *Posttranslational modification and plasma membrane localization of the Drosophila melanogaster presenilin.* Mol Cell Neurosci, 2000. **15**(1): p. 88-98.

107.   Rawlings, N.D. and A.J. Barrett, *MEROPS: the peptidase database.* Nucleic

        Acids Res, 1999. **27**(1): p. 325-31.

108.   Blundell, T., B.L. Sibanda, and L. Pearl, *Three-dimensional structure,*

        specificity and catalytic mechanism of renin. Nature, 1983. **304**(5923): p. 273-

        5.

109.   Zhivotovsky, B., et al., *Caspases: their intracellular localization and*

        translocation during apoptosis. Cell Death Differ, 1999. **6**(7): p. 644-51.

110.   Wajant, H., *The Fas signaling pathway: more than a paradigm.* Science,

        2002. **296**(5573): p. 1635-6.

111.   Boehning, D., et al., *Cytochrome c binds to inositol (1,4,5) trisphosphate*

        receptors, amplifying calcium-dependent apoptosis. Nat Cell Biol, 2003.

        5(12): p. 1051-61.

112.   Motyckova, G. and D.E. Fisher, *Pycnodysostosis: role and regulation of*

        cathepsin K in osteoclast function and human disease. Curr Mol Med, 2002.

        2(5): p. 407-21.

113.   Hook, V., et al., *Cysteine Cathepsins in the secretory vesicle produce active*

        peptides: Cathepsin L generates peptide neurotransmitters and cathepsin B

        produces beta-amyloid of Alzheimer's disease. Biochim Biophys Acta, 2012.

        1824(1): p. 89-104.

114.   Illy, C., et al., *Role of the occluding loop in cathepsin B activity.* J Biol Chem,

        1997. **272**(2): p. 1197-202.

115.   Roshy, S., B.F. Sloane, and K. Moin, *Pericellular cathepsin B and malignant*

        progression. Cancer Metastasis Rev, 2003. **22**(2-3): p. 271-86.

116. Sevenich, L., et al., *Human cathepsin L rescues the neurodegeneration and lethality in cathepsin B/L double-deficient mice.* Biol Chem, 2006. **387**(7): p. 885-91.

117. Campbell, R.L. and P.L. Davies, *Structure-function relationships in calpains.* Biochem J, 2012. **447**(3): p. 335-51.

118. Lebart, M.C. and Y. Benyamin, *Calpain involvement in the remodeling of cytoskeletal anchorage complexes.* FEBS J, 2006. **273**(15): p. 3415-26.

119. Patthy, L., et al., *Kringles: modules specialized for protein binding. Homology of the gelatin-binding region of fibronectin with the kringle structures of proteases.* FEBS Lett, 1984. **171**(1): p. 131-6.

120. Hedstrom, L., *Serine protease mechanism and specificity.* Chem Rev, 2002. **102**(12): p. 4501-24.

121. Hooper, N.M., *Families of zinc metalloproteases.* FEBS Lett, 1994. **354**(1): p. 1-6.

122. Stocker, W., et al., *The metzincins--topological and sequential relations between the astacins, adamalysins, serralysins, and matrixins (collagenases) define a superfamily of zinc-peptidases.* Protein Sci, 1995. **4**(5): p. 823-40.

123. Seals, D.F. and S.A. Courtneidge, *The ADAMs family of metalloproteases: multidomain proteins with multiple functions.* Genes Dev, 2003. **17**(1): p. 7-30.

124. Piccard, H., P.E. Van den Steen, and G. Opdenakker, *Hemopexin domains as multifunctional liganding modules in matrix metalloproteinases and other proteins.* J. Leukoc. Biol., 2007. **81**(4): p. 870-892.

125.   Murphy, G., *Regulation of the proteolytic disintegrin metalloproteinases, the 'Sheddases'*. Semin Cell Dev Biol, 2009. **20**(2): p. 138-45.

126.   Turk, B., D. Turk, and V. Turk, *Protease signalling: the cutting edge.* EMBO J, 2012. **31**(7): p. 1630-43.

127.   Nakayama, K., *Furin: a mammalian subtilisin/Kex2p-like endoprotease involved in processing of a wide variety of precursor proteins.* Biochem J, 1997. **327 (Pt 3)**: p. 625-35.

128.   Black, R.A., et al., *A metalloproteinase disintegrin that releases tumour-necrosis factor-alpha from cells.* Nature, 1997. **385**(6618): p. 729-33.

129.   Adrain, C., et al., *Tumor necrosis factor signaling requires iRhom2 to promote trafficking and activation of TACE.* Science, 2012. **335**(6065): p. 225-8.

130.   Kopan, R., *Notch signaling.* Cold Spring Harb Perspect Biol, 2012. **4**(10).

131.   Silvestri, L., et al., *The serine protease matriptase-2 (TMPRSS6) inhibits hepcidin activation by cleaving membrane hemojuvelin.* Cell Metab, 2008. **8**(6): p. 502-11.

132.   Fyhrquist, F. and O. Saijonmaa, *Renin-angiotensin system revisited.* J Intern Med, 2008. **264**(3): p. 224-36.

133.   Jutras, I. and T.L. Reudelhuber, *Prorenin processing by cathepsin B in vitro and in transfected cells.* FEBS Lett, 1999. **443**(1): p. 48-52.

134.   Mercure, C., et al., *Cathepsin B is not the processing enzyme for mouse prorenin.* Am J Physiol Regul Integr Comp Physiol, 2010. **298**(5): p. R1212-6.

135.   Yvan-Charvet, L. and A. Quignard-Boulange, *Role of adipose tissue renin-angiotensin system in metabolic and inflammatory diseases associated with obesity.* Kidney Int, 2011. **79**(2): p. 162-8.

136.   Coble, J.P., et al., *Activation of the renin-angiotensin system, specifically in the subfornical organ is sufficient to induce fluid intake.* Am J Physiol Regul Integr Comp Physiol, 2014. **307**(4): p. R376-86.

137.   Ocaranza, M.P., et al., *Recent insights and therapeutic perspectives of angiotensin-(1-9) in the cardiovascular system.* Clin Sci (Lond), 2014. **127**(9): p. 549-57.

138.   Nguyen, G., et al., *Pivotal role of the renin/prorenin receptor in angiotensin II production and cellular responses to renin.* J Clin Invest, 2002. **109**(11): p. 1417-27.

139.   Sihn, G., et al., *(Pro)renin receptor: subcellular localizations and functions.* Front Biosci (Elite Ed), 2013. **5**: p. 500-8.

140.   Macfarlane, S.R., et al., *Proteinase-activated receptors.* Pharmacol Rev, 2001. **53**(2): p. 245-82.

141.   Zhao, P., M. Metcalf, and N.W. Bunnett, *Biased signaling of protease-activated receptors.* Front Endocrinol (Lausanne), 2014. **5**: p. 67.

142.   Maun, H.R., D. Kirchhofer, and R.A. Lazarus, *Pseudo-active sites of protease domains: HGF/Met and Sonic hedgehog signaling in cancer.* Biol Chem, 2010. **391**(8): p. 881-92.

143.   Gallet, A., *Hedgehog morphogen: from secretion to reception.* Trends Cell Biol, 2011. **21**(4): p. 238-46.

144. Fuse, N., et al., *Sonic hedgehog protein signals not as a hydrolytic enzyme but as an apparent ligand for patched.* Proc Natl Acad Sci U S A, 1999. **96**(20): p. 10992-9.

145. Williamson, A.L., et al., *A multi-enzyme cascade of hemoglobin proteolysis in the intestine of blood-feeding hookworms.* J Biol Chem, 2004. **279**(34): p. 35950-7.

146. Ranjit, N., et al., *Proteolytic degradation of hemoglobin in the intestine of the human hookworm Necator americanus.* J Infect Dis, 2009. **199**(6): p. 904-12.

147. Knox, D., *Proteases in blood-feeding nematodes and their potential as vaccine candidates.* Adv Exp Med Biol, 2011. **712**: p. 155-76.

148. Gluzman, I.Y., et al., *Order and specificity of the Plasmodium falciparum hemoglobin degradation pathway.* J Clin Invest, 1994. **93**(4): p. 1602-8.

149. Williamson, A.L., et al., *Ancylostoma caninum MTP-1, an astacin-like metalloprotease secreted by infective hookworm larvae, is involved in tissue migration.* Infect Immun, 2006. **74**(2): p. 961-7.

150. Salter, J.P., et al., *Cercarial elastase is encoded by a functionally conserved gene family across multiple species of schistosomes.* J Biol Chem, 2002. **277**(27): p. 24618-24.

151. Fishelson, Z., *Novel mechanisms of immune evasion by Schistosoma mansoni.* Mem Inst Oswaldo Cruz, 1995. **90**(2): p. 289-92.

152. McVeigh, P., et al., *Fasciola hepatica virulence-associated cysteine peptidases: a systems biology perspective.* Microbes Infect, 2012. **14**(4): p. 301-10.

153. McGonigle, L., et al., *The silencing of cysteine proteases in Fasciola hepatica newly excysted juveniles using RNA interference reduces gut penetration.* Int J Parasitol, 2008. **38**(2): p. 149-55.

154. Yao, C., *Major surface protease of trypanosomatids: one size fits all?* Infect Immun, 2010. **78**(1): p. 22-31.

155. Mottram, J.C., G.H. Coombs, and J. Alexander, *Cysteine peptidases as virulence factors of Leishmania.* Curr Opin Microbiol, 2004. **7**(4): p. 375-81.

156. Swenerton, R.K., et al., *Leishmania subtilisin is a maturase for the trypanothione reductase system and contributes to disease pathology.* J Biol Chem, 2010. **285**(41): p. 31120-9.

157. Swenerton, R.K., et al., *The oligopeptidase B of Leishmania regulates parasite enolase and immune evasion.* J Biol Chem, 2011. **286**(1): p. 429-40.

158. Villalta, F., et al., *Molecular analysis of early host cell infection by Trypanosoma cruzi.* Front Biosci, 2008. **13**: p. 3714-34.

159. Mackey, Z.B., et al., *A cathepsin B-like protease is required for host protein degradation in Trypanosoma brucei.* J Biol Chem, 2004. **279**(46): p. 48426-33.

160. Serbielle, C., et al., *Identification of parasite-responsive cysteine proteases in Manduca sexta.* Biol Chem, 2009. **390**(5-6): p. 493-502.

161. Nass, R. and I. Hamza, *The nematode C. elegans as an animal model to explore toxicology in vivo: solid and axenic growth culture conditions and compound exposure parameters.*, in *Current Protocols in Toxicology*, M.D.

Maines, et al., Editors. 2007, John Wiley & Sons, Inc.: New York. p. 1.9.1-1.9.17.

162.   Samuel, T.K., et al., *Culturing Caenorhabditis elegans in axenic liquid media and creation of transgenic worms by microparticle bombardment.* J Vis Exp, 2014(90): p. e51796.

163.   Epstein, H.F. and D.C. Shakes, eds. *Caenorhabditis elegans: Modern Biological Analysis of an Organism*. Methods in Cell Biology, ed. L. Wilson and P. Matsudaira. Vol. 48. 1995, Academic Press: San Diego.

164.   Kamath, R.S., et al., *Systematic functional analysis of the Caenorhabditis elegans genome using RNAi.* Nature, 2003. **421**(6920): p. 231-7.

165.   Reboul, J., et al., *C. elegans ORFeome version 1.1: experimental verification of the genome annotation and resource for proteome-scale protein expression.* Nat Genet, 2003. **34**(1): p. 35-41.

166.   Li, J.M., et al., *Cloning of the Escherichia coli K-12 hemB gene.* J Bacteriol, 1988. **170**(2): p. 1021-5.

167.   Redemann, S., et al., *Codon adaptation-based control of protein expression in C. elegans.* Nat Methods, 2011. **8**(3): p. 250-2.

168.   Larkin, M.A., et al., *Clustal W and Clustal X version 2.0.* Bioinformatics, 2007. **23**(21): p. 2947-8.

169.   Petersen, T.N., et al., *SignalP 4.0: discriminating signal peptides from transmembrane regions.* Nat Methods, 2011. **8**(10): p. 785-6.

170.   Zhang, Y., *I-TASSER server for protein 3D structure prediction.* BMC Bioinformatics, 2008. **9**: p. 40.

171. McGhee, J.D., et al., *ELT-2 is the predominant transcription factor controlling differentiation and function of the C. elegans intestine, from embryo to adult.* Dev Biol, 2009. **327**(2): p. 551-65.

172. Pauli, F., et al., *Chromosomal clustering and GATA transcriptional regulation of intestine-expressed genes in C. elegans.* Development, 2006. **133**(2): p. 287-95.

173. McGhee, J.D., et al., *The ELT-2 GATA-factor and the global regulation of transcription in the C. elegans intestine.* Dev Biol, 2007. **302**(2): p. 627-45.

174. Castino, R., et al., *Prolactin promotes the secretion of active cathepsin D at the basal side of rat mammary acini.* Endocrinology, 2008. **149**(8): p. 4095-105.

175. Kuester, D., et al., *The cathepsin family and their role in colorectal cancer.* Pathol Res Pract, 2008. **204**(7): p. 491-500.

176. Bogitsh, B.J., et al., *Gut-associated immunolocalization of the Schistosoma mansoni cysteine proteases, SmCL1 and SmCL2.* J Parasitol, 2001. **87**(2): p. 237-41.

177. Fares, H. and I. Greenwald, *Genetic analysis of endocytosis in Caenorhabditis elegans: coelomocyte uptake defective mutants.* Genetics, 2001. **159**(1): p. 133-45.

178. Oka, T., et al., *Four subunit a isoforms of Caenorhabditis elegans vacuolar H+-ATPase. Cell-specific expression during development.* J Biol Chem, 2001. **276**(35): p. 33079-85.

179.   Rozengurt, E. and C. Sternini, *Taste receptor signaling in the mammalian gut.* Curr Opin Pharmacol, 2007. **7**(6): p. 557-62.

180.   Arndt, S., et al., *Iron-induced expression of bone morphogenic protein 6 in intestinal cells is the main regulator of hepatic hepcidin expression in vivo.* Gastroenterology, 2010. **138**(1): p. 372-82.

181.   Lee, B.H., et al., *Hyperactive neuroendocrine secretion causes size, feeding, and metabolic defects of C. elegans Bardet-Biedl syndrome mutants.* PLoS Biol, 2011. **9**(12): p. e1001219.

182.   Cao, C., et al., *Placental heme receptor LRP1 correlates with the heme exporter FLVCR1 and neonatal iron status.* Reproduction, 2014. **148**(3): p. 295-302.

183.   Evans, D. and T. Blumenthal, *trans splicing of polycistronic Caenorhabditis elegans pre-mRNAs: analysis of the SL2 RNA.* Mol Cell Biol, 2000. **20**(18): p. 6659-67.

184.   Ding, L. and E.P. Candido, *Association of several small heat-shock proteins with reproductive tissues in the nematode Caenorhabditis elegans.* Biochem J, 2000. **351**(Pt 1): p. 13-7.

185.   Balklava, Z., et al., *Genome-wide analysis identifies a general requirement for polarity proteins in endocytic traffic.* Nat Cell Biol, 2007. **9**(9): p. 1066-73.

186.   Poea-Guyon, S., et al., *The V-ATPase membrane domain is a sensor of granular pH that controls the exocytotic machinery.* J Cell Biol, 2013. **203**(2): p. 283-98.

187. Fruton, J.S., *A history of pepsin and related enzymes.* Q Rev Biol, 2002. **77**(2): p. 127-47.

188. Cousin, C., et al., *Potential role of the (pro)renin receptor in cardiovascular and kidney diseases.* J Nephrol, 2010. **23**(5): p. 508-13.

189. Glondu, M., et al., *A mutated cathepsin-D devoid of its catalytic activity stimulates the growth of cancer cells.* Oncogene, 2001. **20**(47): p. 6920-9.

190. Kang, J., et al., *Essential roles of snap-29 in C. elegans.* Dev Biol, 2011. **355**(1): p. 77-88.

191. Clokey, G.V. and L.A. Jacobson, *The autofluorescent "lipofuscin granules" in the intestinal cells of Caenorhabditis elegans are secondary lysosomes.* Mech Ageing Dev, 1986. **35**(1): p. 79-94.

192. Lehner, B., et al., *Loss of LIN-35, the Caenorhabditis elegans ortholog of the tumor suppressor p105Rb, results in enhanced RNA interference.* Genome Biol, 2006. **7**(1): p. R4.

193. Suzuki, Y., et al., *A BMP homolog acts as a dose-dependent regulator of body size and male tail patterning in Caenorhabditis elegans.* Development, 1999. **126**(2): p. 241-250.

194. Ritter, A.D., et al., *Complex expression dynamics and robustness in C. elegans insulin networks.* Genome Res, 2013. **23**(6): p. 954-65.

195. Li, C., et al., *Neuropeptide gene families in the nematode Caenorhabditis elegans.* Ann N Y Acad Sci, 1999. **897**: p. 239-52.

196.	Liang, J., et al., *The Caenorhabditis elegans schnurri homolog sma-9 mediates stage- and cell type-specific responses to DBL-1 BMP-related signaling.* Development, 2003. **130**(26): p. 6453-64.

197.	Liang, J., et al., *Transcriptional repressor and activator activities of SMA-9 contribute differentially to BMP-related signaling outputs.* Dev Biol, 2007. **305**(2): p. 714-25.

198.	Myers, M.G., Jr. and D.P. Olson, *Central nervous system control of metabolism.* Nature, 2012. **491**(7424): p. 357-63.

199.	Miao, D., S.L. Young, and C.D. Golden, *A meta-analysis of pica and micronutrient status.* Am J Hum Biol, 2014.

200.	Sontag, C., et al., *[Rapid regression of prolonged pagophagia after treatment of iron deficiency].* Presse Med, 2001. **30**(7): p. 321-3.

201.	Osman, Y.M., Y.A. Wali, and O.M. Osman, *Craving for ice and iron-deficiency anemia: a case series from Oman.* Pediatr Hematol Oncol, 2005. **22**(2): p. 127-31.

202.	Li, P., et al., *Expression of recombinant proteins in Pichia pastoris.* Appl Biochem Biotechnol, 2007. **142**(2): p. 105-24.

203.	Backes, B.J., et al., *Synthesis of positional-scanning libraries of fluorogenic peptide substrates to define the extended substrate specificity of plasmin and thrombin.* Nat Biotechnol, 2000. **18**(2): p. 187-93.

204.	Varfaj, F., J.N. Lampe, and P.R. Ortiz de Montellano, *Role of cysteine residues in heme binding to human heme oxygenase-2 elucidated by two-dimensional NMR spectroscopy.* J Biol Chem, 2012. **287**(42): p. 35181-91.

205. Garcia-Santamarina, S., S. Boronat, and E. Hidalgo, *Reversible cysteine oxidation in hydrogen peroxide sensing and signal transduction.* Biochemistry, 2014. **53**(16): p. 2560-80.

206. Kim, B.E., et al., *Cardiac copper deficiency activates a systemic signaling mechanism that communicates with the copper acquisition and storage organs.* Cell Metab, 2010. **11**(5): p. 353-63.

207. Nemeth, E., et al., *Hepcidin regulates cellular iron efflux by binding to ferroportin and inducing its internalization.* Science, 2004. **306**(5704): p. 2090-3.

208. Mills, E., et al., *Mechanisms of brain iron transport: insight into neurodegeneration and CNS disorders.* Future Med Chem, 2010. **2**(1): p. 51-64.

209. Khan, A.A. and J.G. Quigley, *Control of intracellular heme levels: heme transporters and heme oxygenases.* Biochim Biophys Acta, 2011. **1813**(5): p. 668-82.

210. Kool, M., et al., *Analysis of expression of cMOAT (MRP2), MRP3, MRP4, and MRP5, homologues of the multidrug resistance-associated protein gene (MRP1), in human cancer cell lines.* Cancer Res, 1997. **57**(16): p. 3537-47.

211. Rieu, S., et al., *Exosomes released during reticulocyte maturation bind to fibronectin via integrin alpha4beta1.* Eur J Biochem, 2000. **267**(2): p. 583-90.

212. Ratajczak, J., et al., *Biological significance of the different erythropoietic factors secreted by normal human early erythroid cells.* Leuk Lymphoma, 2003. **44**(5): p. 767-74.

213. Kautz, L., et al., *Identification of erythroferrone as an erythroid regulator of iron metabolism.* Nat Genet, 2014. **46**(7): p. 678-84.

214. Andriopoulos, B., Jr., et al., *BMP6 is a key endogenous regulator of hepcidin expression and iron metabolism.* Nat Genet, 2009. **41**(4): p. 482-7.

215. Zhang, X. and Y. Zhang, *DBL-1, a TGF-beta, is essential for Caenorhabditis elegans aversive olfactory learning.* Proc Natl Acad Sci U S A, 2012. **109**(42): p. 17081-6.